Riemannian Computational Geometry

– Convex Hull, Voronoi Diagram and Delaunay-type Triangulation –

リーマン計算幾何

－凸包、ボロノイ図とデローネ型三角形分割－

Kensuke Onishi
大西建輔

①

Riemannian Computational Geometry
— Convex Hull, Voronoi Diagram and Delaunay-type Triangulation —

by

Kensuke Onishi

A Doctoral Thesis

Submitted to

The Graduate School of Information Science

Faculty of Science

The University of Tokyo

on July 3, 1998

in Partial Fulfillment of the Requirements

for the Degree of Doctor of Science

ABSTRACT

In this thesis, *Riemannian computational geometry* is investigated, the main goal being the design of efficient algorithms and data structures for special geometric objects in Riemannian space. Although some geometric objects in Riemannian space, for example *geodesics, the cut locus*, are known from the work of others, the effort has been mainly towards their mathematical characterization. We add a computational aspect to these studies. We gives algorithms for constructing geometric objects, together with bounds on their combinatorial and time complexity. Some properties of those structures are proved and a number of applications are described.

In this thesis, the convex hull, the Voronoi diagram and Delaunay-type triangulations are the principal objects of study. The convex hull is a fundamental object in computational geometry and is used in the construction of the Voronoi diagram and Delaunay-type triangulations. The Voronoi diagram for a set of points, expresses proximity relationships, and has applications in many fields of natural and social science. Delaunay triangulation is a special type of triangulation and is important for finite element methods and computer graphics. Unfortunately, the Delaunay triangulation does not always exist in Riemannian space. We propose a Delaunay-type triangulation, which does always exist in several special types of Riemannian space, and coincides with Delaunay triangulation in the Euclidean case. These objects are known to be efficiently computable in the Euclidean space. In a Riemannian space, the situation is different. For example, the Voronoi diagram is defined in any space with distance, but it is not known whether it is computable in general.

The particular cases of hyperbolic space and dually flat space are highlighted in this thesis. Hyperbolic space has conformal, projective and differential geometric aspects, and is very basic as a Riemannian space. It is of course famous as a non-Euclidean space. The dually flat space is useful because of its connection with statistical estimation and as an extension of Euclidean geometry. For such a space, we can take advantage of the existence of *potential functions* in the algorithms for the Voronoi diagram and the Delaunay-type triangulation, and also of *divergence*, as an extension of the Euclidean distance.

Since we take the position that computation is of great importance, we define these objects constructively, mentioned above. Such objects can be computed efficiently by

means of our algorithms. Our main contribution is the demonstration of relations among these structures: the connections through hyperplane arrangements and convex polytopes. Moreover, the dually flat space, treated in this thesis, has some nice properties, and provides a good framework for posing problems, leading to new developments of computational geometry.

Acknowledgments

This thesis was supervised by Associate Prof. Hiroshi Imai of the University of Tokyo. I could not write this thesis without this various comments, suggestions and advises. He also supported me for going abroad, which helped me to think in a wider perspective. Moreover, he has encouraged me. Such encouragement has been invaluable for me.

Special thanks must go to Prof. Nobuki Takayama of the Kobe university, who gives me very precise and critical comments on my research. I would like to thanks Prof. Mamoru Hoshi of the University of Electro-Communications, who gives me much time for writing this thesis and advises on English. I would like to thanks Prof. Junichi Itoh of Kumamoto University, who gives me advises on the concept of cut locus. Thanks also go to Mr. Shintaro Yoshizawa, who states the global coordinate system in dually flat space.

Also I would like to acknowledge helpful discussion with members of Imai laboratory. Especially, Mrs. Mary Inaba explained about geometric clustering, which is based on Chapter 6.1 of this thesis.

Finally, I would like to thanks my parents, my grandfather, my brother and my sister for their supports in my daily life.

Table of Contents

List of Figures

Chapter 1

Introduction

1.1 From Euclidean Geometry to Riemannian Geometry

Euclidean geometry has been studied since Stoicheia, although its role was fundamentally upset and changed by the discovery of Riemannian geometry. In Euclidean geometry, geometric objects as point sets are the primary focus of research. In Riemannian space, by contrast, it is the local and global structure of the space itself that is usually studied. There have been earlier works on geometric objects in Riemannian space, for example, geodesics (e.g., see [24]) which correspond to straight lines in Euclidean space. Earlier research has mainly considered the properties of such objects, constructive issues being ignored. In this thesis, we propose endowing geometric objects in a Riemannian space with *computational* aspects: the stating of good algorithms; the analysis of complexity and the establishment of theory. This we call *Riemannian computational geometry*.

In Euclidean space, such research is simply called *computational geometry*. Since the latter has numerous applications to geographical information systems, pattern recognition, computer graphics, robotics, etc., there is plenty of reported work in the literature, for example, "Algorithms in Combinatorial Geometry [12]", "Computational Geometry [42]", etc. This thesis is not only a study of geometric objects in Riemannian space, but is also an extension of computational geometry from Euclidean space to Riemannian space.

In this chapter we begin with an explanation of the theoretical aspects (Section 1.2), followed by the applied aspects (Section 1.3) of the thesis. In Section 1.4, the geometric structures and spaces treated in this thesis, are described. Finally, in Section 1.5, the conclusions of each chapter are summarized.

1.2 Theoretical Aspect

Our purpose in this thesis is to research geometric structures with computation in Riemannian space. For our investigation we consider the following problems :

1. What structures can be defined in Riemannian space?
2. What properties have these geometric structures?
3. Can such structures be computed?

To illustrate the first problem, let us consider generalization of hyperplane arrangement in Riemannian space, we first need to ask what a "hyperplane" is in Riemannian space: a hypersurface that has properties mimicking properties of a hyperplane in Euclidean space. Although "hyperplane" is not always defined in a general Riemannian space, it was shown that a ruled real hypersurface has required properties to stand for a hyperplane if the space is a complex Kähler manifold of a constant holomorphic curvature [23]. There are many other geometric structures useful in computational geometry and geometric data processing; However, possibility of their generalization to Riemannian spaces have not been studied well in literature. In this thesis we focus on three structures, the *convex hull*, the *Voronoi diagram* and *Delaunay-type triangulation* in Riemannian spaces. These structures are rather basic in Euclidean space and have been much studied.

The second problem is that although a geometric object is defined in a Riemannian space in a similar way to that in Euclidean space, it may not always have similar characteristics. For example, in [32, 33], the Voronoi diagram in Siegel space, a type of Riemannian space, is stated and expressed as a proximity relationship. A Voronoi diagram can be defined by a positive-valued function. If that function is a *distance* in space, then that diagram provides the proximity relation. Thus, it is proved that the distance can be used as the function defining a Voronoi diagram in some Riemannian space. Not only do we define geometric structures but also study their properties.

We give a high priority to the third problem whether the geometric structures considered in this thesis can be efficiently computed. There has been a little research concerned with computation for geometric structures in Riemannian space: for example, the convex hull in Minkowski space [30], and the Voronoi diagram for points in orbifolds [27]. In particular, in [5], the Voronoi diagram in hyperbolic space is described, using a non-Euclidean metric, and applied to shape reconstruction from plane sections. In this thesis not only each structure but also the relations among objects are investigated. Consequently most of the Riemannian structures in this thesis are researched by a unified approach using *potential functions* and *hyperplane arrangement*.

In this paper, we assume that real RAM(random-access machine) is available for the model of computation (e.g., see [42]). In that model, many operations, for example arithmetic, the comparison of two numbers, trigonometric functions, exponential functions, etc., can be used at unit time.

1.3 Applied Aspect

Since we attach great importance to *computation*, the following application is of particular interest. A statistical parametric space, which is not only an example of a dually flat space, but is also the first such space considered, is the parameter space of a probability density function. It plays an important role in theory of statistical estimation. When the functional form of a probability density function is given without specifying its parameter values, it can be regarded as a function of the parameters. In that parameter space, the values of the parameters can be determined by, for example, a maximum likelihood method. In information geometry [1], a Riemannian geometry is introduced in the statistical parametric space. Then the maximum likelihood method and higher order asymptotic theory are interpreted in term of that geometry. We hope that other descriptions of statistical estimation are provided by geometric objects in statistical parametric space. For example, the parametric space of any discrete distribution can be regarded as a Riemannian space, and a proximity relation in that space can be constructed by our algorithm. Moreover the dually flat space is also the model for geometric clustering.

Another motivation is the implementation of mesh generation in a surface with a Riemannian metric. Such mesh generation has already been studied in [7, 8] and its implementation has been achieved. However, the length between any two points was taken along an Euclidean segment, which provides only an approximation of true distance. We will study a method of mesh generation based on the distance along a *geodesic*. Surface can be separated into three subsets, those for which the curvature is positive, negative or zero. Moreover, a set of points on the surface can be divided into some clusters according to the curvature criterion, and then each cluster can be triangulated. Can a triangulation for surface be make from these triangulations of clusters? Although this study is only in its infancy and the theoretical basis has not yet been established, a few results are obtained in this thesis. In particular, we propose a nice triangulation, called a *Delaunay-type triangulation*, which can be transformed into a structure on a surface *pseudo sphere* in three-dimensional Euclidean space without changing distance. This triangulation is useful for the triangulation of clusters whose points have negative curvature. A suitable triangulation of the cluster of points of positive and of zero curvature, called the Delaunay triangulation, has already been investigated in [35] and [12, 42], respectively.

1.4 Geometric Structure and Target Space

In this thesis we consider three geometric structures: the *convex hull*, the *Voronoi diagram* and *Delaunay triangulation*. Their definition and characterization are described in Chapter 3, 4 and 5, respectively. Here, we explain the nature of these objects. These structures are defined for a finite set of points P.

Convex Hull The minimum convex set including the point set P. In Euclidean space, its boundary is a union of "facets", where a facet is a closed convex subset in a hyperplane. Two- or three-dimensional convex hulls are used in computer graphics, computer aided design, etc.

Voronoi Diagram A partition of the space into "Voronoi regions" of points of P. The Voronoi region of a point $p \in P$ consists of points x in the space such that $f(p, x) \leq f(q, x)$ for any point q in P, where f is a given bivariate function on the space. The Euclidean Voronoi diagram employs the construction of a minimum spanning tree of P, where the edge weight of an edge is provided by the Euclidean distance between end points.

Delaunay Triangulation A triangulation is a division of the convex hull of P by triangles (simplices) such that each vertex of the triangle (simplex) is a point of

P. The Delaunay triangulation is a special one, as each point of P is not included in the circumsphere of each triangle (simplex). In Euclidean space, the Delaunay triangulation is the dual structure to the Voronoi diagram.

These structures are of major interest in computational geometry and are also useful in various fields. We study these objects in *hyperbolic space* and in *dually flat space*. The former is fundamental and well-known in differential geometry. The Voronoi diagram in two-dimensional hyperbolic space is also studied in [5]. The three-dimensional hyperbolic space is related to knot theory [25].

The latter is also a kind of Riemannian space, which has been employed in a geometrical approach to the analysis of statistical estimation, such as the maximum likelihood method. Moreover, in that space, the distance-like function *divergence* and *potential functions* are considered; these are related to parametric estimation [1]. The concept of the dually flat space originated in the field of statistical estimation, and can be applied in various contexts: *parametric family of invertible linear system* [2], *feasible region of linear programming* [51], etc.

1.5 Overview of This Thesis

Chapter 2 contains the background preparatory material of this thesis: previous works about Riemannian space, statistical parametric space and dually flat space are described in Section 2.1, 2.2 and 2.3, respectively. Moreover, some properties of hyperbolic space are proved in Section 2.1.2 and the calculation of the Fisher information matrix is in Section 2.2.3.

In 3) the *Convex hull* in Riemannian space discusses. In Section 3.2 we show that the convex hull of a flat space with a global coordinate system, which contains *dually flat space* as a special case, can be computed by using algorithm of the Euclidean convex hull. Its combinatorial and time complexity are given (Theorem 3.1, Corollary 3.1). In the dually flat space for give set of points there are two convex hulls, called ∇- and ∇^*-convex hull, corresponding to the two different introduced *connections*. Note that there is *two* coordinate systems in *a* dually flat space. In Section 3.3, the convex hull in hyperbolic space is considered. This convex hull is constructed by a Euclidean convex hull algorithm and the linearization method (e.g., see [12]). Moreover, we discuss the convex hull in the prototype two-dimensional hyperbolic space, called *Poincaré space*. In addition, in Section 3.5, a new class of Riemannian space, *linearizable space*, is proposed. This class encompasses the flat space with a global coordinate system, the hyperbolic space and the space defined in Definition 3.5. In that space the convex hull for given set of points is efficiently computable.

In Chapter 4, we explain the *hyperbolic Voronoi diagram* (Section 4.2) and the ∇- and ∇^*-*Voronoi diagram* (Section 4.3). The hyperbolic Voronoi diagram is defined by the *distance* based on the proximity relation in that space. It can be computed by an algorithm of the Euclidean Voronoi diagram and the deletion of some faces. It is also proved that its combinatorial and time complexity equal to that of the Euclidean algorithm (Theorem 4.2). This theorem is shown by the fact that Euclidean and hyperbolic sphere coincide for given points. ∇- and ∇^*-Voronoi diagrams in dually flat space by *divergences* instead of the distance (Section 4.3). Because the divergence does not satisfy the symmetry rule of the distance, two diagrams exist. The diagram can be constructed by the projection of the lower envelope of the hyperplane arrangement in the corresponding coordinate system and the deletion of faces. The difference between the potential function and the tangent hyperplane is equal to the value of the divergence. The combinatorial and time complexities of this diagram are also Euclidean. In addition, the relation between the statistical parametric space of the normal distributions and the Poincaré space is obtained in Section 4.4. The relation between divergence and metric is also stated.

Delaunay and *Delaunay-type triangulations* are described in Chapter 5. Although these structures are the same in Euclidean space, in hyperbolic space and dually flat space they differ. In Section 5.2, the Delaunay graph, which is the dual structure to the hyperbolic Voronoi diagram, is obtained. Since that graph has nice properties, the Delaunay-type triangulation in hyperbolic space is defined by Algorithm 5.2 so that the triangulation contains the Delaunay graph. However, the properties of the Delaunay-type triangulation have not been established yet. In Section 5.4, Delaunay-type triangulation in dually flat space is described. That triangulation is a dual structure of ∇- (or ∇^*-)Voronoi diagram without deletion of faces and has the nice property "the divergence from the center to points of the maximal minimum enclosing sphere of Delaunay-type triangulation minimizes among all triangulations in the dually flat space".

In Chapter 6, we state two applications of the ∇-Voronoi diagram (Section 6.1) and of Delaunay-type triangulation (Section 6.2). The former is a geometric clustering by ∇-Voronoi diagram. In Section 4.3, the ∇- and ∇^*-Voronoi diagrams are treated equally. However, the ∇-Voronoi diagram is more useful than the ∇^*-Voronoi in relation to the statistical estimation. Moreover we obtain the surface triangulation by the Delaunay-type triangulation in Poincaré space. This triangulation may lead to a new mesh-generation method.

Chapter 2

Preliminaries

In this chapter we explain basic concepts of this thesis, i.e., in Section 2.1 *Riemannian geometry*, in Section 2.2 *statistical parametric space* and in Section 2.3 *dually flat space* are stated. Thought most of the research in this chapter has been studied, there are our computations in Section 2.1.2 and Section 2.2.3.

2.1 Riemannian Space

The concept of Riemannian space is studied since nineteenth century. So many topic has been researched, then various books are published, for example, "Riemannian Geometry [15]", "Foundations of Differential Geometry Vol. I & II [24]", "Riemannian Geometry [41]", etc. The basic concepts in Riemannian manifold are explained in Section 2.1. In Section 2.1.2 we state *hyperbolic space*, which is a fundamental Riemannian space and has various aspect. For this space we calculate some functions, *Christoffel's symbol*, *Riemannian curvature*, etc. Some geometric objects, *hyperbolic sphere* and *perpendicular bisector*, are defined and its properties are proved, which are collected in [36].

2.1.1 Definitions and Examples of Riemannian Space

In this section we state some concepts in Riemannian geometry to understand this thesis, i.e., definitions, examples and results without proof are stated. First, Riemannian space is defined.

Definition 2.1 (Riemannian space) *Let R be a d-dimensional manifold and g be a Riemannian metric which defines a positive definite inner product in each tangent space. The pair (R, g) is called* Riemannian space.

Example 2.1 (Euclidean Space) *Suppose $R = \mathbb{R}^d$ is d-dimensional Euclidean space with natural coordinates $x_1, x_2, \ldots, x_d$ and $g = I_d$ is d-dimensional identity matrix, i.e.,* $\mathrm{d}s^2 = \mathrm{d}x_1{}^2 + \mathrm{d}x_2{}^2 + \ldots + \mathrm{d}x_d{}^2$, *called* Euclidean metric.

Example 2.2 (Poincaré Space) *Suppose that $R = \{(x_1, x_2) \mid x_1, x_2 \in \mathbb{R}, x_2 > 0\}$ and $g = (x_2)^{-2} I_2$, i.e., $\mathrm{d}s^2 = \dfrac{\mathrm{d}x_1{}^2 + \mathrm{d}x_2{}^2}{x_2{}^2}$. This space is called* Poincaré space *or* upper half-plane, *written by* $\mathbb{H}$.

In Riemannian space *distance* between two points is defined by Riemannian metric.

Definition 2.2 (Distance on Riemannian space) *On a Riemannian space (R, g) the* arc length *of differentiable curve $\tau = x_t, a \leq t \leq b$, is defined by*

$$L = \int_a^b \sqrt{{}^t\left(\frac{\mathrm{d}x}{\mathrm{d}t}\right) g \left(\frac{\mathrm{d}x}{\mathrm{d}t}\right)} \mathrm{d}t.$$

Given a Riemannian metric g on a connected manifolds R, we define the distance function $d(x, y)$ on R is the infimum of the lengths of all piecewise differentiable curves of class C^∞ joining x and y.

Then we have

$$d(x, y) \geq 0, \quad d(x, y) = d(y, x), \quad d(x, y) + d(y, z) \geq d(x, z). \tag{2.1}$$

Definition 2.3 (Affine Connection) *Suppose (R, g) is a d-dimensional Riemannian space. Let $p, p' \in R$ be points, $[\xi]$ be a local coordinate system of R and $T_p, T_{p'}$ are tangent spaces of R at p and p', respectively. If a function $\Pi_{p,p'} : T_p \to T_{p'}$ is defined*

$$\Pi_{p,p'}\left(\left(\frac{\partial}{\partial \xi^j}\right)_p\right) = \left(\frac{\partial}{\partial \xi^j}\right)_{p'} - \sum_{i,k} d\xi^i \left(\Gamma^k_{ij}\right)_p \left(\frac{\partial}{\partial \xi_k}\right)_{p'}$$

and d^3 functions $\Gamma^k_{ij} : p \mapsto (\Gamma^k_{ij})_p$ are included in a class of C^∞, then affine connection *is given on R and written by ∇. Moreover $\{\Gamma^k_{ij}\}$ is called* connection coefficients *in the coordinate $[\xi]$.*

Affine connection gives a correspondence of vectors on each tangent space. In other words, if the whole connection coefficients are C^∞ and that coordinate system is *global*, then we can regard an affine connection $\Pi_{p,p'}$ as the connection coefficients Γ^i_{jk}.

Definition 2.4 *Suppose (R, g) is a Riemannian space and $\Pi_{p,p'}$ is an affine connection. Let $\gamma : [a, b] \to R$ be a curve on the Riemannian space R joining $\gamma(a)$ and $\gamma(b)$ and the map $X : t \mapsto X(t)$ be a field of vector along the curve γ, i.e., for $\forall \gamma(t)$, $X(t) \in T_{\gamma(t)}$ is decided. If the field of vector X is satisfied the condition*

$$X(t + \mathrm{d}t) = \Pi_{\gamma(t),\gamma(t+\mathrm{d}t)}(X(t)),$$

then X is parallel *on γ.*

Conversely, if γ is given, a parallel field of vector Π_γ on γ is decided. This connection is called parallel displacement *on γ.*

Definition 2.5 *Let X be a field of vector on a Riemannian space R. For any curve on R, if $X_\gamma : t \mapsto X_{\gamma(t)}$ is parallel on γ for a given connection ∇, X is* parallel *on R for ∇.*

Suppose for coordinate $[\xi]$ of R, d basis vector fields $\partial_i = \frac{\partial}{\partial \xi^i} (i = 1, \ldots, d)$ are parallel on R. This coordinate $[\xi^i]$ is called an *affine coordinate system* of ∇. The following conditions are also equivalent :

- $\nabla_{\partial_i} \partial_j = 0 \ \ (\forall i, j)$,
- connection coefficients $\Gamma^k_{ij} \equiv 0 \ \ (\forall i, j, k)$.

Definition 2.6 *Let R be a d-dimensional Riemannian space with metric g. If an affine coordinate system exists for a given connection ∇, then ∇ is said to be* flat.

The condition for flatness is equivalent to the vanishing of the connection coefficients Γ^k_{ij} $(i, j, k = 1, \ldots, d)$ at all points $p \in R$.

Definition 2.7 (Global Coordinate System) *An affine coordinate system is* global *if the same coordinate system is used for all points in the space. Such a coordinate system is called a* global coordinate system.

If flat space has a global coordinate system, the geodesic locally becomes an Euclidean line in that coordinate system.

Definition 2.8 *Let (R, g) be a Riemannian space, ∇ be a connection of R and $\mathcal{T}(R)$ be whole of tangent space of R. For fields of vector $X, Y, Z \in \mathcal{T}(R)$ maps $R : \mathcal{T} \times \mathcal{T} \times \mathcal{T} \to \mathcal{T}, T : \mathcal{T} \times \mathcal{T} \to \mathcal{T}$ are defined as follows :*

$$R(X, Y, Z) = \nabla_X(\nabla_Y Z) - \nabla_Y(\nabla_X Z) - \nabla_{[X,Y]}Z,$$

$$T(X, Y) = \nabla_X Y - \nabla_Y X - [X, Y],$$

where $[X, Y] = \sum_i \left(\sum_j X^j \partial_j X^i - \sum_j Y^j \partial_j X^i \right) \partial_i$ *for* $X = \sum_j X^j \partial_j, Y = \sum_j Y^j \partial_j$. *The R and T are called Riemannian curvature and torsion tensor, respectively.*

If $T = 0$, then connection is symmetric.

Definition 2.9 *Let (R, g) be a Riemannian space, ∇ be a connection of R and $\mathcal{T}(R)$ be whole of tangent space of R. For any fields of vector $X, Y, Z \in \mathcal{T}(R)$, if the following condition is satisfied :*

$$Z\langle X, Y\rangle = \langle \nabla_Z X, Y\rangle + \langle X, \nabla_Z Y\rangle, \tag{2.2}$$

then ∇ is metrical *for g where $\langle , \rangle$ is an inner product by g, i.e., $\langle X, Y\rangle := {}^tX \cdot g \cdot Y$.*

Definition 2.10 (Levi-Civita Connection) *For a Riemannian metric g, if a connection ∇ is metrical and symmetric, then that connection is called* Levi-Civita connection *or* Riemannian connection.

This connection is uniquely determined for a Riemannian metric g. Thus the Levi-Civita connection is given as follows :

$$\Gamma^k_{ij} = \frac{1}{2} \sum_l g^{il}(\partial_k g_{lj} + \partial_j g_{lk} - \partial_l g_{jk})$$

where g^{ij} is the inverse of g. These connection coefficients are also called *Christoffel's symbols.*

Example 2.3 1. **(Euclidean Space)** *All Γ^k_{ij} are equal to 0 for any i, j, k.*

2. **(Poincaré Space)** *The connection coefficients of Levi-Civita connection of Poincaré space are calculated by the metric $g = (x_2)^{-2} I_2$.*

$$\Gamma^1_{12} = \Gamma^2_{21} = -\Gamma^2_{11} = \Gamma^2_{22} = -{x_2}^{-1},$$

$$\Gamma^i_{jk} = 0 \quad \textit{Otherwise}.$$

In Riemannian space there exists a structure like a Euclidean line which called *geodesic*.

Definition 2.11 (Geodesic) *Let $\gamma(t)$ be a curve of C^∞-class in Riemannian space (R, g). $\gamma(t)$ is a* geodesic *if the field of vector $X = \frac{d\gamma}{dt}$ defined along γ is parallel along γ, that is, if $\nabla_X X$ exists and equals zero for all t.*

This condition is rewrite by the representation by component γ^i:

$$\frac{d^2\gamma^k(t)}{dt^2} + \sum_{i,j} \frac{d\gamma^i(t)}{dt}\frac{d\gamma^j(t)}{dt}(\Gamma^k_{ij})_{\gamma(t)} = 0 \quad (k = 1, \cdots, d). \tag{2.3}$$

Thus we get the geodesic in any Riemannian space if these differential equations can be solved. Although it is difficult to solve these equation in general, there are several special cases in which we can obtain the exact solutions:

Example 2.4 (Euclidean Space) *In Euclidean space, the connection coefficients Γ^i_{jk} $(\forall i, j, k = 1, \ldots, d)$ are equal to 0. Thus, the differential equations satisfied by geodesics are*

$$\frac{d^2\gamma^k(t)}{dt^2} = 0 \quad (k = 1, \cdots, d).$$

The solutions are straight lines.

Example 2.5 (Poincaré Space) *The above differential equations become*

$$\left\{ \begin{array}{rcl} \dfrac{d^2\gamma^1}{dt} - \dfrac{2}{\gamma^2}\dfrac{d\gamma^1}{dt}\dfrac{d\gamma^2}{dt} & = & 0 \\ \dfrac{d^2\gamma^2}{dt} - \dfrac{1}{\gamma^2}\left\{\left(\dfrac{d\gamma^2}{dt}\right)^2 - \left(\dfrac{d\gamma^1}{dt}\right)^2\right\} & = & 0. \end{array} \right. \tag{2.4}$$

There are two types of solutions:

$$(x_1 - a)^2 + {x_2}^2 = b^2 \text{ or } \ x = a$$

where a, b are constants, depending on initial conditions.

In addition, the concepts of *minimizing geodesic* and *completeness of manifold* are introduced.

Definition 2.12 (Minimizing Geodesic, [24, p.166]) *A geodesic joining two points x and y of a Riemannian manifold M is called* minimizing *if its length is equal to the distance $d(x, y)$.*

Definition 2.13 (Completeness of Manifold, [24, p.172]) *A Riemannian manifold R is said to be complete if the Riemannian connection is complete, that is, if every geodesic M can be extended for arbitrarily large values of its canonical parameter.*

Moreover the following theorem holds.

Theorem 2.1 ([24, p.172]) *If M is a connected complete Riemannian manifold, then any two points x and y of M can be joined by a minimizing geodesic.*

2.1.2 Hyperbolic Space

In this section, we discuss *hyperbolic space*, which is the most important Riemannian space in differential geometry, having uses in the analysis of manifolds (see [52]) and in knot theory (see [25]). The detail of this section is also described in [36].

Definition 2.14 (Hyperbolic Space) *Let $\mathbb{H}^d = \{(x_1, \cdots, x_d) \mid x_i \in \mathbb{R}, x_d > 0\}$ be a Riemannian manifold with Riemannian metric $\mathrm{d}s^2 = \dfrac{\mathrm{d}{x_1}^2 + \cdots + \mathrm{d}{x_d}^2}{{x_d}^2}$. This manifold is called d-*dimensional hyperbolic space.

[Remark] Two-dimensional hyperbolic space becomes Poincaré space. Defining hyperbolic space as above, we can replace the metric by $\mathrm{d}\tilde{s}^2 = c \cdot \mathrm{d}s^2$ for any positive constant c. By an appropriate choice of c, the space has -1 scalar curvature. The following arguments for $\mathrm{d}s$ directly carry over to a case such as $\mathrm{d}\tilde{s}^2$, and therefore we deal only with the above case. Moreover this space is realizable as a parametric space of a multinomial normal distribution whose variance-covariance matrix is $\sigma^2 I_d$. Then its *Fisher information matrix* is similar with the metric of hyperbolic space. When the matrix is regarded as Riemannian metric, the parametric space becomes Riemannian space [1].

We assume that Levi-Civita connection is introduced to the hyperbolic space. The Christoffel's symbols Γ^i_{jk} of this space are given by

$$\Gamma^i_{jk} = \begin{cases} -\dfrac{1}{x_d} & (i = j,\ k = d \text{ or } i = k,\ j = d\ (i = 1, \ldots, d)), \\ \dfrac{1}{x_d} & (j = k,\ i = d\ (j = 1, \ldots, d-1)), \\ 0 & \textit{otherwise}. \end{cases} \tag{2.5}$$

From these symbols, the Riemannian curvature $R^i_{jkl} = -\Gamma^i_{jk,l} + \Gamma^i_{jl,k} + \sum_{h=1}^{d}\left(-\Gamma^h_{jk}\Gamma^i_{hl} + \Gamma^h_{jl}\Gamma^i_{hk}\right)$ can be calculated when $i = k$ is satisfied:

$$R^i_{jil} = \begin{cases} -\dfrac{1}{{x_d}^2} & (j = l,\ i \neq j,\ i \neq d,\ j \neq d) \text{ or } (j = l,\ i \neq j,\ i = d,\ j \neq d), \\ -\dfrac{1}{{x_d}^2} & (j = l,\ i \neq j,\ i \neq d,\ j = d), \\ 0 & \text{otherwise}. \end{cases}$$

Moreover the Ricci tensor $R_{jl} = \sum_i R^i_{jil}$ becomes

$$R_{jl} = \begin{cases} -\dfrac{d-1}{{x_d}^2} & (j = l), \\ 0 & (j \neq l). \end{cases}$$

Finally, we obtain a scalar curvature

$$R = -d(d-1). \tag{2.6}$$

Thus this space has a negative constant curvature.

A *geodesic* in $\mathbb{H}^d$, which corresponds to a straight line in Euclidean space, is considered. Using Christoffel's symbols, the differential equations (2.3) for a geodesic are :

$$\begin{cases} \dfrac{\mathrm{d}^2\gamma^i}{\mathrm{d}t^2} - \dfrac{2}{\gamma^d}\cdot\dfrac{\mathrm{d}\gamma^i}{\mathrm{d}t}\cdot\dfrac{\mathrm{d}\gamma^d}{\mathrm{d}t} = 0 \quad (i = 1, \cdots, d-1) \\ \dfrac{\mathrm{d}^2\gamma^d}{\mathrm{d}t^2} - \dfrac{1}{\gamma^d}\left\{\sum_{j=1}^{d-1}\left(\dfrac{\mathrm{d}\gamma^j}{\mathrm{d}t}\right)^2 - \left(\dfrac{\mathrm{d}\gamma^d}{\mathrm{d}t}\right)^2\right\} = 0. \end{cases} \tag{2.7}$$

Those simultaneous differential equations can be solved as follows:

1. For an initial condition of special form $(x_1(0), \ldots, x_d(0)) = (a_1, \ldots, a_d)$ and $\left(\frac{\mathrm{d}x_1(0)}{\mathrm{d}t}, \ldots, \frac{\mathrm{d}x_d(0)}{\mathrm{d}t}\right) = (b_1, 0, \ldots, 0, b_d)$, and using the solution of the differential equations (2.4), we can construct solutions of (2.7) as

$$(x_1, \cdots, x_d) = (c\cos\theta - p, a_2, \ldots, a_{d-1}, c\sin\theta) \quad (c > 0, 0 < \theta < 2\pi)$$

or

$$(x_1, \cdots, x_d) = (a_1, a_2, \ldots, a_{d-1}, c) \quad (c > 0).$$

2. For the more general initial condition $(x_1(0), \ldots, x_d(0)) = (a_1, \ldots, a_d)$ and $\left(\frac{dx_1(0)}{dt}, \ldots, \frac{dx_d(0)}{dt}\right) = (b_1, b_2, \ldots, b_d)$, the simultaneous differential equations are solved by reduction to case 1.

   Consider a matrix $T = \begin{pmatrix} G & 0 \\ 0 & 1 \end{pmatrix}$, where G is a $(d-1)$-dimensional orthogonal matrix, we can translate the initial condition of case 2 into that of case 1.

   The solution is translated by the inverse of T, leading to the geodesic, as described in Lemma 2.1.

Lemma 2.1 *A geodesic on d-dimensional hyperbolic space $\mathbb{H}^d$ is expressed as*

$$(x_1 - p)^2 + {x_n}^2 = R, \; x_i = a_i \; (i = 2, \ldots, d-1) \tag{2.8}$$

or

$$x_i = a_i \; (i = 1, \ldots, d), \; x_d > 0 \tag{2.9}$$

by a transformation in the set :

$$\left\{ \begin{pmatrix} G & 0 \\ 0 & 1 \end{pmatrix} \cdot \boldsymbol{x} + \boldsymbol{a} \right\} \tag{2.10}$$

where G is $(d-1)$-dimensional orthogonal matrix, $\boldsymbol{x} = {}^t(x_1, \ldots, x_d) \in \mathbb{H}^d$, $\boldsymbol{a} = {}^t(a_1, \ldots, a_{d-1}, 0) \in \mathbb{R}^d$

Proof:

Case $(x_1 - p)^2 + {x_n}^2 = R, \; x_i = a_i \; (i = 2, \ldots, d-1)$ **:**

As G is an orthogonal transformation, the proof starts from the solution of the differential equations above.

Therefore, we consider only $\boldsymbol{a}$. However, $\boldsymbol{a}$ is a parallel displacement, which does not change the x_d-coordinate, and hence the inverse can be constructed. Thus, using these transformations, the geodesic is included in the case.

Case $x_i = a_i \; (i = 1, \ldots, d), \; x_d > 0$ **:**

The solution of this case is a particular solution of the differential equations above and is a half-line that is orthogonal to $x_d = 0$. Using a transformation as above, the geodesic is included in this case.

□

Secondly, by measuring a distance along the geodesic, the following lemma is proved.

Lemma 2.2 *For two points $p^{(1)}, p^{(2)}$ in the d-dimensional hyperbolic space, the distance of $p^{(1)}$ and $p^{(2)}$ can be expressed as*

$$d(p^{(1)}, p^{(2)}) = \frac{1}{2}\log\left(\frac{1+\cos\beta}{1-\cos\beta}\cdot\frac{1-\cos\alpha}{1+\cos\alpha}\right) \tag{2.11}$$

where α, β are constants depending on $p^{(1)}, p^{(2)}$. When $p^{(1)}, p^{(2)}$ are translated into $\tilde{p}^{(1)}(a_{11}, a_{12}, \ldots, a_{1(d-1)}, a_{1d})$ and $\tilde{p}^{(2)}(a_{21}, a_{12}, \ldots, a_{1(d-1)}, a_{2d})$, then α, β are satisfied the following equations: $c\cdot\cos\alpha - q = a_{11}$, $c\cdot\sin\alpha = a_{1d}$, $c\cdot\cos\beta - q = a_{21}$, $c\cdot\sin\beta = a_{2d}$ and $q = \dfrac{{a_{21}}^2 - {a_{11}}^2 + {a_{2d}}^2 - {a_{1d}}^2}{2(a_{21}-a_{11})}$, $c = \left\{\dfrac{-(a_{11}+a_{21})^2 + {a_{1d}}^2 - {a_{2d}}^2}{2(a_{21}-a_{11})}\right\}^2 + {a_{1d}}^2$.

Proof: Any $p^{(1)}, p^{(2)}$ can be translated into $\tilde{p}^{(1)}(a_{11}, a_{12}, \ldots, a_{1(d-1)}, a_{1d})$ and $\tilde{p}^{(2)}(a_{21}, a_{12}, \ldots, a_{1(d-1)}, a_{2d})$ by an element in the set (2.10). Thus, there is an intersection H of hyperplanes $x_i = a_{1i}$ $(i = 2, \ldots, d-1)$ leaving invariant the distance of $p^{(1)}$ and $p^{(2)}$.

Considering the restriction to H, the geodesic segment connecting two points is parameterized as

$$(x_1, \cdots, x_d) = (c\cos\theta - p, a_{12}, \cdots, a_{1(d-1)}, c\sin\theta)$$

where p, c are constants depending on $a_{11}, a_{21}, a_{1d}, a_{2d}$. The distance along the geodesic segment is

$$\begin{aligned}\int_\alpha^\beta \sqrt{\frac{\sum \mathrm{d}{x_i}^2}{{x_d}^2}} &= \int_\alpha^\beta \sqrt{\frac{\sum\left(\frac{\mathrm{d}x_i}{\mathrm{d}\theta}\right)^2}{{x_d}^2}}\mathrm{d}\theta = \int_\alpha^\beta \sqrt{\frac{1}{\sin^2\theta}}\mathrm{d}\theta \\ &= \frac{1}{2}\log\frac{1+\cos\beta}{1-\cos\beta}\cdot\frac{1-\cos\alpha}{1+\cos\alpha}\end{aligned}$$

where α, β are values of θ which depend on $\tilde{p}^{(1)}, \tilde{p}^{(2)}$. When the geodesic is expressed as $(x_1, \ldots, x_d) = (a_{11}, \ldots, a_{1(d-1)}, t)$, this lemma can be proved in a similar way. □

Now we prove that hyperbolic space is complete.

Lemma 2.3 *Hyperbolic space is complete.*

Proof: Any geodesic in hyperbolic space is a half-circle. Although it looks like a finite segment, appearances are deceptive. In this space, the distance from a point to a point on $x_d = 0$ is infinite because ${x_d}^2$ is in the denominator of the metric formula, and blows up if x_d is near to zero. In Definition 2.13, its parameter is a length, so any geodesic can be extended for arbitrarily large values. □

Using the lemma above, we can measure the distance between two points. Furthermore, we can define a sphere in the space, which is important for the construction of the *Voronoi diagram*.

Definition 2.15 *A set of points equidistant from a point $O \in \mathbb{H}^d$ is called a* hyperbolic sphere. *The point O is called the* hyperbolic center.

Lemma 2.4 *The hyperbolic sphere which has a hyperbolic center $(a_1, \ldots, a_d) \in \mathbb{H}^d$ and a radius r is expressed as follows :*

$$\sum_{i=1}^{d-1}(x_i - a_i)^2 + (x_d - a_d \cosh r)^2 = (a_d \sinh r)^2.$$

Proof: The hyperbolic center $(a_1, \ldots, a_{d-1}, a_d)$ becomes a point $(0, \ldots, 0, a_d)$ by a $(d-1)$-dimensional parallel displacement. Since the x_d-coordinate is not changed, the distance is also invariant. The restriction to the intersection of $x_i = a_i$ $(i = 2, \ldots, d-1)$, has the same structure as the Poincaré space $\mathbb{H}$.

The hyperbolic sphere with hyperbolic center (a_1, a_d) and radius r in $\mathbb{H}$ is expressed as

$$(x_1 - a_1)^2 + (x_d - a_d \cosh r)^2 = (a_d \sinh r)^2$$

as described in [40]. Moreover, equation (2.11) defines distance in the Poincaré space by that reduction.

Since the distance on $\mathbb{H}^d$ is not changed by a $(d-1)$-dimensional congruence transformation, the surface is transformed into the following:

$$\sum_{i=1}^{d-1} {x_i}^2 + (x_d - a_d \cosh r)^2 = (a_d \sinh r)^2$$

by a $(d-1)$-dimensional orthogonal transformation. The hyperbolic center $(0, \ldots, 0, a_d)$ moves to $(a_1, \ldots, a_{d-1}, a_d)$ using the inverse of the parallel displacement. □

The hyperbolic sphere has the same characteristics as the Euclidean sphere, but their centers are different. The centers are always included in the sphere.

Now we can define a *perpendicular bisector*, which is the basic element in the construction of a Voronoi diagram in hyperbolic space and expresses the proximity relations for two given points and is like a facet in $\mathbb{R}^d$.

Definition 2.16 *The set of points at the same distance from two points is called a* perpendicular bisector.

Lemma 2.5 *For two points $p^{(1)}(a_{11}, \ldots, a_{1d}), p^{(2)}(a_{21}, \ldots, a_{2d})$ in d-dimensional hyperbolic space, the perpendicular bisector can be expressed as*

$$\sum_{i=1}^{d-1}\left(x_i - \frac{a_{1d}a_{2i} - a_{2d}a_{1i}}{2(a_{1d} - a_{2d})}\right)^2 + x_d{}^2 = \sum_{i=1}^{d-1}\left\{\frac{(a_{1d}a_{2i} - a_{2d}a_{1i})^2}{4(a_{1d} - a_{2d})^2} - \frac{a_{1d}a_{2i}{}^2 - a_{2d}a_{1i}{}^2}{a_{1d} - a_{2d}}\right\} + a_{1d}a_{2d}$$

when $a_{1d} \neq a_{2d}$, and

$$\sum_{i=1}^{d-1}\left\{(a_{2i} - a_{1i})x_i + (a_{2i}{}^2 - a_{1i}{}^2)\right\} = 0$$

when $a_{1d} = a_{2d}$.

Proof: Each hyperbolic sphere C_k with hyperbolic center $p^{(k)}, (k = 1, 2)$ and radius r is expressed as

$$C_k \;:\; \sum_{i=1}^{d-1}(x_i - a_{ik})^2 + (x_d - a_{dk}\cosh r)^2 = (a_{dk}\sinh r)^2 \quad (k = 1, 2).$$

If we eliminate r from these equations, we get the equation above. □

Thus, we define a class of surfaces in hyperbolic space.

Definition 2.17 *A surface which is expressed as either*

$$\sum_{i=1}^{d-1}(x - p_i)^2 + x_d{}^2 = R^2 \tag{2.12}$$

or

$$\sum_{i=1}^{d-1} p_i x_i + p_d = 0 \tag{2.13}$$

is called a hyperbolic plane *where $p_i \in \mathbb{R}$.*

[**Remark**] The surface in Lemma 2.5 is a kind of hyperbolic plane.

Definition 2.18 *A set of points P is* non-degenerate *in the d-dimensional hyperbolic space if a hyperbolic plane is uniquely determined for any d points in P and there does not exist a hyperbolic plane including $d+1$ points in P.*

For a non-degenerate point set, the hyperbolic plane is uniquely determined.

Moreover we define a *half-space* in hyperbolic space that corresponds to half-space in Euclidean space.

Definition 2.19 *For a hyperbolic plane C, each of the two connected components C^+ and C^- of $\mathbb{H}^d \setminus C$ is called* half-space.

Although this space becomes *convex*, its proof is in Section 3.3.

2.2 Statistical Parametric Space

Statistical parametric space is defined as a parametric space of probability density function, which has the close relation to the statistical estimation. In Section 2.2 we explain its definition, example, characterizations and relation to the statistical estimation. In Section 2.2.3 we write down computations of Fisher information matrix.

2.2.1 Definitions and Examples of Statistical Parametric Space

Definition 2.20 (Statistical Parameter Space) *For a family of distributions over a domain which are determined by d real-valued parameters $[\xi_1, \ldots, \xi_d]$, the structure of this family is identified with $S = \{[\xi_1, \ldots, \xi_d] \mid [\xi_1, \ldots, \xi_d]$ corresponds one-to-one to a distribution in the family $\}$, which is called the* statistical parameter space *of this family of distributions.*

Here we define an example of a statistical parametric space, called *exponential family*, that contains the parametric space of normal distribution, Poisson distribution, etc.

Definition 2.21 (Exponential Family) *The* exponential family *is a family of probability distributions whose probability density function $p(x;\theta)$ (x is a random variable (vector in general) and θ is a parameter (vector in general) determining the distribution) is expressed as*

$$p(x;\theta) = \exp\left(C(x) + \sum_{i=1}^{d} \theta^i F_i(x) - \psi(\theta)\right)$$

for $\theta = [\theta^1, \ldots, \theta^d]$ and functions $C(x)$, $F_i(x)$ ($i = 1, \ldots, d$) of x and a function $\psi(\theta)$ of θ.

Here, since $\int p(x;\theta)\mathrm{d}x = 1$, the function ψ for each θ is determined as follows:

$$\psi(\theta) = \log \int \exp\left(C(x) + \sum_{i=1}^{n} \theta^i F_i(x)\right) \mathrm{d}x. \tag{2.14}$$

Example 2.6 *1. For the one-dimensional normal distribution the probability density function with mean μ and standard deviation σ is $p(x;\theta)$ of type in the exponential family with*

$$C(x) = 0,\ F_1(x) = x,\ F_2(x) = x^2,$$
$$\theta^1 = \frac{\mu}{\sigma^2},\ \theta^2 = -\frac{1}{2\sigma^2},$$
$$\psi(\theta) = \frac{\mu^2}{2\sigma^2} + \log(\sqrt{2\pi}\sigma) = -\frac{(\theta^1)^2}{4\theta^2} + \frac{1}{2}\log\left(-\frac{\pi}{\theta^2}\right)$$

2. *For the one-dimensional Poisson distribution the probability density function is* $e^{-\xi}\frac{\xi^x}{x!}$ *with random variable* x *on* $\{0, 1, 2, \cdots\}$ *with parameter space* $\{\xi \mid \xi > 0\}$. *For this distribution.* $C(x) = -\log x!$, $F(x) = x$, $\theta = \log \xi$, $\psi(\theta) = \xi = e^{\theta}$.

3. *For the distribution on a finite set* $\{x_0, x_1, \ldots, x_d\}$, *the probability that* x_i *occurs is* ξ_i *with parameter space* $\{[\xi_1, \ldots, \xi_d] \mid \xi_i > 0, \sum_{i=1}^{d} \xi_i < 1\}$. *For this distribution,* $C(x) = 0$, $F_i(x) = 1$ *when* $x = x_i$ *and 0 when* $x \neq x_i$, $\theta^i = \log \frac{\xi_i}{1 - \sum_{j=1}^{d} \xi_j}$ *and* $\psi(\theta) = \log\left(1 + \sum_{i=1}^{d} \exp \theta^i\right)$.

The statistical parametric space, however, is only a parametric space of probability distribution. Since we want to regard this space as Riemannian space, we use a *metric* called the *Fisher information matrix*, which is famous in statistics. This idea was first considered in [44].

Definition 2.22 (Fisher information matrix) *For continuous probability density function* $p(x;\xi)$, *the element of the matrix*

$$g_{ij} = \int \frac{\partial}{\partial \xi_i} \log p(x;\xi) \cdot \frac{\partial}{\partial \xi_j} \log p(x;\xi) \cdot p(x;\xi) \mathrm{d}x,$$

and $(g_{ij})_{i,j=1,\ldots,d}$ *is called the* Fisher information matrix.

For a discrete probability density function, this matrix is defined like this:

$$g_{ij} = \sum_x \frac{\partial}{\partial \xi_i} \log p(x;\xi) \cdot \frac{\partial}{\partial \xi_j} \log p(x;\xi) \cdot p(x;\xi).$$

This matrix is related to the error of estimation [11], i.e., the matrix gives a bound of squared error of any unbiased estimator. For various distributions this matrix is computed in Section 2.2.3.

The Fisher information matrix can be regarded as a Riemannian metric,

$$\mathrm{d}s^2 = (\mathrm{d}\xi_1, \ldots, \mathrm{d}\xi_d) \cdot \{g_{ij}\} \cdot \begin{pmatrix} \mathrm{d}\xi_1 \\ \vdots \\ \mathrm{d}\xi_d \end{pmatrix},$$

and with this metric $\mathrm{d}s^2$, called the *Fisher metric*, the statistical parameter space can be considered a Riemannian space $(R, g) = (\xi, \mathrm{d}s^2)$.

Definition 2.23 (**α-Connection [3]**) *Let $R = \{p_\xi\}$ be a d-dimensional statistical parametric space with Fisher metric g. For any real number α the following functions are defined:*

$$\left(\Gamma^{(\alpha)}_{ij,k}\right)_\xi = \int \left(\partial_i\partial_j \log p_\xi + \frac{1-\alpha}{2}\partial_i \log p_\xi \partial_j \log p_\xi\right) \cdot (\partial_k \log p_\xi) \cdot p_\xi \mathrm{d}x. \qquad (2.15)$$

These functions are α-connection $\nabla^{(\alpha)}$ *on R.*

In particular, $\nabla^{(1)}$ *is called* exponential connection $\nabla^{(e)}$ *and* $\nabla^{(-1)}$ *is called* mixture connection $\nabla^{(m)}$.

The metric g is smooth and symmetric, hence Levi-Civita connection (Definition 2.10) can be introduced in the statistical parametric space. For example, the statistical parametric space of a normal distribution is equal to a Poincaré space as a Riemannian manifold if the Levi-Civita connection is introduced. In [31], however, α-connection is introduced because $\nabla^{(\alpha)}$-connection has a close relation to statistical estimation. That relation is described in Section 2.2.2. In this thesis the *α-connection* is used as a connection of such a parametric space.

The following lemmas about the exponential family were proved in [3].

Lemma 2.6 (**[3]**) *The exponential family is $\nabla^{(e)}$-flat.*

Lemma 2.7 (**[3]**) *The following is equivalent for a statistical parametric space R with Fisher metric g:*

- *$\nabla^{(\alpha)}$-connection is flat (R is $\nabla^{(\alpha)}$-flat).*
- *$\nabla^{(-\alpha)}$-connection is flat (R is $\nabla^{(-\alpha)}$-flat).*

If e- and m-connection are introduced in the exponential family R with Fisher metric g, then that becomes *dually flat space*. There is an *affine coordinate system* in flat space. Since this space has two flat connections, there are two coordinate systems: the *natural parameter* $[\theta]$ and the *expectation parameter* $[\eta], \eta_i = \int F_i(x)p(x;\theta)dx$, which correspond to exponential and mixture connections, respectively.

2.2.2 Statistical Estimation

We state the relation between the maximum likelihood estimation and these connections. First we explain the *statistical estimation*, more details of which are in [1, 29]. Statistical estimation finds information of unknown probability density function from observed values in the probabilistic space. When let $x_{(1)}, \ldots, x_{(n)}$ be independent observed value of stochastic vector by a probability function, it is a statistical estimator to give the parameters ξ of original function $p(x;\xi)$ by $x^{(n)} = (x_{(1)}, \ldots, x_{(n)})$.

Definition 2.24 *Let $p_{(n)}(x^{(n)};\xi) = \prod_{i=1}^{n} p(x_{(i)}, \xi)$. We consider $p_{(n)}(x^{(n)};\xi)$ as a function of the parameter ξ, and call it* **likelihood function**. *The value of ξ maximizing this function is called the* maximum likelihood estimator, *and maximize $p_{(n)}(x^{(n)};\xi)$ at $\hat{\xi}$. That is*

$$\max_{\xi} p_{(n)}(x^{(n)};\xi) = p_{(n)}(x^{(n)};\hat{\xi})$$

where $p_{(n)}(x^{(n)};\xi)$ is a probability density function of $x^{(n)}$. Such estimation is called maximum likelihood estimation.

For example, we consider the maximum likelihood estimation of the exponential family (Definition 2.21) is considered, setting $C(x) \equiv 0$ and $x_i := F_i(x)$. Then the probability density function becomes

$$p(x;\theta) = \exp\left(\sum_{i=1}^{d} \theta^i x_i - \psi(\theta)\right).$$

Since each x_i is independent, $p_{(n)}(x^{(n)};\theta)$ becomes

$$p_{(n)}(x^{(n)};\theta) = \prod_{i=1}^{n} p(x_{(i)};\theta) = \exp\left[\sum_{j=1}^{d} n\left\{\theta^j \bar{x}_j - \psi(\theta)\right\}\right] \tag{2.16}$$

where

$$\bar{x} = \frac{1}{n}\sum_{i=1}^{n} x_{(i)}. \tag{2.17}$$

In statistical parametric space with θ-coordinate system if consider the problem that a maximized problem of equation (2.16). By differentiation we obtain

$$\bar{x}_i = \partial\psi(\theta) = \eta_i.$$

Therefore the maximum likelihood estimator is given in η-coordinate system of the statistical parametric space of the exponential family. That is, this estimation for exponential family is $\bar{x}$ and we need only compute its θ-coordinate expression $\theta = \theta(\eta(\bar{x}))$.

2.2.3 Fisher Information Matrix

In this section some results of computation of Fisher information matrix. That matrix has a relation with an error bound of the statistical estimation and is regarded as Riemannian metric ([44, 1]). Since we cannot find their calculations, such matrices are computed for various distributions. In addition, we state some computations and some acquired knowledge in this section.

Firstly we prove an equation about Fisher information matrix.

Lemma 2.8 ([1]) *Let $\{g_{ij}\}$ be a Fisher metric. The following equation is proved.*

$$g_{ij} = -\int \left\{ \frac{\partial^2}{\partial \xi_i \partial \xi_j} \log p(x;\xi) \right\} \cdot p(x;\xi) \mathrm{d}x.$$

Proof: Suppose an exchange of the order among differentiation and integration. These equations are shown.

$$\int \frac{\partial}{\partial \xi_i} p(x;\xi)\mathrm{d}x = \frac{\partial}{\partial \xi_i} \int p(x;\xi)\mathrm{d}x = \frac{\partial}{\partial \xi_i} 1 = 0.$$

$$0 = \int \frac{\partial}{\partial \xi_i} p(x;\xi)\mathrm{d}x = \int \frac{\frac{\partial p(x;\xi)}{\partial \xi_i}}{p(x;\xi)} \cdot p(x;\xi)\mathrm{d}x = \int \frac{\partial \log p(x;\xi)}{\partial \xi_i} \cdot p(x;\xi)\mathrm{d}x.$$

Each side of this equation differentiate partially $\partial/\partial \xi_j$.

$$0 = \int \left\{ \frac{\partial^2}{\partial \xi_i \partial \xi_j} \log p(x;\xi) \right\} p(x;\xi)\mathrm{d}x + \int \frac{\partial \log p(x;\xi)}{\partial \xi_i} \cdot \frac{\partial p(x;\xi)}{\partial \xi_j} \mathrm{d}x$$

The former part becomes right-hand member and the latter is equal to the definition of g_{ij}. Above equation is proved. □

[Remark] This equation is shown for discrete Fisher information matrix. In such a case, the integration is replaced with the summation. Since this equation is so useful to compute Fisher information matrix, we use this equation in this section.

One-dimensional Continuous Distribution

Here, we describe the calculation of Fisher information matrix for one-dimensional continuous distributions, i.e., uniform, normal, gamma, beta, Cauchy, F, inverse gamma, Pareto and Weibull distributions.

Uniform distribution : The probability density function is expressed by

$$p(x; a, b) = \frac{1}{b-a} I_{(a,b)}(x)$$

where $I_{(a,b)}(x) = 1$ if $x \in (a, b)$ and $= 0$ if $x \notin (a, b)$, called characteristic function. Thus we consider a subspace of 2-dimensional Euclidean space as follows :

$$\{(a, b) \mid a, b \in \mathbb{R},\ a < b\}.$$

The Fisher information matrix g becomes

$$g = \frac{1}{(b-a)^2} \begin{pmatrix} 1 & -1 \\ -1 & 1 \end{pmatrix}.$$

Normal distribution : The normal distribution is already defined in Example 2.6. Its parametric space is

$$\{(\mu, \sigma) \mid \mu, \sigma \in \mathbb{R}, \sigma > 0\}$$

and Fisher information matrix becomes

$$g = \frac{1}{\sigma^2} \begin{pmatrix} 1 & 0 \\ 0 & 2 \end{pmatrix}.$$

This space can be regard as Poincaré space. The different between this space and Poincaré space is the introduced *connection*. The former has exponential and mixture connections, the latter has Levi-Civita connection.

Gamma distribution : The probability density function is expressed by

$$p(x; \alpha, \beta) = \frac{1}{\Gamma(\alpha)} \left(\frac{x}{\beta}\right)^{\alpha-1} \exp\left(-\frac{x}{\beta}\right) \frac{1}{\beta} I_{(0,\infty)}(x),$$

where $\alpha > 0$, $\beta > 0$ and $\Gamma(\alpha)$ is gamma function and is defined as follows :

$$\Gamma(\alpha) := \int_0^\infty x^{\alpha-1} e^{-x} \mathrm{d}x.$$

We state some properties of the gamma function :

- $\Gamma(1) = \Gamma(2) = 1$,
- $\Gamma(1/2) = \sqrt{\pi}$,
- $\Gamma(\alpha + 1) = \alpha\Gamma(\alpha)$,

- $\Gamma(\alpha+1) = \alpha!$ where α is a positive integer.

The statistical parametric space is

$$\{(\alpha, \beta) \mid \alpha, \beta \in \mathbb{R},\ \alpha > 0, \beta > 0\}.$$

The Fisher information matrix becomes like this :

$$g = \begin{pmatrix} -\partial_1\partial_1 \log p & \frac{1}{\beta} \\ \frac{1}{\beta} & \frac{\alpha}{\beta^2} \end{pmatrix}$$

where

$$\partial_1\partial_1 \log p(x; \alpha, \beta) = -\frac{\Gamma(\alpha)'' \cdot \Gamma(\alpha) - \{\Gamma(\alpha)'\}^2}{\Gamma(\alpha)^2}.$$

The $'$ and $''$ represent differentiation and quadric by α, respectively.

Beta distribution : The probability density function is expressed by two positive real numbers p, q

$$p(x; \xi) = \frac{1}{B(p,q)} x^{p-1}(1-x)^{q-1} I_{(0,1)}(x)$$

where $\xi = [\xi_i] = [p, q]$, $B(p, q)$ is the beta function and defined like this :

$$B(p,q) = \int_0^1 x^{p-1}(1-x)^{q-1}\mathrm{d}x \quad (p > 0, q > 0).$$

The Fisher information matrix is

$$\begin{pmatrix} -\partial_1\partial_1 l_\xi & -\partial_1\partial_2 l_\xi \\ -\partial_1\partial_2 l_\xi & -\partial_2\partial_2 l_\xi \end{pmatrix}$$

where

$$\begin{aligned} \partial_1\partial_1 l_\xi &= \frac{-\{\partial_1\partial_1 B(p,q)\}B(p,q) + \{\partial_1 B(p,q)\}^2}{B(p,q)^2}, \\ \partial_1\partial_2 l_\xi &= \frac{-\{\partial_1\partial_2 B(p,q)\}B(p,q) + \partial_1 B(p,q) \cdot \partial_2 B(p,q)}{B(p,q)^2}, \\ \partial_2\partial_2 l_\xi &= \frac{-\{\partial_2\partial_2 B(p,q)\}B(p,q) + \{\partial_2 B(p,q)\}^2}{B(p,q)^2}, \end{aligned}$$

$$\partial_1 B(p,q) = \int_0^1 x^{p-1}(1-x)^{q-1} \log x \mathrm{d}x,$$

$$
\begin{aligned}
\partial_2 B(p,q) &= -\int_0^1 x^{p-1}(1-x)^{q-1}\log(1-x)\mathrm{d}x,\\
\partial_1\partial_1 B(p,q) &= \int_0^1 x^{p-1}(1-x)^{q-1}(\log x)^2\mathrm{d}x,\\
&= \frac{\Gamma(p)\cdot\Gamma(q)}{\Gamma(p+q)}\left[\{Poly\Gamma(0,p)-Poly\Gamma(0,p+q)\}^2+Poly\Gamma(1,p)-Poly\Gamma(1,p+q)\right]\\
\partial_1\partial_2 B(p,q) &= -\int_0^1 x^{p-1}(1-x)^{q-1}\log x\log(1-x)\mathrm{d}x,\\
\partial_2\partial_2 B(p,q) &= \int_0^1 x^{p-1}(1-x)^{q-1}\{\log(1-x)\}^2\mathrm{d}x
\end{aligned}
$$

and $Poly\Gamma(n,x)$ is nth differentiation of $\dfrac{\mathrm{d}\log\Gamma(x)}{\mathrm{d}x}$.

Cauchy distribution : The probability density function is expressed by a real number α and a positive real number β as

$$p(x;\alpha,\beta)=\frac{1}{\pi}\left\{1+\left(\frac{x-\alpha}{\beta}\right)^2\right\}^{-1}\cdot\frac{1}{\beta}\quad(x\in\mathbb{R}).$$

This distribution is called Cauchy distribution and written by Cauchy(α,β).

The Fisher information matrix becomes like this :

$$g=\begin{pmatrix}\dfrac{1}{2\beta^2} & 0\\ 0 & \dfrac{3}{2\beta^2}\end{pmatrix}.$$

This matrix is much similar to the matrix of one-dimensional normal distribution. The statistical parametric space of Cauchy distribution is regarded as the space of one-dimensional normal distribution.

F distribution : The probability density function is expressed by positive real numbers ν_1,ν_2 as

$$p(x;\nu_1,\nu_2)=\frac{1}{B\left(\frac{\nu_1}{2},\frac{\nu_2}{2}\right)}\left(\frac{\nu_1}{\nu_2}x\right)^{\frac{\nu_1}{2}-1}\left(1+\frac{\nu_2}{\nu_1}x\right)^{-\frac{\nu_1+\nu_2}{2}}\frac{\nu_1}{\nu_2}I_{(0,\infty)}(x).$$

This distribution is called F *distribution.*

$$
\begin{aligned}
\partial_1\partial_1 f &= \partial_1\left\{-\frac{\partial_1 B(\nu_1/2,\nu_2/2)}{B(\nu_1/2,\nu_2/2)}\right\}-\frac{\nu_2}{\nu_1}\cdot\frac{\nu_2-x^2\nu_1}{(\nu_2+\nu_1x)^2}\\
\partial_1\partial_2 f=\partial_2\partial_1 f &= \partial_2\left\{-\frac{\partial_1 B(\nu_1/2,\nu_2/2)}{B(\nu_1/2,\nu_2/2)}\right\}-\frac{\nu_2-x^2\nu_1}{(\nu_2+\nu_1x)^2}\\
\partial_1\partial_1 f &= \partial_1\left\{-\frac{\partial_1 B(\nu_1/2,\nu_2/2)}{B(\nu_1/2,\nu_2/2)}\right\}-\frac{\nu_1}{\nu_2}\cdot\frac{\nu_2-x^2\nu_1}{(\nu_2+\nu_1x)^2}
\end{aligned}
$$

By these equations we can get Fisher information matrix $g_{ij} = -\int \partial_i \partial_j \log p \cdot p \cdot dx$.

Inverse gamma distribution : When the random variable z follows gamma distribution, the distribution by the random variable $x = z^{-1}$ is called *inverse gamma distribution*. The probability density function becomes

$$p(x; \alpha, \beta) = \frac{1}{\Gamma(\alpha)} \left(\frac{1}{\beta x}\right)^{\alpha-1} \exp\left(-\frac{1}{\beta x}\right) \frac{1}{\beta x^2} I_{(0,\infty)}(x).$$

Moreover the Fisher information matrix is

$$g = \begin{pmatrix} -Poly\Gamma(1, \alpha) & \frac{1}{\beta} \\ \frac{1}{\beta} & \frac{\alpha}{\beta^2} \end{pmatrix}.$$

This matrix is equal to the gamma distribution.

Pareto distribution : By $\alpha > 1$ and $\beta > 0$ the probability density function is expressed as

$$p(x; \alpha, \beta) = (\alpha - 1) \left(\frac{x}{\beta}\right)^{-\alpha} \frac{1}{\beta} I_{(\beta,\infty)}(x)$$

which is called *Pareto distribution*.

The Fisher information matrix becomes

$$g = \begin{pmatrix} \frac{1}{(\alpha-1)^2} & -\frac{1}{\beta} \\ -\frac{1}{\beta} & \frac{\alpha-1}{\beta^2} \end{pmatrix}.$$

Weibull distribution : The probability density function is expressed by a positive real numbers α, β as

$$p(x; \alpha, \beta) = \alpha \left(\frac{x}{\beta}\right)^{\alpha-1} \exp\left(-\left(\frac{x}{\beta}\right)^{\alpha}\right) \frac{1}{\beta} I_{(0,\infty)}(x).$$

This distribution is called *Weibull distribution*.

The matrix becomes

$$\begin{pmatrix} (12C + 6C^2 + \pi + 12\alpha \log \beta - 12\alpha C \log \beta + 6\alpha^2(\log \beta)^2 + 6)/6\alpha^2 & (\alpha \log \beta - C)/\beta \\ (\alpha \log \beta - C)/\beta & \alpha^2/\beta \end{pmatrix}$$

where $C = \lim_{n\to\infty} \left(1 + \frac{1}{2} + \cdots + \frac{1}{n} - \log n\right) \simeq 0.577216\cdots$ is Euler number.

Some Fisher information matrices of one-dimensional continuous distribution are computed. We arrange the acquired knowledge by computation.

- Fisher information matrices for uniform distribution, normal distribution, Cauchy distribution, Pareto distribution and Weibull distribution are calculated. The others is partly computed.
- Parametric space of gamma distribution is equal to the space of inverse gamma distribution as a Riemannian space. It is not need to classify the parametric space of gamma distribution and of inverse gamma distribution as a Riemannian space.
- Parametric space of one-dimensional normal distribution is also equal to the space of Cauchy distribution as a Riemannian space. These spaces are regarded as the same.
- The matrix of Pareto distribution is easy to deal with, that is a nice space to study geometric objects.

Higher-dimensional Continuous Distribution

Moreover d-dimensional normal distribution is considered. The probability density function is expressed as

$$p(x;\xi) = 2\pi^{-d/2}|\Sigma|^{-1/2}\exp\left\{-\frac{1}{2}{}^t(x-\mu)\Sigma^{-1}(x-\mu)\right\}$$

where x is a d-dimensional stochastic vector, $\mu \in \mathbb{R}^d$ is a means vector and Σ is a variance-covariance matrix, which is positive definite and symmetric. General case of this distribution is so difficult, we deal with a special case, i.e., variance-covariance matrix is equal to $\sigma^2 I_d$. In this case the Fisher information matrix becomes

$$g = \begin{pmatrix} \sigma^{-2} & 0 & \cdots & 0 \\ 0 & \ddots & \cdots & \vdots \\ \vdots & \vdots & \sigma^{-2} & 0 \\ 0 & \cdots & 0 & 2d\sigma^{-2} \end{pmatrix}.$$

Thus this parametric space is regarded as $(d+1)$-*dimensional hyperbolic space*, which is described in Section 2.1.2. The geometry changes by what connection is introduced.

In addition, for general two-dimensional normal distribution Fisher information matrix is computed. The parametric space of that distribution is expressed as $\xi = [\xi_i] = [\mu_1, \mu_2, \sigma_1, \sigma_2, \sigma_{12}]$, $\Sigma = \begin{pmatrix} {\sigma_1}^2 & {\sigma_{12}}^2 \\ {\sigma_{12}}^2 & {\sigma_2}^2 \end{pmatrix}$, $|\Sigma| = {\sigma_1}^2{\sigma_2}^2 - {\sigma_{12}}^4$.

Its Fisher information matrix becomes

$$\begin{pmatrix} {\sigma_2}^2/|\Sigma| & -{\sigma_{12}}^2/|\Sigma| & 0 & 0 & 0 \\ -{\sigma_{12}}^2/|\Sigma| & {\sigma_1}^2/|\Sigma| & 0 & 0 & 0 \\ 0 & 0 & 2{\sigma_1}^2{\sigma_2}^4/|\Sigma|^2 & 2\sigma_1\sigma_2{\sigma_{12}}^4/|\Sigma|^2 & -4\sigma_1{\sigma_2}^2{\sigma_{12}}^3/|\Sigma|^2 \\ 0 & 0 & 2\sigma_1\sigma_2{\sigma_{12}}^4/|\Sigma|^2 & 2{\sigma_1}^4{\sigma_2}^2/|\Sigma|^2 & -4{\sigma_1}^2\sigma_2{\sigma_{12}}^3/|\Sigma|^2 \\ 0 & 0 & -4\sigma_1{\sigma_2}^2{\sigma_{12}}^3/|\Sigma|^2 & -4{\sigma_1}^2\sigma_2{\sigma_{12}}^3/|\Sigma|^2 & 4{\sigma_{12}}^2({\sigma_1}^2{\sigma_2}^2 + {\sigma_{12}}^4)/|\Sigma|^2 \end{pmatrix}.$$

These distributions are a kind of multivariate normal distribution. For general multivariate normal distribution Fisher information matrix can be computed as same as two-dimensional case.

Discrete Distribution

In this section we describe the calculation of Fisher information matrix of discrete distributions, i.e., binomial, Poisson, negative binomial, hypergeometric and negative hypergeometric distribution.

Binomial distribution : For a positive real number n and a real number p $(0 < p < 1)$, the probability density function is expressed as

$$p(x; n, p) = \begin{pmatrix} n \\ x \end{pmatrix} p^x (1-p)^{n-x}$$

where $x = 0, 1, \ldots, n$.

The Fisher information matrix becomes

$$\begin{aligned} g_{11} &= \sum_{x=1}^{n} (\partial_1 \log p(x; n, p))^2 \cdot p(x; n, p), \\ g_{12} = g_{21} &= \sum_{x=1}^{n} \partial_1 \log p(x; n, p) \cdot \partial_2 \log p(x; n, p) \cdot p(x; n, p) = \frac{1}{1-p}, \\ g_{22} &= \sum_{x=1}^{n} (\partial_2 \log p(x; n, p))^2 \cdot p(x; n, p). \end{aligned}$$

The $g_{12} = g_{21}$ can be computed but otherwise cannot.

Poisson distribution : The Poisson distribution is already defined in Example 2.6. The Fisher information matrix becomes

$$g_{11} = \sum_{x=0}^{\infty} - \left(-\frac{x}{\lambda^2}\right) \cdot e^{-\lambda}\frac{\lambda^x}{x!} = \frac{e^{-\lambda}}{\lambda}\left\{\frac{\lambda^{-1}}{(-1)!} + e^{\lambda}\right\} = \frac{e^{-\lambda}}{\lambda^2(-1)!} + \frac{1}{\lambda}.$$

Negative binomial distribution : For a positive integer r and a real number p $(0 < p < 1)$, the probability density function becomes

$$p(x;r,p) = \begin{pmatrix} r+x-1 \\ x \end{pmatrix} p^r(1-p)^x \quad (x = 0, 1, 2, \cdots)$$

which is called *negative binomial distribution*. Its Fisher information matrix becomes

$$\begin{aligned} g_{11} &= \sum_{x=1}^{\infty}(\partial_1 \log p(x;r,p))^2 \cdot p(x;r,p), \\ g_{12} = g_{21} &= \sum_{x=1}^{\infty} \partial_1 \log p(x;r,p) \cdot \partial_2 \log p(x;r,p) \cdot p(x;r,p) = -\frac{1}{p}, \\ g_{22} &= \sum_{x=1}^{\infty}(\partial_2 \log p(x;r,p))^2 \cdot p(x;r,p). \end{aligned}$$

The $g_{12} = g_{21}$ can be calculated but the others cannot.

Hypergeometric distribution : For positive integers n, N $(n \leq N)$ and a rational number p $(0 < p < 1)$ such that Np is an integer the probability density function is expressed as

$$p(x;n,p,N) = \frac{\begin{pmatrix} Np \\ x \end{pmatrix}\begin{pmatrix} N(1-p) \\ n-x \end{pmatrix}}{\begin{pmatrix} N \\ n \end{pmatrix}}$$

which is called *hypergeometric distribution* and $x = 0, \ldots, n$. By $q = Np$ above equation is rewritten like this

$$p(x;n,N,q) = \frac{\begin{pmatrix} q \\ x \end{pmatrix}\begin{pmatrix} N-q \\ n-x \end{pmatrix}}{\begin{pmatrix} N \\ n \end{pmatrix}}.$$

$$
\begin{aligned}
\partial_1 p(x;n,N,q) &= -\frac{\partial_1\Gamma(N-q-n+x+1)}{\Gamma(N-q-n+x+1)} - \frac{\partial_1\Gamma(n-x+1)}{\Gamma(n-x+1)} + \frac{\partial_1\Gamma(N-n+1)}{\Gamma(N-n+1)} + \frac{\partial_1\Gamma(n+}{\Gamma(n+1} \\
\partial_2 p(x;n,N,q) &= \frac{\partial_2\Gamma(N-q+1)}{\Gamma(N-q+1)} - \frac{\partial_2\Gamma(N-q-n+x+1)}{\Gamma(N-q-n+x+1)} - \frac{\partial_2\Gamma(N+1)}{\Gamma(N+1)} + \frac{\partial_2\Gamma(N-n+1}{\Gamma(N-n+1)} \\
\partial_3 p(x;n,N,q) &= \frac{\partial_3\Gamma(q+1)}{\Gamma(q+1)} - \frac{\partial_3\Gamma(q-x+1)}{\Gamma(q-x+1)} + \frac{\partial_3\Gamma(N-q+1)}{\Gamma(N-q+1)} - \frac{\partial_3\Gamma(N-q-n+x+1)}{\Gamma(N-q-n+x+1)}
\end{aligned}
$$

However the x retain in the quadratic differential, the Fisher information cannot be computed.

Negative hypergeometric distribution : For a positive integer N and a positive rational number p $(0 < p < 1)$ such that Np is an integer and a positive integer r $(r \leq Np)$ the probability density function is expressed as

$$
p(x;r,p,N) = \frac{1}{\begin{pmatrix} N \\ Np \end{pmatrix}} \begin{pmatrix} x+r-1 \\ x \end{pmatrix} \begin{pmatrix} N-x+r \\ Np-r \end{pmatrix} \quad (x = 0, 1, \cdots, N(1-p))
$$

which is called *negative hypergeometric distribution*. By $q = Np$ and the gamma function this function is rewritten

$$
\begin{aligned}
\log p(x;r,N,q) &= \log\Gamma(N-q+1)\Gamma(q+1)\Gamma(x+r)\Gamma(N-x-r+1) \\
&\quad -\log\Gamma(N+1)\Gamma(r)\Gamma(x+1)\Gamma(N-x-q+1)\Gamma(q-r+1).
\end{aligned}
$$

This function differentiate partially in the coordinate system $[\xi] = [r, q, N]$ $(r \leq q)$.

$$
\begin{aligned}
\partial_1 \log p &= \frac{\partial_1\Gamma(x+r)}{\Gamma(x+r)} + \frac{\partial_1\Gamma(N-x-r+1)}{\Gamma(N-x-r+1)} - \frac{\partial_1\Gamma(r)}{\Gamma(r)} - \frac{\partial_1\Gamma(q-r+1)}{\Gamma(q-r+1)}, \\
\partial_2 \log p &= \frac{\partial_2\Gamma(N-q+1)}{\Gamma(N-q+1)} + \frac{\partial_2\Gamma(q+1)}{\Gamma(q+1)} - \frac{\partial_2\Gamma(N-x-q+1)}{\Gamma(N-x-q+1)} - \frac{\partial_2\Gamma(q-r+1)}{\Gamma(q-r+1)}, \\
\partial_3 \log p &= \frac{\partial_3\Gamma(N-q+1)}{\Gamma(N-q+1)} + \frac{\partial_3\Gamma(N-x-r+1)}{\Gamma(N-x-r+1)} - \frac{\partial_3\Gamma(N+1)}{\Gamma(N+1)} - \frac{\partial_3\Gamma(N-x-q+1)}{\Gamma(N-x-q+1)}.
\end{aligned}
$$

However the matrix cannot be calculated.

Some Fisher information matrices of discrete distribution are calculated. Here, we state some knowledge.

- Fisher information matrix for Poisson distribution is computed. The others is partly done.

- There are no good distribution for research. The parametric space of Poisson distribution is one dimension and is included in the exponential family (Example 2.6).

- The parametric space of all discrete distribution in a certain dimension becomes $\nabla^{(e)}$- and $\nabla^{(m)}$-flat ([3]). In this section we consider its submanifold however these spaces do not have so nice properties, i.e., the discrete distribution must be treated as one manifold.

2.3 Dually Flat Space

This section describes *dually flat space* ([1, 3]), which is a kind of Riemannian space and includes *statistical parametric space* [1], *feasible region of linear programming* [51], *parametric family of invertible linear system* [2], etc.. We define this space and give some examples. We also explain the two coordinate system, the potential functions and divergences in this space. These concepts are extensions of the corresponding concepts applicable to Euclidean space, and there is also an extension of the Pythagorean theorem (Theorem 2.2).

2.3.1 Definitions and Examples of Dually Flat Space

Definition 2.25 (Dually Flat Space) *Let (R, g) be a Riemannian space with two affine connections ∇, ∇^*. The 4-tuple (R, g, ∇, ∇^*) is a* dually flat space *if the Riemannian space satisfies the following conditions:*

- *For $\forall X, Y, Z$ vector field of R*

$$Z\langle X, Y\rangle = \langle \nabla_Z X, Y\rangle + \langle X, \nabla^*_Z Y\rangle. \tag{2.18}$$

  The connections ∇ and ∇^* are dual *about g if they satisfy this condition.*

- *∇ and ∇^* is flat.*

[Remark] If the $\nabla = \nabla^*$ then the condition (2.18) becomes the condition of metrical connection [24]. Thus this dual condition is a natural extension of metrical connection. In the other words, metrical connection is self-dual.

Example 2.7 (Euclidean Space) *Let $R = \mathbb{R}^d$ be a Riemannian space with a metric $g = I_d$. In this case the connection ∇ and ∇^* is the same and self-dual. This space is called d-dimensional Euclidean space.*

Example 2.8 (Statistical Parametric Space of One-dimensional Normal Distributions) *Let $R = [\mu, \sigma](\sigma > 0)$ be a Riemannian space with Riemannian metric $g = \frac{1}{\sigma^2}\begin{pmatrix} 1 & 0 \\ 0 & 2 \end{pmatrix}$. This space is the parameter space of the normal distribution. That is, the normal distribution is given like this:*

$$p(x;\xi) = \frac{1}{\sqrt{2\pi}\sigma}\exp\left\{-\frac{(x-\mu)^2}{2\sigma^2}\right\} \qquad (2.19)$$

The parametric space $[\xi] = [\mu, \sigma]$ has the metric which is called the Fisher information matrix (Definition 2.22). This space becomes dually flat space by introducing e-connection *and* m-connection *(Definition 2.23).*

Example 2.9 (Statistical Parametric Space of the Exponential Family) *The probability density function is already defined in Definition 2.21. Its Fisher information matrix becomes*

$$g_{ij} = \frac{\partial^2}{\partial\theta^i\partial\theta^j}\psi(\theta)$$

where $\psi(\theta)$ is given by equation (2.14). In this space exponential *and* mixture connections *are also introduced.*

By a coordinate system $[\xi]$ the condition (2.18) becomes

$$\partial_k g_{ij} = \Gamma_{ki,j} + \Gamma^*_{kj,i}$$

where $\Gamma_{ij,k} = \sum_h \Gamma^h_{ij} g_{hk}$ and $\Gamma^*_{ij,k} = \sum_h \Gamma^{h*}_{ij} g_{hk}$. $\Gamma^k_{ij}, \Gamma^{k*}_{ij}$ are respectively the connection coefficients for ∇ and ∇^*.

Since the dually flat space is flat, there exist affine coordinate systems such that $\Gamma^i_{jk}, \Gamma^{i*}_{jk} \equiv 0$. The one for ∇-connection is called θ-coordinate, and the one for ∇^*-connection is called η-coordinate. These coordinates are called a *dual coordinate system* if this condition is satisfied:

$$\left\langle \frac{\partial}{\partial\theta^i}, \frac{\partial}{\partial\eta_j} \right\rangle = \delta^j_i.$$

[Remark] In this paper we use the following notations: $\partial_i = \dfrac{\partial}{\partial\theta^i}, \partial^j = \dfrac{\partial}{\partial\eta_j}$.

Example 2.10 (Dual Coordinates) *1. For Euclidean space the dual coordinate systems are $\theta^i = \eta_i$.*

2. For the parametric space of one-dimensional normal distributions the dual coordinate systems become

$$[\theta^1, \theta^2] = \left[\frac{\mu}{\sigma^2}, -\frac{1}{2\sigma^2}\right], \quad [\eta_1, \eta_2] = \left[\mu, \mu^2 + \sigma^2\right].$$

3. For the parametric space of the exponential family its dual coordinate systems become

$$[\theta^1, \ldots, \theta^d], \; \eta_i = \int F_i(x) p(x;\theta) \mathrm{d}x,$$

these coordinate systems are called natural parameter *and* expectation parameter, *respectively.*

Let $\psi, \varphi : R \to \mathbb{R}$ be functions such that

$$\partial_i \psi = \eta_i, \quad \partial^j \varphi = \theta^j. \tag{2.20}$$

Those differential equations can be solved if $\partial_i \eta_j = \partial_j \eta_i, \partial^i \theta^j = \partial^j \theta^i$. In this paper we suppose these conditions. By this assumption the differential equations above have solutions. Moreover these functions are convex in Euclidean space because the quadratic differentiations of these functions is the metric of Riemannian space and the metric is a positive definite matrix.

Thus the following equations are proved:

$$\partial_i \partial_j \psi = g_{ij}, \quad \partial^i \partial^j \psi = g^{ij}, \tag{2.21}$$

$$\psi + \varphi - \sum_i \theta^i \eta_i = 0, \tag{2.22}$$

where g_{ij} is an expression of g in the θ-coordinate system and g^{ij} is in the η-coordinate system. The transformation defined by equation (2.20) and (2.22) is a *Legendre transformation* and the functions ψ and φ are called *potential functions.*

Example 2.11 (Potential Functions) *1. For Euclidean space the potential functions become*

$$\psi = \varphi = \frac{1}{2} \sum (\theta^i)^2.$$

Therefore it is also stated that Euclidean space is self-dual.

2. *For the parametric space of normal distribution, the potential functions become*

$$\begin{aligned} \psi &= \frac{\mu^2}{2\sigma^2} + \log(\sqrt{2\pi}\sigma) &= -\frac{(\theta^1)^2}{4\theta^2} + \frac{1}{2}\log\left(-\frac{\pi}{\theta^2}\right), \\ \varphi &= -\log(\sqrt{2\pi}\sigma) - \frac{1}{2}. \end{aligned}$$

3. *For the statistical parametric space of the exponential family, the potential functions are given by equation (2.14) and become*

$$\varphi(\theta) = \int (\log p(x;\theta) - C(x)) \cdot p(x;\theta) \mathrm{d}x.$$

This function φ *is an entropy [11] if* $C(x) \equiv 0$.

In the dually flat space *divergence* can be defined, which is a distance-like function. In Section 4.3 we use this divergence instead of distance.

Definition 2.26 (Divergence) *By these dual coordinate systems and potential functions a mapping* $D : R \times R \to \mathbb{R}$ *is defined as follows;*

$$D(\theta \,\|\, \tilde{\theta}) = \psi(\theta) + \varphi(\tilde{\theta}) - \sum_{i=1}^{d} \theta^i(\theta)\eta_i(\tilde{\theta}). \tag{2.23}$$

This function is called ∇-divergence *and is distance-like function in the dually flat space. Another divergence, called* ∇^*-divergence, *is defined:*

$$D^*(\theta \,\|\, \tilde{\theta}) = \psi(\tilde{\theta}) + \varphi(\theta) - \sum_{i=1}^{d} \theta^i(\tilde{\theta})\eta_i(\theta). \tag{2.24}$$

The divergence does not satisfy the symmetry of the distance, but the value of this function is non-negative and vanishes if and only if two points are the same.

[**Remark**] By this definition we can get the following property of divergence

$$D^*(\theta \,\|\, \tilde{\theta}) = D(\tilde{\theta} \,\|\, \theta). \tag{2.25}$$

Example 2.12 (∇- and ∇^*-divergence) *1. Euclidean space [1], the* ∇- *and* ∇^*-*divergences are the same.*

$$D(p \,\|\, q) = D^*(p \,\|\, q) = \frac{1}{2}\sum_{i=1}^{d}\left\{\theta^i(p) - \theta^i(q)\right\}^2.$$

This divergence is a half of the square of Euclidean distance.

2. *Statistical parametric space of one-dimensional normal distributions [37], the ∇- and ∇^*-divergences are expressed as follows*

$$D(\xi^{(2)}||\xi^{(1)}) = D^*(\xi^{(1)}||\xi^{(2)}) = \log\frac{\sigma^{(2)}}{\sigma^{(1)}} + \frac{\left(\sigma^{(1)}\right)^2 + \left(\mu^{(1)} - \mu^{(2)}\right)^2}{2(\sigma^{(2)})^2} - \frac{1}{2} \quad (2.26)$$

where $\xi^{(1)} = [\mu^{(1)}, \sigma^{(1)}], \xi^{(2)} = [\mu^{(2)}, \sigma^{(2)}]$. *This divergence is the calculation of* Kullback-Leibler divergence [11] *for the normal distribution.*

3. *Statistical parametric space of exponential family, the ∇- and ∇^*-divergences are expressed as follows:*

$$D(p\|q) = D^*(q\|p) = \int q \log\frac{q}{p} dx.$$

The ∇^*-divergence is Kullback-Leibler divergence, *which is famous and useful in information theory* [11].

For three points in the dually flat space, a Pythagorean theorem like a Euclidean space is proved.

Theorem 2.2 (Pythagorean theorem [1]) *Suppose three points p, q, r in the dually flat space. If the ∇-geodesic connecting p, q and the ∇^*-geodesic connecting q, r intersect orthogonally at q, then*

$$D(p\|r) = D(p\|q) + D(q\|r).$$

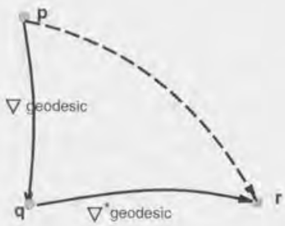

Figure 2.1: Pythagorean theorem in dually flat space

This theorem is an extension of Pythagorean theorem in Euclidean space.

2.3.2 Other Examples of Dually Flat Space

In this section we describe other dually flat spaces, i.e., feasible region of linear programming [51] and parametric family of invertible linear system [2].

The linear programming is well-known and studied field in mathematical programming. The feasible region is a subspace of Euclidean and a polytope. The space is also regarded as dually flat space.

Example 2.13 (Feasible Region of Linear Programming [51]) *Let $M = \{\theta \mid A\theta - b > 0,\ A = \left(a_i^l\right), b = (b^l), l = 1, \ldots, m\}$ be a convex region. On the space we deal with minimization problem below function: $V(\theta) = c^{\,t}\,\theta\ \left(c = (c_i) \in \mathbb{R}^d, \theta = (\theta_i) \in M\right)$.*

The potential function on M is defined as follows :

$$\psi = -\sum_{l=1}^{m} \log\left(\sum_i a_i^l \theta^i - b^l\right).$$

This function is convex on M and called log barrier function *which actually used in the interior point method. Moreover η-coordinate can be calculated like this :*

$$\eta_j = \partial_j \psi(\theta) = -\sum_{l=1}^{m} \frac{a_j^l}{\sum_k a_k^l \theta^k - b^l}.$$

The η is expressed by vector $\eta(\theta) = A^t[A\theta - b]^{-1}1_m$, where $[z]$ is the diagonal matrix such that the diagonal element is the vector z.

The previous example is a feasible region of linear programming. The other is stated, i.e., *parametric family of invertive linear system*, which is also considered as dually flat space. That space is defined

$$L := \left\{S(\omega) \;\middle|\; \int_{-\pi}^{\pi} |\log S(\omega)|^2 \mathrm{d}\omega < \infty\right\}$$

which is called *system space* and $S(\omega)$ is called spectrum. The metric and the connection are introduced into this space like this :

$$g_{ij}(\xi) = \langle e_i, e_j \rangle = \frac{1}{2\pi}\int \partial_i \log S(\omega;\xi)\partial_j \log S(\omega;\xi)\mathrm{d}\omega,$$

$$\Gamma_{ij,k}^{(\alpha)} = \frac{1}{2\pi}\int \{\partial_i\partial_j \log S(\omega;\xi) - \alpha\partial_i \log S(\omega;\xi)\partial_j \log S(\omega;\xi)\}\,\partial_k \log S\mathrm{d}\omega$$

where ξ is the local coordinate system of $\log S(\omega)$ and its relation is

$$\log S(\omega) = \sum_{t=0}^{\infty} \xi_t e_t(\omega).$$

Theorem 2.3 ([2]) *The system space L is α-flat for all α and the α-coordinate system $c^{(\alpha)}$ is its affine coordinate system.*

The coordinate system $c^{(\alpha)}$ is defined as follows : suppose the Taylor expansion of α-spectrum

$$R^{(\alpha)}(\omega) = \sum_{i=1}^{\infty} c_i^{(\alpha)} e_i(\omega),$$

the expansion coefficients $[c^{(\alpha)}] = [c_1^{(\alpha)}, c_2^{(\alpha)}, \ldots]$ is regarded as the α-coordinate system where α-spectrum is

$$R^{(\alpha)} = \begin{cases} -\dfrac{1}{\alpha} S(\omega)^{-\alpha} & (\alpha \neq 0) \\ \log S(\omega) & (\alpha = 0) \end{cases} \qquad \forall \alpha \in \mathbb{R}.$$

These $c^{(\alpha)}$ and $c^{(-\alpha)}$ become dual coordinate systems.

Moreover the potential functions becomes

$$\psi_\alpha = \frac{2}{\alpha} H + \frac{1}{2\alpha^2} \ (\alpha \neq 0), \quad \psi_0 = \frac{1}{4\pi} \int \{\log S(\omega)\}^2 \mathrm{d}\omega$$

where $H = \dfrac{1}{4\pi} \displaystyle\int \log S(\omega) \mathrm{d}\omega + \frac{1}{2} \log(2\pi e)$.

Thus the α-divergence is described as follows:

$$D_\alpha(S_1(\omega), S_2(\omega)) = \begin{cases} \dfrac{1}{2\pi\alpha^2} \displaystyle\int \left\{ \left(\frac{S_2}{S_1} \right)^\alpha - 1 - \alpha \log \frac{S_2}{S_1} \right\} \mathrm{d}\omega & (\alpha \neq 0), \\ \dfrac{1}{4\pi} \displaystyle\int (\log S_2 - \log S_1)^2 \mathrm{d}\omega & (\alpha = 0). \end{cases}$$

In latter section we mainly discuss geometric structure in the dually flat space with global coordinate system, however these spaces, statistical parametric space, feasible region of linear programming and parametric family of invertive linear system, are always in our mind.

Chapter 3

Convex Hull

The convex hull of a finite set of points is of basic interest because convex hulls are so familiar to us in two-dimensional and three-dimensional Euclidean space, computer graphics, etc. Moreover, high dimensional convex hulls are used for linear programming, games theory, the analysis of manifolds, and are also of interest in their own right.

3.1 Convex Hull in Riemannian Space

The goal of this section is to define an extension of the convex hull concept to Riemannian space. First, let us mention some earlier works in this field: for example, in [9] the convex hull in manifolds of pinched negative curvature, and in [30] the construction of the convex hull in Minkowski space are considered. In these papers, *convexity* is defined by *geodesics* (e.g., see [24]). Evidently, the uniqueness of a geodesic between any two points is necessary for the definition of convexity. In this section we assume the uniqueness of geodesics, i.e. only *complete spaces* (Definition 2.13) are considered.

Definition 3.1 (Convexity on Riemannian Space) *A subset S of a complete Riemannian space R is said to be* convex, *if, for any two points θ and $\tilde{\theta}$ in S there exists a minimizing geodesic joining θ and $\tilde{\theta}$ which is included in S.*

[Remark] In a general Riemannian space, for a given point p and direction, a unique geodesic is determined, and provides the distance t from p by arc length. This distance has the property that (1) there is a point q and a positive real number $s = d(p, q)$ such that $t < s$ or (2) t can take an any real value. A *cut point* of p is a such point q. The set of all the cut point of p is called the *cut locus* of p (e.g., see [24]). For example, for a point on a sphere, the antipodal point is the cut locus. This set is more difficult to define in the context of Riemannian space (see Fig 3.1). In [21] any compact subset of the cut locus has finite 1-dimensional Hausdorff measure in a complete surface with a Riemannian metric of class C^2, and in [22] the existence of a cut locus that is fractal is proved. The Voronoi diagram in Riemannian space is defined as the set of cut loci for finite point sets.

Figure 3.1: Cut locus for sphere and ellipsoid

Since in any complete manifold there is a minimizing geodesic (Theorem 2.1), the convex hull is defined by convexity in that space.

Definition 3.2 (Convex Hull) *For a given finite set of points P the convex hull* CH(P) *is defined as the intersection of all convex sets including P.*

The concept of a convex hull in a general Riemannian space is more difficult, because there is cut locus and no hypersurface analogous to the Euclidean hyperplane. However, in some cases the convex hull can be constructed. We shall consider a *flat space* with a *global coordinate system* and a *hyperbolic space* in Sections 3.2 and 3.3, respectively. Since the hyperbolic space is complete (Lemma 2.3), any two points are connected by a minimizing geodesic and the length of the geodesic is given by the distance between the two points. We prove that the convex hull in these spaces can be constructed by an algorithm for the convex hull, as in Euclidean space. Dually flat space is also flat, and the convex hull in that space is also efficiently computable if the flat space has a global coordinate system.

Moreover we propose a class of Riemannian spaces, namely *linearizable spaces*, in the section 3.5, in which the convex hull can be constructed. That class includes flat space with a global coordinate system, the hyperbolic space, etc.

3.2 Flat Space

In this section we obtain the *convex hull* in *flat space*. Flat space is special amongst Riemannian spaces, in that there is an *affine coordinate system*. By virtue of that coordinate system, the flat space is locally regarded as Euclidean space; in particular, the geodesic segment becomes a segment of Euclidean space in the affine coordinate system. In addition, we treat flat space with a global coordinate system (Definition 2.7); it is possible that such a local coordinate system extends to the whole space, which then becomes a *global coordinate system*. Although it is not known that this space is complete, we can at least prove the following lemma :

Lemma 3.1 *In any flat space with a global coordinate system, there exists a unique geodesic segment connecting any two points.*

Proof: Such a space is regarded as a subset of Euclidean space, i.e., a geodesic segment is a Euclidean segment as a point set. Since in Euclidean space any two points are connected by a unique segment, in such flat space the equality is true. □

Convexity was defined for complete Riemannian spaces (Definition 3.1). However, in a flat space with a global coordinate system, the geodesic segment between any two points is unique. Thus convexity is defined and is equal to the convexity in Euclidean space as a point set. Therefore, computationally, the convex hull can be defined and constructed by means of the *Euclidean convex hull algorithm*. Because the structure is convex, the whole of the convex hull is included in flat space. In particular, no part of the convex hull is removed, unlike the construction of the Voronoi diagram (Section 4).

We work up above facts into theorem.

Theorem 3.1 *The convex hull in a flat space with global affine coordinate system is equal to Euclidean convex hull and can be efficiently constructed by the Euclidean convex hull algorithm.*

Proof: In flat space, any geodesic segment becomes a Euclidean segment using the *global coordinate system*. When the flat space does not use the global coordinate system, there exists a transformation which is a bijection. The transformation is applied to the original space. In the mapped space we can consider the convex hull.

Since we proved the uniqueness of geodesic in this space, the convexity of the flat space is Euclidean. Thus the structure of the convex hull is also Euclidean. Moreover, as the flat space is a subset of Euclidean, the whole of the convex hull is included in the flat space. Because of the uniqueness of geodesics and the definition of convexity, the convex hull in the flat space consists of geodesic segments and is Euclidean by the global coordinate system. Thus the algorithm for the Euclidean convex hull can be applied to a set of points in the flat space. □

The following corollary follows immediately:

Corollary 3.1 *For a set of n points in d-dimensional flat space with a global coordinate, the combinatorial complexity of the convex hull is $F = O(n^{\lfloor d/2 \rfloor})$ and the time complexity is $O(F \log n)$.*

Proof: By theorem 3.1 the convex hull in that space has Euclidean structure. Thus we can use the *upper bound theorem for Euclidean convex polytope* (e.g., see [12, 42]). Its time complexity of Euclidean is proved in [48]. □

In the dually flat space for a set of points two convex hulls can be considered since there exist two affine coordinate systems. These are called the ∇- and the ∇^*-*convex hulls*. They do not always have the same structure, because *two* distinct convexities are defined in the space.

Example 3.1 *Let $P = \{(0, 2a-\varepsilon), (0, a), (-a, 2a), (a, 2a) \mid a \gg \varepsilon > 0\}$ be a set of points in the parametric space of one-dimensional normal distribution. The ∇^*-convex hull consists of three points $\mathrm{CH}(P_\eta) = \{(0, a), (-a, 2a), (a, 2a)\}$ and $\{(-a, 5a^2), (a, 5a^2), (0, a^2)\}$ in θ-coordinate system, but the ∇-convex hull has four vertices $\mathrm{CH}(P_\theta) = \{(0, 2a - \varepsilon), (0, a), (-a, 2a), (a, 2a)\}$ and*

$$\mathrm{CH}(P_\theta) = \left\{ \left(0, -\frac{1}{2(2a+\varepsilon)^2}\right), \left(-\frac{1}{4a}, -\frac{1}{8a^2}\right), \left(\frac{1}{4a}, -\frac{1}{8a^2}\right), \left(0, -\frac{1}{2a^2}\right) \right\}$$

in η-coordinate system. The transformations for each coordinate are given by $(\theta^1, \theta^2) = \left(\frac{x}{y^2}, -\frac{1}{2y^2}\right)$, $(\eta_1, \eta_2) = (x, x^2 + y^2)$.

In flat space, the convex hull can be calculated. This result is based on the *flatness* and the *global coordinate system*.

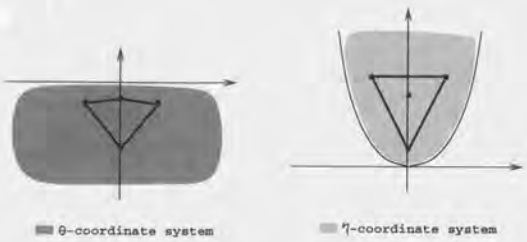

Figure 3.2: ∇-convex hull (left) and ∇^*-convex hull (right)

3.3 Hyperbolic Space

In Section 2.1.2 we define the *hyperbolic sphere*, the *hyperbolic plane* and the related *half-space* for a hyperbolic space. We also define *convexity* on a complete Riemannian space. Since hyperbolic space is complete (Lemma 2.3), the convex hull, called *hyperbolic convex hull*, is automatically defined. In this section we state some properties of the hyperbolic convex hull: the convexity of the half-space and the structure of hyperbolic convex hull are proved. In addition, the construction algorithm and the analysis of its complexity is provided in Theorem 3.2. By that algorithm the hyperbolic convex hull can be computed efficiently.

Firstly, we state the convexity of the half-space of the Poincaré space $\mathbb{H}$ to prove the convexity in the hyperbolic space.

Lemma 3.2 *The half-space of the Poincaré space* $\mathbb{H}$ *is convex.*

Proof: We prove that if $a_1, a_2 \in C^+$, then $C_{a_1,a_2} \subset C^+$ where C_{a_1,a_2} is the geodesic segment that connects two points a_1 and a_2. Suppose that C and C_{a_1,a_2} are on circles C' and C'_{a_1,a_2} in the Euclidean plane respectively. These two circles intersect at most two points and these centers of the circles C', C'_{a_1,a_2} are on x-axis. Therefore, one of the intersection is in the upper half-plane and the other is in the lower half-plane. Thus two geodesic cross at most one point in $\mathbb{H}$. Hence, if $a_1, a_2 \in C^+$, then C_{a_1,a_2} is in C^+. To finish the proof, we need to consider the case in which C is on $x = c$ can be proved in a similar way. $\square$

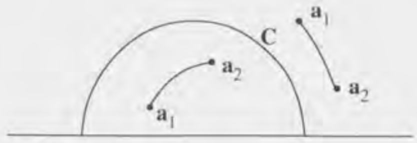

Figure 3.3: Convexity in Poincaré space

By above lemma, the convexity of the half-space of the hyperbolic space $\mathbb{H}^d$ can be obtained.

Lemma 3.3 *The half-space of the d-dimensional hyperbolic space $\mathbb{H}^d$ is convex.*

Proof: Let C be a hyperbolic plane and C^+, C^- be half-spaces determined by C. For $a_1, a_2 \in C^+(C^-)$, let L be a geodesic segment connecting these two points. There are 4 cases :

1. The geodesic is (2.8) and the hyperbolic plane is (2.12).
2. The geodesic is (2.9) and the hyperbolic plane is (2.12).
3. The geodesic is (2.8) and the hyperbolic plane is (2.13).
4. The geodesic is (2.9) and the hyperbolic plane is (2.13).

Cases 2,3 and 4 are trivial. Consider only the case 1. Without loss of generality, the geodesic C_{a_1,a_2} can be expressed as $(x_1 - p_1)^2 + x_d{}^2 = R$, $x_i = p_i$ $(i = 2, \ldots, d-1)$ and the hyperbolic plane C can be expressed as $\sum_i (x_i - q_i)^2 + x_d = R$.
Let the hyperbolic plane be restricted to $x_i = p_i$ $(i = 2, \ldots, d-1)$. Thus the hyperbolic plane can be expressed as

$$(x_1 - q_1)^2 + x_d{}^2 = R' - \sum_{i=2}^{d-1} (p_i - q_i)^2.$$

If the right-hand side of the equation above is positive, then it is possible that the geodesic segment and the hyperbolic plane intersect.

Suppose the right-hand side is positive, then this lemma is reduced to the convexity of the Poincaré space $\mathbb{H}$, as was proved in Lemma 3.2. □

This corollary is easily proved by these lemmas.

Corollary 3.2 *The intersection of half-spaces in the hyperbolic space is convex.*

Proof: A half-space in the hyperbolic space is convex (Lemma 3.3). The intersection of half-spaces is also convex because any points of the intersection are connected by the geodesic segment from each half-space. Thus the geodesic segment is included in the intersection. □

For hyperbolic space the *linearization technique* can be applied. Linearization is a method in which the original structure is embedded in a different dimensional space, so that it is a structure in its own dimension (e.g., see [12]). For hyperbolic space, we consider the following transformation:

$$X_i := x_i \; (i = 1, \cdots, d), \quad X_d := x_1^2 + \cdots + x_d^2. \tag{3.1}$$

By this transformation, hyperbolic plane is mapped to a hyperplane in Euclidean space:

$$-\sum_{i=1}^{d-1} 2p_i X_i + X_d + \sum_{i=1}^{d-1} p_i^2 - R = 0 \text{ or } \sum_{i=1}^{d-1} p_i X_i + p_d = 0.$$

We can prove the following lemma:

Lemma 3.4 *The non-degeneration point set of hyperbolic plane and of linearized space is equivalent.*

Proof: Let $P = \{p^{(i)} \; ; \; i = 1, \ldots, d\}$ be a set of points in the hyperbolic space. The degeneration of hyperbolic plane depends on the existence of solution of following simultaneous equations :

$$\begin{aligned}
& \textstyle\sum_{i=1}^{d-1} \left(p^{(j)i} - q_i\right)^2 + (p^{(j)d})^2 = R \quad (j = 1, \ldots, d), \\
\Longleftrightarrow \quad & \det\left[p^{(j)i} - p^{(1)i}\right] \neq 0 \qquad (i = 1, \cdots, d-1, j = 2, \cdots, d), \\
\Longleftrightarrow \quad & \det\left[p^{(j)i}\right] \neq 0 \qquad (i = 1, \cdots, d-1, j = 2, \cdots, d),
\end{aligned}$$

where $q(q_1, \ldots, q_{d-1}, 0)$, R are the center, the radius of circumscribed sphere of P The determinant of above equation is equal to the degeneracy of the linearized set of points $\tilde{P}$ by equation (3.1) □

We can prove the following theorem:

Theorem 3.2 *The convex hulls for given points in hyperbolic space and for linearized points in Euclidean space are equivalent in a face-lattice.*

Proof: By the linearization the connective relations among faces are unchanged. Thus, at least the structure corresponds to the Euclidean. We state that hyperbolic space contains the whole convex hull. This structure is convex; for any two points the connecting geodesic segment is included within that space, and that geodesic is in the interior of the convex hull. Therefore the whole of the convex hull is included in that space. □

The hyperbolic convex hull can be constructed by a Euclidean algorithm and inverse mapping.

Algorithm (Convex Hull in the Hyperbolic Space)

1. `Transform the given set of points by equation (3.1).`
2. `Compute the convex hull (the space is regarded as Euclidean space).`
3. `Calculate the inverse of that convex hull.`

Then the following corollary is immediately proved:

Corollary 3.3 *For a given set of n points P in the d-dimensional hyperbolic space* $\mathbb{H}^d$ *the combinatorial complexity of convex hull* $\mathrm{CH}(P)$ *is bounded by* $F = O(n^{\lceil d/2 \rceil})$ *and the time complexity is* $O(F \log n)$.

Proof: The combinatorial complexity is that of the Euclidean convex hull. Since the first and third step of algorithm are linear on the number of points and of faces, the overall time do not exceed the time of second step. That time complexity is also equal to Euclidean.

For the combinatorial and time complexity of Euclidean convex hull, refer to [12] and [48], respectively. □

Hyperbolic convex hull can be computed by the existence of global coordinate system and the of linearized transformation.

3.4 Poincaré Space

Poincaré space is well-known as a non-Euclidean space, a fundamental Riemannian space and two-dimensional hyperbolic space, i.e., the above algorithm can be applied. However that space is also a subset of two-dimensional Euclidean space as a set of points and some special algorithms of convex hull can be considered. In this section we explain two algorithms such that *incremental method* and *Graham's scan* in Section 3.4.1 and Section 3.4.2, respectively. In two-dimensional space convex hull can be express by list, i.e., in this section we use doubly linked list and combinatorial complexity of that convex hull is bounded by $O(n)$.

3.4.1 Incremental Method

The incremental method of the convex hull is a most fundamental algorithm. The key of this method is that the structure adding a point is always *convex hull* in each stage of the algorithm.

The algorithm is written like this :

Algorithm (Incremental Method for Convex Hull in the Poincaré space)

1. Sort given set of points $P = \{p^{(i)} ; i = 1, \ldots, d\}$ by Euclidean distance between the origin and each point and replace their indexes of points $p^{(i)}$ such that its index is equal to the order of the Euclidean distance from the origin.
2. Make convex hull CH(P_3) of $\{p^{(1)}, p^{(2)}, p^{(3)}\}$.
3. **For** $i = 4$ **to** $i = n$
   Make CH(P_i) from CH(P_{i-1}).

The CH(P_n) is the convex hull of P.

We only discuss the third stage above algorithm. If the part works well, we can get the convex hull in the Poincaré space. We firstly prove this lemma.

Lemma 3.5 *Suppose* $\{p^{(i)};\ i = 1, \ldots, n\}$ *is a set of points such that its index is the order of Euclidean distance from the origin. The point* $p^{(j)}$ *is not included in* $\mathrm{CH}(\{p^{(1)}, \ldots, p^{(j-1)}\})$, $(j = 4, \ldots, n)$.

Proof: Consider a curve C such that the center is the origin and the radius is equal to Euclidean distance between the origin and $p^{(j-1)}$, i.e., the C becomes geodesic and is expressed as $x^2+y^2 = d(O, p^{(j-1)})^2$ where O is the origin and $d(\cdot,\cdot)$ is Euclidean distance. By the geodesic C the Poincaré space is divided into two half-space. The part including the origin is called C^+ and another is called C^-. The C^+ contains $\mathrm{CH}(\{p^{(1)}, \ldots, p^{(i-1)}\})$ and the C^- contains $p^{(i)}$ because the points are sorted by Euclidean distance. □

Above lemma shows we have no need to check whether the point is included in the convex hull or not in each stage. In addition, the following lemma is also proved.

Lemma 3.6 *The convex hull* CH(P) *is expressed by* doubly linked list *(e.g., see [42]) and* `prev`(v), `next`(v), *which is previous, next point in that list, respectively. Suppose a point p which stays in the outside of* CH(P) *and make* CH($P \cup \{p\}$) *from* CH(P). *If* `prev`(v) *and* `next`(v) *is included in $C^+_{p,v}$ for a vertex v of convex hull, then the geodesic segment $C_{p,v}$ becomes the edge of* CH($P \cup \{p\}$) *where $C_{p,v}$ is the geodesic segment joining p, v and $C^+_{p,v}$ is the half-space determined by $C_{p,v}$ and contains* CH(P).

Proof: Suppose a separation of $\mathbb{H}$ by geodesic lines $C_1 = C_{v,\mathtt{next}(v)}, C_2 = C_{v,\mathtt{prev}(v)}$. The $\mathbb{H}$ is divided into four parts. Let R be a region including CH(P) among the division and the C be a geodesic line including $C_{p,v}$. When add C into the separation, C intersects C_1, C_2 at v. If `prev`(v), `next`(v) $\in C^+$(or C^-), then $R \subset C^+$(or C^-) where C^+, C^- are half-spaces determined by C. Thus $C_{p,v}$ becomes supporting line of CH(P). □

In the third step we only change the connection of the points, i.e., for any adding point p there exist *upper supporting point* $p_{u.s.p}$ (*lower supporting point* $p_{l.s.p}$) which is a point such that the half-space decided by geodesic segment $C_{p,p_{u.s.p}}$ ($C_{p,p_{l.s.p}}$) includes all point of convex hull. Thus we only find $p_{u.s.p}$ and $p_{l.s.p}$ for adding points.

Procedure (Make CH(P_i) from CH(P_{i-1}))

1. (Search upper supporting point)

   $v = p^{(i-1)}$;

   while `(1)` **do**

       `Consider a geodesic` $C_{v,p^{(i)}}$.

       if `(prev(`v`) and next(`v`)` $\in C^+_{v,p^{(i)}}$`)`

       then v `is an upper supporting point (`$p_{u.s.p} = v$`);` **end**;

       else v `=prev(`v`);`

   end;

2. (Search lower supporting point)

   This point can be found similarly.

3. (Change the link of points)

   `prev(`$p^{(i)}$`)=`$p_{u.s.p}$, `next(`$p^{(i)}$`)=`$p_{l.s.p}$ and `next(`$p_{u.s.p}$`)=prev(`$p_{l.s.p}$`)` $= p^{(i)}$.

The `prev`(v) is the previous point and the `next`(v) is the next point in the doubly linked list.

Finally we obtain the time complexity of this algorithm.

Theorem 3.3 *For a set of n points the time complexity of the convex hull in the Poincaré space is $O(n \log n)$ by incremental method.*

Proof: Since n points are sorted in the first step, its time complexity is $O(n \log n)$. Suppose the reconnection and the check of nodes require constant time. The cost of the stage 3 is linear for the number of the search and the reconnection of nodes. So we count the number, which becomes complexity.

The reconnection of nodes happens at most n times because the insertion happens at most n times. Moreover if a node is searched once, then the node remove from the list. Thus the number is $O(n)$. The whole of the time complexity is $O(n \log n)$. □

3.4.2 Graham's Scan

In this section we deal with *Graham's scan*. This algorithm is based on the sorting of an *angle*. Since the *angle* can be defined in the Poincaré space, we can apply this algorithm.

Definition 3.3 (Angle on the Poincaré Space) *Let a_1, a_2, a_3 be distinct points in $\mathbb{H}$. The* angle *$\angle a_1, a_2, a_3$ in the Poincaré space is defined as an angle from l_1 to l_2 where l_1, l_2 is the tangent line of the geodesic segment C_{a_1,a_2} at a_2 and of C_{a_2,a_3} at a_2 respectively.*

Moreover the key of this algorithm is that all points are regarded as on the boundary of convex hull and remove actually interior points. Graham's scan is described like this:

Algorithm 3.1 (Graham's Scan)

1. Find a point q where q attains the minimum of x_1-coordinate among given point set P

2. The point q is regarded as an origin and sort P by the angle $\angle a_i, q, e$ (e is ${}^t(1, 0)$) and

Figure 3.4: Angle in Poincaré space

the Euclidean distance from q. Set $START$ to the point which has the minimum angle and the boolean variable, when true, indicates that vertex $START$ has been reached through forward scan, not backtracking.
3.(Scan)

```
begin  v = START; w = prev(v); f = false;
   while (next(v) ≠ START or f = false) do
      begin if (next(v) = w) then  f = true;
         if (The angle ∠v,next(v),next(next(v)) from l_{next(v),v} to l_{next(v),next(next(v))}
         is more than π.)
            then next(v);
         else begin Remove next(v);
               v = prev(v);
            end
      end
end.
```

where the `next(v)` *and the* `prev(v)` *are the next and previous points of v in the doubly linked list, respectively.*

The problem above algorithm is the judgment of deleting point. The decision is done by the signed area of triangle $\triangle v$`next`(v)`next`(`next`(v)). This signed area can be computed if the coordinate of points is given. This method is used in not only Euclidean but also Poincaré space because its decision is the same.

Here we prove this lemma about the analysis of the time complexity of this algorithm. By this lemma that sort is bounded by $O(n \log n)$.

Lemma 3.7 (Sorting by Angle) *Let $P = \{p^{(0)}, p^{(1)}, \ldots, p^{(n)}\}$ be a set of distinct points in $\mathbb{H}$ where $p^{(0)}$ is a point of P s.t. the x_1-coordinate is minimum and x_2-coordinate is positive.*

The sorting by angle between x_1-axis and the tangent line of geodesic segment joining $p^{(0)}, p^{(i)}$ at $p^{(0)}$ is equal to the sorting by $c^{(i)}$ where $c^{(i)}$ is a center of equation $C_{p^{(0)}p^{(i)}}$ when that geodesic is regarded as the circle in the Euclidean space.

Proof: Suppose two geodesic segments $C_i = C_{p^{(0)},p^{(i)}}, C_j = C_{p^{(0)},p^{(j)}}$ and $p^{(k)}(x_1^{(k)}, x_2^{(k)})$ $(k = 0, i, j)$. Moreover the center of the equation of C_i, C_j (since that geodesic is half-circle, there is a center) is $O_i(c^{(i)}, 0), O_j(c^{(j)}, 0)$. The tangent vector at $p^{(0)}$ is $(x_2^{(0)}, c^{(i)} - x_1^{(0)}), (x_2^{(0)}, c^{(j)} - x_1^{(0)})$. Its order of tangent vector is equal to the x_2-coordinate of C_i at $x_1 = x_1^{(0)} + \varepsilon$ where ε is a positive real number and sufficient small. Consider this function:

$$f(x_1, i) := {x_2}^2 = (x_1^{(0)} - c^{(i)})^2 + (x_2^{(0)})^2 - (x_1 - c^{(i)})^2$$

which is given the value of ${x_2}^2$ of C_i. The value of this function at $x_1 = x_1^{(0)} + \varepsilon$ becomes

$$f(x_1^{(0)} + \varepsilon, i) = -2\varepsilon(x_1^{(0)} - c^{(i)}) - \varepsilon^2 + (x_2^{(0)})^2.$$

After all the difference is

$$f(x_1^{(0)} + \varepsilon, i) - f(x^{(0)} + \varepsilon, j) = 2\varepsilon(c^{(i)} - c^{(j)}).$$

Thus this value depend on the value $c^{(i)}, c^{(j)}$. So we compute $c^{(i)}$ $(i = 1, \ldots, n)$ instead of sorting the tangent vector. □

We obtain the time complexity of this algorithm.

Theorem 3.4 *For a set of n points in $\mathbb{H}$ the time complexity of Graham's scan is $O(n \log n)$.*

Proof: In the algorithm since the set of points is sorted, that stage costs $O(n \log n)$. Suppose the judgment of the angle is done constant time, then the number of decision is n times, i.e., the scan stage is $O(n)$ time. Thus the time complexity of Graham's scan is also $O(n \log n)$. □

In Section 3.4.1 and Section 3.4.2 incremental algorithm and Graham's scan are dealt with, respectively. In both methods the convex hull for n points can be computed in $O(n \log n)$ time. Its complexity is equal to Euclidean version.

3.5 Linearizable Space

Earlier, we described algorithms for the computation of a convex hull in flat space (Section 3.2) and in hyperbolic space (Section 3.3). We now propose a class of Riemannian space, namely *linearizable space*, which includes flat space with a global coordinate system and hyperbolic space, and in that space a convex hull can be efficiently calculated.

Definition 3.4 (Linearizable Space) *A Riemannian space is* linearizable *if there exists a global coordinate system such that any geodesic segment can be expressed as a Euclidean segment as a set of points. That coordinate system is called a* linearized coordinate system.

We show that a convex hull in a linearizable space can be efficiently constructed.

Theorem 3.5 (Convex Hull in Linearizable Space) *For a set of points in a linearizable space the convex hull can be computed by the algorithm of the Euclidean convex hull.*

Proof: In the space there is a global coordinate system: any geodesic segment in the space is regarded as a Euclidean segment. Suppose that such coordinate system is used on the linearizable space.

For any two points, the geodesic segment is unique, because the geodesic joining two points becomes a Euclidean segment and as that coordinate system is global, the expression is unique. Thus the convexity of the space is Euclidean. The convex hull in that space has same structure of that of the Euclidean convex hull. In particular, the Euclidean convex hull algorithm can be applied. □

When the convex hull has the same structure as Euclidean, we get the following corollary:

Corollary 3.4 *For a set of n points in d-dimensional linearizable space, the combinatorial complexity of the convex hull is $F = O(n^{\lfloor d/2 \rfloor})$ and the time complexity is $O(F \log n)$.*

Proof: Since the convex hull has the same structure as Euclidean (Theorem 3.5), the upper-bound theorem for Euclidean convex polytope ([12]) can be applied. The combinatorial complexity of the Euclidean convex hull is proved in [48]. □

In addition, we deal with the classification of space.

Lemma 3.8 *Linearizable space contains these spaces:*

- *flat space with global coordinate system,*
- *hyperbolic space.*

Proof:

Flat Space : Since this space has a global coordinate system, a local geodesic segment can be extended to the whole space. In addition, since that space is flat, the extended geodesic segment is a Euclidean segment as a set of points.

Hyperbolic Space : In the hyperbolic space, suppose the coordinate system is transformed by the equation (3.1). In that coordinate system, any geodesic segment is regarded as a Euclidean segment as a set of points.

□

We give an example of a linearizable space.

Definition 3.5 *Let* $S = \{(x_1, y_1, \ldots, x_d, y_d) \mid x_i, y_i \in \mathbb{R}, y_i > 0\ (i = 1, \ldots, d)\}$ *be a Riemannian space with the metric*

$$\mathrm{d}s^2 = \sum_{i=1}^{d} \frac{\mathrm{d}x_i{}^2 + \mathrm{d}y_i{}^2}{y_i{}^2}.$$

[Remark] This space is realized by a statistical parametric space of a multivariate normal distribution with its variance-covariance

$$\Sigma = \begin{pmatrix} \sigma_1{}^2 & 0 & \cdots & 0 \\ 0 & \ddots & \cdots & \vdots \\ \vdots & \vdots & \sigma_{d-1}{}^2 & 0 \\ 0 & \cdots & 0 & \sigma_d{}^2 \end{pmatrix}.$$

Its parametric space is $2d$-dimensional space $[\xi] = [\mu_1, \sigma_1, \ldots, \mu_d, \sigma_d]$ and the Fisher information matrix of this space becomes

$$g_{ij} = \begin{cases} \xi_{2k}{}^{-2} & = \sigma_k{}^{-2} \quad (i = j = 2k-1) \\ 2\xi_{2k}{}^{-2} & = 2\sigma_k{}^{-2} \quad (i = j = 2k) \\ 0 & \quad\quad\quad\quad (Otherwise) \end{cases}$$

where $k = 1, \ldots, d$. This space with Fisher metric is equal to the space in Definition 3.5 as a Riemannian space. i.e., if Levi-Civita connection is introduced in this space, then this space is an extension of hyperbolic space and if α-connection is introduced, then this space is regarded as a statistical parametric space. Moreover the convex hull is efficiently computed in each space. However Voronoi diagram is not efficiently computed in this space, because Lemma 2.4 is not proved.

Lemma 3.9 *The above space S is included in the class of linearizable space.*

Proof: The geodesic in S is expressed as

$$x_1 = r_i \cos t_i - p_i,\ y_i = r_i \sin t_i \quad (i = 1, \cdots, d)$$

by d pairs of equation (2.4) for (x_i, y_i). Using the linearization technique, we consider the following transformation:

$$X_i = x_i, Y_i = {x_i}^2 + {y_i}^2$$

Since the linearized coordinate system of S is given, the proof is concluded. □

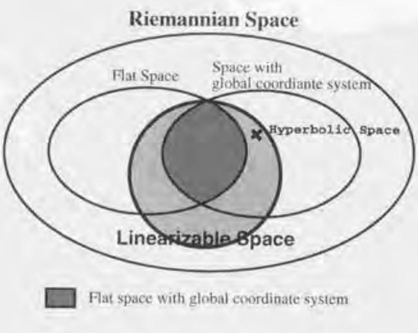

Figure 3.5: The relation between flat space, hyperbolic space and linearizable space

We show the relationship between flat space, hyperbolic space and linearizable space in Figure 3.5. However the complete relation is not known :

- Is there a space that is contained the class of linearizable space and have no global coordinate system?

- Is there a space that is contained in flat space and is not contained in linearizable space ?
- Is there a space which is linearizable space and is not flat and has no global coordinate?

Finally we claim that convex hull depends only on the convexity of the space: if the geodesic in the Riemannian space is linearizable, then the structure of the convex hull in the space is Euclidean. Such a space is called a *linearizable space*.

Chapter 4

Voronoi Diagram

The aim of this chapter is to discuss the proximity relation in Riemannian space, leading to the *Voronoi diagram*. That is defined in general Riemannian space. Since our purpose is to construct a geometric structure, the hyperbolic space and the dually flat space are treated and we propose efficient algorithms, i.e., in these spaces Voronoi diagram can be constructed by our algorithms.

4.1 Voronoi Diagram in Riemannian Space

The Voronoi diagram is a well-known geometric and mathematical object because it is simple to define and has applications in a number of sciences: biology, physics, archaeology, etc. First we provide a general definition.

Definition 4.1 *Let* $P = \{p^{(i)} \ ; \ i = 1, \ldots, n\}$ *be a set of* n *points in the space* S. *The* Voronoi polygon $\mathrm{Vor}(p^{(i)})$ *of* P *is defined as follows:*

$$\mathrm{Vor}(p^{(i)}) = \left\{ x \in S \mid d(x, p^{(i)}) \leq d(x, p^{(j)}) \ \forall j \neq i \right\} \tag{4.1}$$

where $d : S \times S \to \mathbb{R}$ *is a distance function. The Voronoi polygons for* P *partition* S *and constitute the* Voronoi diagram. *The vertices of the Voronoi polygons are called* Voronoi points *and the k-dimensional faces of Voronoi polygons are called* Voronoi k-faces.

This definition uses proximity relations between points in the space, based on a certain distance function. There are some different criteria used in the literature, for example, L_p metric [42], power diagram (see [12, pp.327–328]), Laguerre Voronoi diagram [19], etc. In Section 4.2 we deal with the Voronoi diagram in hyperbolic space.

called the *hyperbolic Voronoi diagram*. This Voronoi diagram can be efficiently computed by using the Euclidean Voronoi diagram and the deleting some faces. There is an equivalence between the Euclidean and hyperbolic spheres for given points (Lemma 4.2). Since for a certain point configuration there is no such sphere, some faces must be removed. The conditions for existence of a sphere is given in Lemma 4.2. Using these properties a constructive algorithm for hyperbolic Voronoi diagram is provided in Algorithm 4.1.

The original criterion of Voronoi diagram is the Euclidean distance. In that case there are much research and so interesting results, for example, the relation to hyperplane arrangement, to Delaunay triangulation, etc. Voronoi diagrams in Section 4.3, called ∇- and ∇^*-*Voronoi diagram*, also satisfy these properties i.e., the dually flat space is an extension of Euclidean. That diagram is also constructed by the projection of the envelope of a hyperplane arrangement and the deletion of some faces (Theorem 4.4, Theorem 4.5).

Moreover the relation among hyperbolic, ∇- and ∇^*-Voronoi diagram are stated in Section 4.4, i.e., we describe the relation between Fisher metric and divergence, the characterization of Voronoi diagram in the Poincaré space and the statistical parametric space of one-dimensional normal distributions.

Figure 4.1: Voronoi diagram in Euclidean space

4.2 Hyperbolic Space

In this section a Voronoi diagram in hyperbolic space, called the *hyperbolic Voronoi diagram* is explained (the details of this section is also described in [36]). In that space the distance function is already given in equation (2.11) and the perpendicular bisector is a *hyperbolic plane* (Lemma 2.5). We can define the Voronoi diagram in the hyperbolic space immediately:

Definition 4.2 (Hyperbolic Voronoi Diagram) *The* hyperbolic Voronoi diagram *is defined so that the equation (2.11) is regarded as the criterion of Definition 4.1. Each term of this Voronoi diagram affixes* hyperbolic.

This lemma is immediate:

Lemma 4.1 *Each hyperbolic Voronoi polygon is a convex set in the hyperbolic space.*

Proof: By the definition, the hyperbolic Voronoi polygon of a point is the intersection of the half-spaces. Since each half-space is convex, the Voronoi polygon is also convex. □

By this lemma, it is evident that the polygon becomes *convex hull* in hyperbolic space : each region can be linearized and looks like Euclidean convex hull.

Here, we describe the structure of the hyperbolic Voronoi diagram. Consider the following equation satisfied by distinct $(d+1)$ points $p^{(i)}(p_{i1}, p_{i2}, \ldots, p_{id})$:

$$\begin{vmatrix} 1 & p_{11} & p_{12} & \cdots & p_{1d} & \sum_{j=1}^{d} {p_{1j}}^2 \\ 1 & p_{21} & p_{22} & \cdots & p_{2d} & \sum_{j=1}^{d} {p_{2j}}^2 \\ \vdots & \vdots & \vdots & \vdots & \ddots & \vdots \\ 1 & x_1 & x_2 & \cdots & x_d & \sum_{j=1}^{d} {x_j}^2 \end{vmatrix} = 0. \tag{4.2}$$

in both the hyperbolic and the Euclidean spaces. This equation gives the same surface, a *sphere*, in both hyperbolic (Lemma 2.4) and Euclidean space.

By expanding the determinant, we have

$$\alpha_{d+1}\left(\sum_{j=1}^{d} {x_j}^2\right) + \sum_{j=1}^{d}\left\{(-1)^{d-j+1}\alpha_j x_j\right\} + (-1)^{d+1}\alpha_0 = 0 \tag{4.3}$$

where $\alpha_j (j = 0, \ldots, d+1)$ are constant numbers depending on p_{ij}.

The sign of this determinant (4.2) shows whether the point $(x_1, x_2, \ldots, x_d)$ is included in the sphere (4.3) or not. Moreover, the sphere expresses the circumscribed sphere of the d-simplex of $(d+1)$ points. Thus the center of this sphere is a Voronoi point in the Euclidean space and the *hyperbolic center* (Definition 2.15) is a hyperbolic Voronoi point in the hyperbolic space. The hyperbolic sphere is justly included in the hyperbolic space. Therefore the following lemma has been established:

Figure 4.2: Sphere and the center on the Euclidean and hyperbolic space

Lemma 4.2 *Given $(d+1)$ non-degenerate points in the d-dimensional hyperbolic space, the set consisting of points equidistant from the given $(d+1)$ points, if exists, consists of only one point. Moreover, the necessary and sufficient condition for the existence of the sphere for the given points is that the surface is included in the hyperbolic space. Such a condition can be rewritten in terms of the α_i:*

$$\alpha_{d+1} \neq 0, \quad \alpha_d \cdot \alpha_{d+1} > 0, \quad 0 < (-1)^{d+1} 4\alpha_0\alpha_{d+1} - \sum_{j=1}^{d-1} {\alpha_j}^2 < {\alpha_d}^2. \tag{4.4}$$

Proof: For non-degenerate points in the Euclidean space, a sphere is always determined; however for the hyperbolic space the sphere does not always exist, because the distance from a point to $x_d = 0$ is infinity and the hyperbolic sphere is always included in that space. Thus the necessary and sufficient condition becomes above.

The first condition of (4.4) is expressed as the condition of non-degeneration of the set of points. Since the hyperbolic sphere and the above equation are the same surface, we can compare the equation of the hyperbolic sphere with the equation determined by the $(d+1)$ points. Then, we get the following :

$$\left\{ \begin{aligned} a_j &= (-1)^{d-j} \frac{\alpha_j}{2\alpha_{d+1}} \quad (j = 1, \cdots, d-1), \\ a_d \cosh r &= \frac{\alpha_d}{2\alpha_{d+1}}, \\ (a_d \sinh r)^2 &= (-1)^d \cdot \frac{\alpha_0}{\alpha_{d+1}} + \sum_{j=1}^{d} \frac{{\alpha_j}^2}{4{\alpha_{d+1}}^2}, \end{aligned} \right. \tag{4.5}$$

where $p(a_1, \ldots, a_d)$ is its hyperbolic center and $r > 0$ is the radius of the hyperbolic sphere. Then we can get the point p by solving the above simultaneous equations. Since the hyperbolic sphere is included in $\mathbb{H}^d$, the x_d-coordinate of p is positive and the left side of the third equation of (4.5) also is positive. Also, using the standard relations between the hyperbolic trigonometric functions $\cosh^2 r - \sinh^2 r = 1$, we obtain

$$\left(\frac{\alpha_d}{2\alpha_{d+1}}\right)^2 - (-1)^d \cdot \frac{\alpha_0}{\alpha_{d+1}} - \sum_{j=1}^{d} \frac{{\alpha_j}^2}{4{\alpha_{d+1}}^2} > 0.$$

From those equations we get the above condition.

Conversely if the condition is satisfied, the simultaneous equations always have a unique solution which is included in $\mathbb{H}^d$. □

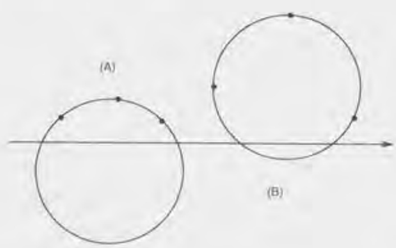

Figure 4.3: Not hyperbolic sphere, (A) hyperbolic center $\notin \mathbb{H}^d$, (B) sphere intersects $x_d = 0$.

Definition 4.3 *A geometric structure is a hyperbolic Delaunay graph, denoted by* H-Del(·), *if its dual structure is that of hyperbolic Voronoi diagram: the k-face of the hyperbolic Voronoi diagram becomes the* $(d-k+1)$*-face of the hyperbolic Delaunay graph. In particular, the d-dimensional face is the hyperbolic d-simplex, which is defined as a d-dimensional hyperbolic convex hull by just* $d+1$ *points.*

In Euclidean space, such dual structure is a *Delaunay triangulation*. In our case, however that is not always true. for example, the dual of Fig 4.5 has only 0-faces and 1-faces; there are neither 2-faces nor 3-faces.

Thus we have the following theorem:

Theorem 4.1 *Suppose that a set of points P in d-dimensional hyperbolic space is given. Then the face lattice of the hyperbolic Delaunay graph* H-Del(P) *is a subgraph of the face lattice of d-dimensional Delaunay triangulation in Euclidean space.*

Proof: Let v be a vertex of the hyperbolic Voronoi diagram. The point v is a point equidistant from $(d+1)$ sites of P. These sites form a hyperbolic d-simplex of H-Del.

Moreover, these $(d+1)$ points of the d-simplex determine a circumscribed sphere. This circumscribed sphere is the same surface in both d-dimensional hyperbolic space and d-dimensional Euclidean space (Lemma 4.2). Therefore the d-simplex does not change in either Euclidean space or hyperbolic space. Thus H-Del(P) is a subgraph of Del(P). □

[**Remark**] The Voronoi diagram and the hyperbolic Voronoi diagram for a set of points may have the same structure as a face lattice. However if $(d+1)$ points do not satisfy the condition (4.4), then the equidistant point always exists in Euclidean space, but does not in the hyperbolic space. Delaunay triangulation is defined in Definition 5.3 and denote Del(P)

From Theorem 4.1, we derive the following corollary related to the construction of the hyperbolic Voronoi diagram.

Corollary 4.1 *For a given set of points $P = \{p^{(i)} \in \mathbb{R}^d : i = 1, \ldots, n,\ x_d(p^{(i)}) > 0\}$, the following is obtained as a face lattice :*

$$\text{lower-hull}(P') = \text{Del}(P) \supset \text{H-Del}(P) = \text{Vor}(P)$$

where lower-hull(P') *is a structure consisting of faces whose outward normal vector has negative x_d-coordinate, $P' = \{(p^{(i)}, \sum_j x_j(p^{(i)})^2) \mid i = 1, \ldots, n\} \subset \mathbb{R}^{d+1}$ and $x_j(p^{(i)})$ is the x_j-coordinate of the point $p^{(i)}$.*

Proof: The first equation is a well-known fact; its proof appeared in [12]. It is proved that Del(P) includes H-Del(P) as a face lattice in the theorem 4.1 above. The last equation is part of the definition of H-Del(P). □

Using this corollary, we design the following algorithm.

Algorithm 4.1 (hyperbolic Voronoi diagram)

1. Construct Del(P) from the set of points P when hyperbolic space is regarded as Euclidean space.

2. The H-Del(P) is made up of the Del(P): remove the vertices that do not satisfy the condition (4.4) and some faces from face lattice of the Del(P).

3. Transform the H-Del(P) to the hyperbolic Voronoi diagram.

We comment on the second stage of above algorithm. Suppose Delaunay triangulation is already completed and the data structure of Delaunay triangulation is face lattice (see Fig.4.4).

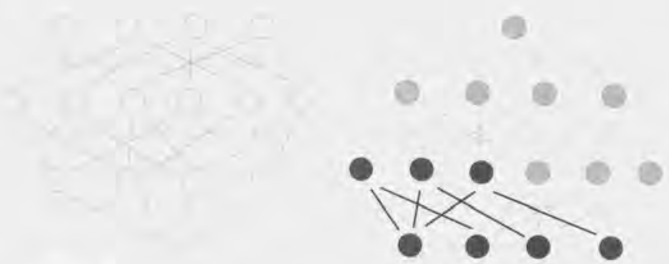

Figure 4.4: Face lattices of three-dimensional simplex and of hyperbolic Delaunay graph.

Fig.4.4 show the change of the face lattice of a 3-dimensional simplex by above procedure (gray nodes and broken line are removed from the face lattice). The latter is a dual structure of hyperbolic Voronoi diagram.

Fig. 4.5 corresponds to the right side face lattice of Fig. 4.4.

Since the hyperbolic Delaunay graph is a subgraph of the Euclidean Delaunay triangulation as a face lattice, the nodes of the lattice are divided into two types : the nodes that are to remain and those that are to be removed. When a Voronoi point which is not included in $\mathbb{H}^d$ is found (the necessary and sufficient condition is (4.4)) from $d+1$ points, the node of Voronoi point is removed. We check every node as to whether it will remain or not. Moreover, the following property is proved.

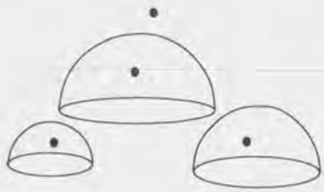

Figure 4.5: Hyperbolic Voronoi diagram for 4 points

Lemma 4.3 *Given the Delaunay graph for a set of points. If a node of Delaunay graph contains no points for removal, then that node is retained in the Delaunay graph. In addition, any superface of removed face also removed.*

Proof: At least remaining hyperbolic simplex is equal to Euclidean and it is need not be remove. We consider only a removed simplex S. All subfaces of that simplex is not taken off. For example, in Fig 4.6 one 2-face is retained. If a k-face of such a simplex is removed, then any superface of the k-face is also removed. This structure is the dual of Voronoi diagram and in that space a k-face does not exist if and only if $d-k$ hyperbolic planes do not intersect. In addition, $d-k$ hyperbolic planes do not intersect, therefore $l(> d-k)$ hyperbolic planes that include previous $d-k$ planes do not intersect either.

□

Figure 4.6: Not all faces of removed simplex and its face lattice

The following procedure is considered by above lemma. This procedure is applied to removed simplex.

Procedure (Mark the remaining node of the simplex)

1. `Mark` $(d+1)$ `vertices of the` d`-simplex;`

2. $Q = \{$`every pairs of points`$\}$;
   `/* set of the face of` d`-simplex */`
   `/* and each face is expressed by the set of vertices of` d`-simplex */`

3. $R = \emptyset$;

4. **while** $(Q \neq \emptyset)$ **do**

   $v \in Q$;

   if `(there exists a node corresponding to` v `in the hyperbolic Voronoi diagram)` **do**

   `Mark the node;`

   $R := R \cup \{v\}$;

   end;

   $Q := Q \setminus \{v\}$;

   end;

5. $Q = \{\{u\} \cup \{w\} \mid u, w \in R,$ `the Hamming distance is` $d(u, w) = 2\ \}$
   if $(Q = \emptyset \parallel |u| = d + 1 (u \in Q))$

   end;

   else

   goto 3;

After this procedure is applied to removed simplex, any unmarked node is removed from the face lattice of the Euclidean Delaunay graph. The remainder graph is just a hyperbolic Delaunay graph for given points.

Moreover, the combinatorial complexity of this structure is proved:

Corollary 4.2 *Let P be a set of n points in the d-dimensional hyperbolic space $\mathbb{H}^d$. The number of k-faces of the hyperbolic Voronoi diagram is $O(n^{\min\{d+1-k, \lfloor d/2 \rfloor\}})$, for $0 \leq k \leq d$.*

Proof: The hyperbolic Voronoi diagram is a subgraph of the Euclidean Voronoi diagram. Thus the number of hyperbolic k-faces is bounded by the number of k-faces of Voronoi diagram in $\mathbb{R}^d$. □

The time complexity of the algorithm is obtained:

Theorem 4.2 *For n points in the d-dimensional hyperbolic space, the hyperbolic Voronoi diagram can be constructed in $O(n^{\lceil (d+1)/2 \rceil} \log n)$ time.*

Proof: Let $F = O(n^{\lceil (d+1)/2 \rceil})$. Firstly, consider the time of construction of the d-dimensional Delaunay triangulation. It can be built in $O(F \log n)$ time (e.g., see [12]).

Secondly consider the second step of our algorithm as follows. Examine all vertices of $\mathrm{Del}(P)$; if a vertex does not satisfy condition (4.4), then remove that vertex and the faces that include that vertex. The number of this operation is at most the sum of the face number. Therefore the 2nd step completed in $O(n^{\lceil (d+1)/2 \rceil})$.

Finally, the third step is only relabeling faces; this operation is also linear for the sum of the face number. Thus this step has the same time complexity with the 2nd step. □

We show that the face lattice of the hyperbolic Voronoi diagram is a subgraph of the Euclidean Voronoi diagram. The hyperbolic Voronoi diagram is characterized by the *Euclidean potential function*.

In addition, a higher-order Voronoi diagram can be considered. The *kth-order Voronoi diagram* is a division of the whole space corresponding to $k(< n)$th nearest region for given n points (detailed definition is in [12, pp.315–319]). In the two-dimensional case, the combinatorial complexity of the kth-order Voronoi diagram is $O(k(n-k))$ and is a tight bound ([12]). For $d \geq 3$, its combinatorial complexity is analyzed by Euclidean potential function in [10], i.e., the sum of the number of faces of the jth-order Voronoi diagram, $j \leq k$, is $O(n^{\lfloor d/2 \rfloor} k^{\lceil d/2 \rceil + 1})$.

In the hyperbolic space the kth-order hyperbolic Voronoi diagram is similarly defined as Euclidean. Moreover, since hyperbolic Voronoi diagram is characterized by a *Euclidean potential function*, its combinatorial complexity is similarly bounded.

Theorem 4.3 *For a set of n points in the d-dimensional hyperbolic space, and a positive integer $k(< n)$, the kth-order hyperbolic Voronoi diagram is a subset of the kth-order Euclidean Voronoi diagram as a face lattice.*

Moreover its combinatorial complexity is bounded by $O(k(n-k))$ *when* $d = 2$ *and* $O(n^{\lfloor d/2 \rfloor} k^{\lceil d/2 \rceil + 1})$ *for* $d \geq 3$.

Proof: When a Voronoi diagram, that is 1st-order Voronoi diagram, for give generators is considered, suppose a sphere that includes no generator and whose boundary is on $d+1$ generators; the center of the sphere becomes a Voronoi point in the Voronoi diagram. In the kth-order Voronoi diagram, similarly suppose a sphere that includes $k-1$ generators and whose boundary on $d+1$ generators. By Lemma 4.2 for $d+1$ non-degenerate generators, the sphere is unique in both the Euclidean space and the hyperbolic space. Since those spheres for given generators are the same, at least kth-order hyperbolic Voronoi diagram is also a subgraph of kth-order Euclidean Voronoi diagram, as a face lattice.

Therefore, by the upper bound for the Euclidean kth-order Voronoi diagram (see [12, 10]) the above bound is also proved. □

Theorem 4.1, 4.2 show that the hyperplane arrangement in Euclidean space gives the information for the whole of the higher-order Voronoi diagrams. In other words, the k-level, that is a set of kth hyperplanes in the order of y-axis, of above hyperplane arrangement corresponds to kth-order Voronoi diagram in both Euclidean and hyperbolic space where the y-axis is an adding axis, and we consider such a hyperplane arrangement in the space $[x_1, \ldots, x_d, y]$.

Hyperbolic Voronoi diagrams are also dealt with in [5, 6]. The difference between our approach is explained here. In [5] they consider the *pencil of sphere* and *identity between Euclidean and hyperbolic spheres*, that is, in d-dimensional hyperbolic space suppose two spheres

$$\Sigma_1 : \sum_{i=1}^{d-1}(x_i - p_i)^2 + (x_d - p_d \cosh r)^2 = (p_d \sinh r)^2, \quad \Sigma_2 : \sum_{i=1}^{d-1}(x_i - p_i)^2 + (x_d + p_d \cosh r)^2 = (p_d \sinh r)^2$$

and their pencil

$$\begin{aligned} \mathcal{F} &:= \{\Sigma : \exists \lambda \in \mathbb{R}, \forall X \in \mathbb{R}^d, \Sigma(X) = \lambda \Sigma_1(X) + (1-\lambda)\Sigma_2(X)\} \\ &= \left\{ \Sigma(X) = \sum_{i=1}^{d-1}(x_i - p_i)^2 + \{x_d - (1-2\lambda)p_d \cosh r\}^2 + {p_d}^2 - (1-2\lambda)(p_d \cosh r)^2. \right\} \end{aligned}$$

Its power function $\psi(\Sigma)$ becomes

$$\psi(\Sigma) := (C, C^2 - R^2) = (p_1, \cdots, p_{d-1}, (1-2\lambda)p_d \cosh r, p_d^2)$$

where C and R are the center and the radius of the sphere Σ, respectively. Thus, an increase of the x_d-coordinate corresponds to an increase of the radius of the hyperbolic sphere. The algorithm is designed by this fact. Therefore in the $(d+1)$-dimensional Euclidean space $[x_1, \ldots, x_d, y]$ consider the Euclidean potential function and the hyperplane arrangement to construct the Euclidean Voronoi diagram and then project the lower envelope with respect to the x_d-coordinate to the potential function parallel to x_d-axis. In addition, project that object to $\mathbb{H}^d$, and the structure becomes the hyperbolic Voronoi diagram.

Consequently, in [5, 6] a hyperbolic Voronoi diagram is computed by enlarging hyperbolic sphere: the intersection of hyperbolic spheres corresponds to the boundary of the hyperbolic Voronoi region. However, in our thesis we look at each Voronoi point and the identity of the sphere, to determine whether the point is included in the hyperbolic space. The relationship to the Euclidean hyperplane arrangement is thereby described and the property of the higher-order Voronoi diagram is also proved.

4.3 Dually Flat Space

This section deals with Voronoi diagrams in the dually flat space, is called ∇-Voronoi diagram and ∇^*-Voronoi diagram. The dually flat space was already described in Section 2.3. In that space, like in the Euclidean space, there are *potential functions* and *divergence*. In addition, since the relation between potential function and divergence can be also shown, some properties of potential function are proved. This work is an extension of [37, 38].

4.3.1 Voronoi Diagrams in Dually Flat Space

Firstly, these diagrams are defined by ∇-divergence and ∇^*-divergence.

Definition 4.4 (∇-Voronoi Diagram) *For a set of n points $\{p^{(j)} : j = 1, \ldots, n\}$ in the dually flat space, the Voronoi region $V(p^{(j)})$ of $p^{(j)}$ is defined by*

$$V(p^{(j)}) = \bigcap_{k \neq j} \left\{ p \;\middle|\; D(p \,\|\, p^{(j)}) < D(p \,\|\, p^{(k)}) \right\}.$$

$V(p^{(j)})(j = 1, \cdots, n)$ portions the dually flat space R, which is called the ∇-Voronoi diagram of these points.

Definition 4.5 (∇^*-Voronoi diagram) *The ∇^*-Voronoi diagram is defined by replacing*

$$D(p \,\|\, p^{(j)}) < D(p \,\|\, p^{(k)})$$

in the definition of the ∇-Voronoi diagram with

$$D^*(p \,\|\, p^{(j)}) < D^*(p \,\|\, p^{(k)}). \tag{4.6}$$

[Remark] Because the divergence does not satisfies the symmetry of the distance, two different Voronoi diagrams are defined in the dually flat space. However there is the relation (2.25), however, we can rewrite equation (4.6) using ∇-divergence:

$$D(p^{(j)} \,\|\, p) < D(p^{(k)} \,\|\, p).$$

Thus two Voronoi diagrams are defined, but the difference between these only is the direction of the divergence: from a generator to a point or from a point to a generator. Moreover the boundary of the $\nabla(\nabla^*)$-Voronoi region consists of the $\nabla(\nabla^*)$-geodesic segments, respectively.

The ∇- and ∇^*-Voronoi diagrams for a set of points might have the same structure as a face lattice but sometime their structures are different.

Example 4.1 ∇- and ∇^*-Voronoi diagrams for a set of points do not always have the same structure. For example, let $P = \{(-a, 1), (0, b), (a, 1) \mid a, b > 0,\ \sqrt{a^2+1} < b \leq e^a\}$ be a set of points in the statistical parametric space of one-dimensional normal distributions. In the ∇-Voronoi diagram for P there is a point equidistant from three points, but in the ∇^*-Voronoi diagram for P there is no such point (Fig. 4.7).

In this section we suppose that a dually flat space has a *global coordinate system* because unless there is such a coordinate system, we specify only a local property of a geometric structure.

Lemma 4.4 *The following conditions are equivalent in dually flat space:*

- *there exists a global coordinate system.*
- *there exists a unique potential function. That is, the function is defined over the entire space.*

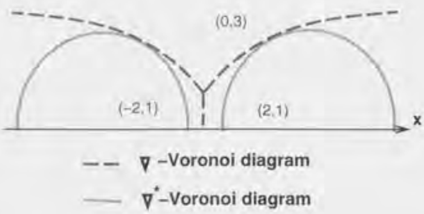

Figure 4.7: ∇- and ∇^*-Voronoi diagrams for P

Proof: Relations (2.20) specify the relation between the coordinate system and the potential function. In general, these relations are proved only in the local coordinate system. But if the coordinate system is global, this relation between the coordinate system and the potential function is expanded to the whole space, i.e., a unique potential function in the coordinate system is defined.

Conversely, if such a potential function exists, then its derivative becomes the global coordinate system. □

Example 4.2 *The statistical parametric space has a* global coordinate system. *Since the potential function in the parametric space is actually written, by the above lemma the space has a global coordinate system.*

4.3.2 ∇-Voronoi Diagram

In this section we specify the structure of the ∇-Voronoi diagram in the dually flat space R for n given point $\theta^{(j)}$. We also give an algorithm for the construction of the ∇-Voronoi diagram.

We suppose an additional axis y to R so that we can consider a space $[R, y]$ in which we consider n hypersurfaces

$$y = D(\theta \| \theta^{(j)}) \quad (j = 1, \cdots, n).$$

Lemma 4.5 *Suppose a point $\tilde{\theta}$, the potential function ψ in the dually flat space R, and a space $[R, y] = [\theta, y]$. The difference between $-\psi(\theta)$ and the value of the y-coordinate at*

θ in the tangent hyperplane of the potential function ψ at $\tilde{\theta}$ is equal to the ∇-divergence from θ to $\tilde{\theta}$.

Proof: The tangent hyperplane is expressed as

$$y = -\sum_i \left(\theta^i - \tilde{\theta}^i\right) \frac{\partial \psi(\tilde{\theta})}{\partial \theta^i} - \psi(\tilde{\theta}) = -\sum_i \left(\theta^i - \tilde{\theta}^i\right) \eta_i(\tilde{\theta}) - \psi(\tilde{\theta}).$$

Because the potential function is strictly convex and the tangent hyperplane is above the function, the difference becomes

$$\begin{aligned} -\sum_{i=1}^{d}(\theta^i - \tilde{\theta}^i)\eta_i(\tilde{\theta}) - \psi(\tilde{\theta}) - (-\psi(\theta)) &= \psi(\theta) + \varphi(\tilde{\theta}) - \sum_{i=1}^{d} \theta^i \eta_i(\tilde{\theta}) \\ &= D(\theta \| \tilde{\theta}). \end{aligned}$$

□

[Remark] This equation can also be proved in the Euclidean space. Recall the example of ∇- and ∇^*-divergence in Euclidean space, and the difference between the potential function and the tangent hyperplane becomes the half of the square of the Euclidean distance. This fact to show the relation between hyperplane arrangement and the Euclidean Voronoi diagram was used in [12, 42].

By the theory of Voronoi diagrams (e.g., see [12]), the projection of the lower envelope of that hyperplane arrangement becomes a Euclidean Voronoi diagram. In the dually flat space the projection of the lower envelope of these hypersurfaces to the space R becomes the ∇-Voronoi diagram. In the θ-coordinate system suppose a mapping from $[R, y]$ to itself by $[\theta, y] \mapsto [\theta, y - \psi]$. The hypersurface is mapped to

$$y = -\left(\sum_{i=1}^{d} \theta^i \eta_i(\theta^{(j)}) - \varphi(\theta^{(j)})\right).$$

This image of the hypersurface is the *hyperplane* in the space $[\theta, y]$. Because the $\theta^{(j)}$ is a generator and constant, the $\varphi(\theta^{(j)})$ is also constant. Moreover the map retains the above-below relation with respect to the y-direction because of the strictly convexity of potential function.

So we state next theorem.

Theorem 4.4 *For a set of n points $\{\theta^{(j)}\ ;\ j = 1, \ldots, n\}$ in the d-dimensional dually flat space with global coordinate system, a ∇-Voronoi diagram is the projection of the* *lower envelope of n hyperplanes*

$$y = -\left(\sum_{i=1}^{d} \theta^i \eta_i(\theta^{(j)}) - \varphi(\theta^{(j)})\right) \tag{4.7}$$

($j = 1, \ldots, n$) to the dually flat space R which is a subset of d-dimensional Euclidean space as a face lattice and hence the combinatorial complexity F is $O(n^{\lceil (d+1)/2 \rceil})$ and the time complexity is $O(F \log n)$.

Proof: The projection to R means $[\theta, y] \mapsto [\theta]$. As mentioned above, the original lifting-up map keeps the above-below relation is unchanged, and for the hyperplane for $\theta^{(j)}$ attaining the lower envelope at $[\theta]$,

$$\min_k D(\theta \| \theta^{(k)}) = D(\theta \| \theta^{(j)}).$$

To derive the combinatorial complexity, we apply the upper bound theorem for convex polytopes with n facets in the $(d+1)$-dimensional Euclidean space. To derive the time complexity, we can use any convex hull algorithm in computational geometry. □

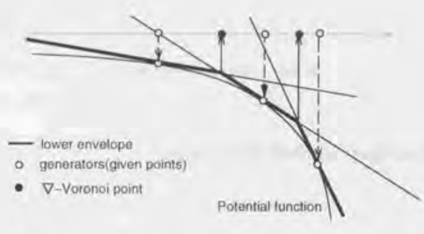

Figure 4.8: Potential function and the tangent hyperplane at each generator

By this theorem we have the following corollary.

Corollary 4.3 *Each Voronoi region of the ∇-Voronoi diagram is nonempty and it is a convex polyhedron in the θ-coordinate system, ignoring the part at infinity.*

Proof: Since each of Voronoi region is included in the generator, the space is nonempty. Moreover, in the θ-coordinate system, all of Voronoi regions consist of half-spaces of hyperplane. Thus the Voronoi region is convex and the polyhedron in the θ-coordinate system. □

The upper envelope, whose projection becomes the farthest ∇-Voronoi diagram, which is naturally defined, can be obtained. The higher-order Voronoi diagram is also defined in the space by ∇-divergence as same as in Euclidean. We can get the relation between the hyperplane arrangement and all higher-order ∇-Voronoi diagrams.

Corollary 4.4 (Higher-order ∇-Voronoi Diagram) *The hyperplane arrangement by equation (4.7) has the complete information of all higher-order ∇-Voronoi diagrams. In other words, the face lattice of the all higher-order ∇-Voronoi diagrams and of the hyperplane arrangement in the θ-coordinate system in the above theorem is the same except for some faces which is not included in the diagram.*

Proof: This corollary can be proved easily because by Lemma 4.5 and Theorem 4.4, the k-level of that hyperplane arrangement corresponds to the kth-order ∇-Voronoi diagram.

It should be noted that the arrangement of hyperplanes in the theorem is defined in the whole θ-coordinate system $[\theta]$, regarding it as $\mathbb{R}^d$. The ∇-Voronoi diagran, however, is defined on $\theta(R)$, which may not be the whole $\mathbb{R}^d$, and may be a proper subset. In such a case, part $\mathbb{R}^d - \theta(R)$ should be cut out, via the projection to R stated in the theorem. □

Moreover, the complexity of the kth-order ∇-Voronoi diagram is bounded.

Corollary 4.5 *For a set of n points in the d-dimensional dually flat space with a global coordinate system, the combinatorial complexity of the kth-order ∇-Voronoi diagram is $O(k(n-k))$ when $d = 2$ and is $O(n^{\lfloor d/2 \rfloor} k^{\lceil d/2 \rceil + 1})$ when $d \geq 3$.*

Proof: The face lattice of the kth-order ∇-Voronoi diagram corresponds to the k-level of above hyperplane arrangement (Corollary 4.4). Thus its combinatorial complexity is bounded by the k-level of the hyperplane arrangement when $d \geq 3$ [10].

A proof of the bound on combinatorial complexity when $d = 2$ given in [26, 12]. The essence of that proof is based on the following:

- the correspondence between the kth-order Voronoi diagram and the k-level of the hyperplane arrangement;

- the graph of the upper (or lower) part of any cell in the k-level is connected, planar and no cycles without the upper graph of the topmost cell and the lower graph of the bottommost cell;

  and

- the Euler relation for planar graph.

So the hyperplane arrangement (4.7) also satisfies these conditions above, because the first is already stated and the second is proved similarly as in Euclidean. In addition, since the hyperplane arrangement is regarded as Euclidean, the Euler relation can be used.

More specifically, the analysis in [12] can be applied to the hyperplane arrangement for n tangent hyperplanes of a strictly convex function. □

The following algorithm can be used to generate the ∇-Voronoi diagram in the dually flat space.

Algorithm (∇-Voronoi diagram)

```
1. Map the given set of points to the θ-coordinate system.
2. Construct the Voronoi diagram for such points by using the potential
   function ψ, i.e, by computing a tangent hyperplane arrangement of
   the transformed set and projecting the arrangement to θ-space.
3. Remove faces which are not included in ∇-Voronoi diagram.
```

Steps 1 and 2 are already explained however in Step 3 we decide which face is included in ∇-Voronoi diagram. That face can be determined by the following theorem.

Theorem 4.5 *In the space $[R, y] = [\eta, y]$, consider the lower boundary of the ∇^*-convex hull of n points $[-\eta^{(j)}, -\psi(\eta^{(j)})]$ $(j = 1, \ldots, n)$ by regarding this space as the $(d+1)$-dimensional Euclidean space. In the face lattice of the lower boundary of this convex hull, delete each face which does not have a supporting hyperplane at the face (i.e., hyperplane containing this face and all other points not in this face are located in one proper side of the hyperplane) given by $-\sum_{i=1}^{d} \eta_i \theta^i + c$ for $\theta = \theta(q)$ with some $q \in R$ and a constant c.*

Then the sublattice consisting of the remaining faces on the lower boundary of the convex hull is dual to the lattice of the ∇-Voronoi diagram.

Proof: This is basically the point-hyperplane duality sometimes called polarity (e.g., see [12, 42]). That is the hyperplanes (4.7) are regarded as the points in the η-coordinate system. Since this polarity keeps the above-below relation unchanged, the lower part of the hyperplane arrangement maps the lower part of the convex hull of those points. Thus the lower boundary of the convex hull in the dual space contains all the information of the ∇-Voronoi diagram. However some part of this ∇-Voronoi diagram, i.e., if the supporting hyperplane of such face does not satisfy the above equation, such face is not included in the ∇-Voronoi diagram. □

So we define *unbounded region* in the dually flat space and the hyperbolic space.

Definition 4.6 *Let R be a region in the dually flat space (hyperbolic space). That region is* unbounded *if when a point p in R and a direction are given, then the geodesic from p with that direction is contained in R and for any point q on the geodesic there exists a point r on the geodesic s.t. $D(p \| q) < D(p \| r)$ ($d(p,q) < d(p,r)$), respectively. In other words, such a geodesic can be extended infinitely in the direction.*

Example 4.3 *In the statistical parametric space of the normal distribution (Example 2.6) there is an* infinite boundary*. That is, in the η-coordinate system $R = \{(\eta_1, \eta_2) \| \eta_2 > {\eta_1}^2\}$ and its boundary becomes*

$$\eta_2 = {\eta_1}^2.$$

So the divergence from any point to boundary point increases (see equation (2.26)).

Lemma 4.6 *If a region in the dually flat space with global coordinate system has a part of the infinite boundary, then the region is unbounded.*

Proof: In that space there is a potential function s.t. that function is defined only in the space and its value at a point on the infinite boundary diverges. The divergence is the difference between potential function and its conjugate function (Definition 2.26). Therefore the value of divergence also diverges at such a point. So suppose a point in the region with a part of infinite boundary and a direction to the infinite boundary, then the geodesic from that point can be extended. Thus that region is unbounded. □

We next give a theorem characterizing unbounded Voronoi regions.

Theorem 4.6 *1. In Theorem 4.5, in the space $[R, y] = [\eta, y]$, consider the face lattice of the whole lower boundary of the ∇^*-convex hull of n points $[-\eta^{(j)}, -\varphi(\eta^{(j)})]$ $(j = 1, \ldots, n)$.*

Then the Voronoi region of $\theta^{(j)}$ is unbounded in R iff there exists a sequence of points $\theta^{(l)} \in R$ diverging to infinity in R and constants $c^{(l)}$ such that $-\sum_{i=1}^{d} \theta^{(l)i}\eta_i^{(j)} + c^{(l)}$ is a supporting hyperplane to the hull at $[-\eta^{(j)}, -\varphi]$.

2. If $\eta^{(j)}$ is on the boundary of the ∇^*-convex hull of $\eta^{(k)}$ $(k = 1, \ldots, n)$, the Voronoi region of $\theta^{(j)}$ is unbounded in R.

Proof: It should be noted that the boundary of the space is regarded as being at infinity, i.e., the divergence from any point in the space to a boundary point diverges to infinity. These results are based on the duality between θ- and η-coordinate systems. Then (1) is basically characterizes unbounded Voronoi regions in the dual setting.

As for (2), $\theta^{(j)}$ has an unbounded region when the lower hull in Theorem 4.5 is projected to $[\theta]$ regarded as $\mathbb{R}^d$. Then, restricting $\mathbb{R}^d$ to $\theta(R)$, it remains unbounded. □

It should be noted that the converse of (2) in this theorem is not necessarily true.

We now compare the ∇-Voronoi diagram with the Euclidean Voronoi diagram. For n points $\xi^{(j)}$ $(j = 1, \ldots, n)$ in $\mathbb{R}^d$, by considering an additional axis y, the Euclidean Voronoi diagram is the projection to the original space of the lower envelope of the tangent hyperplanes at $\xi^{(j)}$ to a parabolic surface $y = \frac{1}{2}\|\xi\|^2$, where $\|\cdot\|$ is the L_2 norm. Its dual structure, the Delaunay triangulation, is the projection to the original space of the lower convex hull of points $(\xi^{(j)}, \frac{1}{2}\|\xi^{(j)}\|^2)$.

Thus, by making correspondence between $y = \psi(\theta)$ and $y = \frac{1}{2}\|\xi\|^2$ and recalling $\partial^i\varphi = \theta^i$ and $\varphi + \psi = \sum_{i=1}^{d} \theta^i\eta_i$, everything corresponds to each other, except that in the ∇-Voronoi diagram the part of the lower envelope of $\mathbb{R}^d - \theta(R)$ is meaningless.

This may be viewed as a computational-geometric interpretation of the dual connection and dually flat space formed by the Kullback-Leibler divergence [1, 3], or we should say that this is an implication of the Legendre transformation.

4.3.3 ∇^*-Voronoi Diagram

In this section we investigate the ∇^*-Voronoi diagram on the manifold R for n given points in the dually flat space. By the duality between θ and η, everything carries over when their roles are interchanged.

By considering the map

$$[\eta, y] \mapsto [\eta, y - \varphi]$$

and hyperplanes $y = -\left(\sum_{i=1}^{d} \theta^i(\bar{\eta})\eta_i - \psi(\bar{\eta})\right)$, we can rewrite theorem 4.4 for the ∇^*-Voronoi diagram.

Theorem 4.7 *For a set of n points $\{\eta^{(j)} ; j = 1, \ldots, n\}$ in the d-dimensional dually flat space with global coordinate system, the ∇^*-Voronoi diagram is the projection of the lower envelope of n hyperplanes*

$$y = -\left(\sum_{i=1}^{d} \theta^i(\eta^{(j)})\eta_i - \psi(\eta^{(j)})\right) \tag{4.8}$$

$(j = 1, \ldots, n)$ to the dually flat space R which is a subset of d-dimensional Euclidean space as a face lattice and hence the combinatorial complexity F is $O(n^{\lceil(d+1)/2\rceil})$ and the time complexity is $O(F \log n)$.

Other corresponding theorems can be obtained similarly. In fact, from the viewpoint of convex analysis, these duality results can all be regarded as results of the Legendre transform between θ- and η-coordinate systems. Since we are treating a finite set of 'points', these dualities correspond completely to the well-known duality results in computational geometry.

In the dually flat space, the ∇- and ∇^*-Voronoi diagrams are characterized by the potential functions ψ and φ, respectively. Thus these diagram is based on the potential functions. Suppose a twice differentiable and strictly convex function $\psi(\theta)$ on the space R. A discussion similar to the one above applies: the divergence is defined by ψ, and the *conjugate function* φ of ψ and the η-coordinate system are defined like this :

$$[\eta_i] := \frac{\partial \psi}{\partial \theta^i}, \quad [\eta] = \left\{ \frac{\partial \psi(\theta)}{\partial \theta}; \theta \in R \right\}.$$

Therefore these theories can be considered to be a kind of convex analysis ([45]).

4.4 Relation of Hyperbolic, ∇- and ∇^*-Voronoi Diagram

In the previous sections we described about the hyperbolic Voronoi diagram (Section 4.2) and the ∇- and ∇^*-Voronoi diagram (Section 4.3). Each structure is independently defined, but there is a relation between them.

We first deal with the relation between the metric and the divergence.

Lemma 4.7 *The infinitesimal change of divergence approximates the sum of the Fisher metric ignoring the higher-order part. That is,*

$$D(\theta + d\theta \| \theta) = \sum_{i,j} g_{ij} d\theta^i d\theta^j + O((d\theta)^3).$$

Proof: By expanding $D(\theta + d\theta \| \theta)$ at θ, we get

$$\begin{aligned} D(\theta + d\theta \| \theta) &= \sum_{i,j} \partial_i \partial_j \psi(\theta) \mathrm{d}\theta^i d\theta_j + O((d\theta)^3) \\ &= \sum_{i,j} g_{ij} d\theta^i d\theta^j + O((d\theta)^3). \end{aligned}$$

□

So we get the relation that the infinitesimal change of ∇-divergence equals the sum of the metric and the change of the third order. Moreover the third order is used as a *connection* in the dually flat space.

For the ∇^*-divergence the following relation is also proved:

$$D^*(\eta + d\eta \| \eta) = \sum_{i,j} g^{ij} d\eta_i d\eta_j + O((d\eta)^3).$$

[**Remark**] This relation for Kullback-Leibler divergence is already shown in [44].

Now we explain the relation between the parametric space of one-dimensional normal distributions with Levi-Civita connection [36] and with dual connection. We consider n one-dimensional normal distributions $p^{(j)}$ with $[\mu^{(j)}, \sigma^{(j)}]$ $(j = 1, \ldots, n)$. We simply call the Voronoi diagram by Fisher metric with the Levi-Civita connection *hyperbolic Voronoi diagram* [36].

In the case of Euclidean Voronoi diagrams of points, unbounded Voronoi regions are characterized by the convex hull of given points. That is, the Voronoi region of a point is unbounded iff it is on the boundary of the convex hull (e.g., see [12, 42]). As we have seen so far, the ∇-Voronoi, ∇^*-Voronoi, and hyperbolic Voronoi diagrams all have polytopal structure, where the convexity plays a crucial role. In connection with the convexity, we analyze unbounded Voronoi regions in these diagrams and compare their properties.

We consider points with the largest σ value among given points in the $[\mu, \sigma]$ upper-half plane, and we show that the ∇^*-Voronoi and hyperbolic Voronoi diagrams share similar structure for these points because their geodesic is regarded as the same. Let

$$P_{\max} = \left\{ p^{(j)} \,\middle|\, \sigma^{(j)} = \max_k \sigma^{(k)} \right\}.$$

Theorem 4.8 *In both the* ∇^**-Voronoi and hyperbolic Voronoi diagrams, the following hold.*

1. *When* $|P_{\max}| = 1$, *for any* σ *and* $\mu = \pm M$ *with sufficiently large* $M > 0$, *a point* $[\mu, \sigma]$ *belongs to the Voronoi region of* $p^{(j)} \in P_{\max}$.

2. *Otherwise,* $|P_{\max}| > 1$. *For any* σ *and* $\mu = M$ ($\mu = -M$, *respectively) for sufficiently large* $M > 0$, $[\mu, \sigma]$ *belongs to the Voronoi region of* $p^{(j)} \in P_{\max}$ *with* $\mu^{(j)}$ *maximum (minimum, respectively). For sufficiently large* σ, *the Voronoi regions are ordered in the increasing order of* $\mu^{(j)}$ ($p^{(j)} \in P_{\max}$) *with Voronoi edge parallel to the* σ*-axis in the* $[\mu, \sigma]$*-plane.*

Proof: Voronoi edges are upper circular arcs in both cases, and then checking the equation of hyperbolic space and the parametric space of one-dimensional normal distribution, we obtain the theorem. □

Thus, at infinity except on the μ-axis in the $[\mu, \sigma]$-plane, the ∇^*-Voronoi and hyperbolic Voronoi diagrams have the same structure.

With regard to the μ-axis at infinity, for unbounded Voronoi regions in ∇^*-Voronoi diagram, Theorem 4.6 shows that the convex hull in the η-coordinate system provides a subset of points whose Voronoi regions are unbounded (it also gives a complete characterization for the unboundedness, which cannot be interpreted directly from the convexity).

We previously defined the convexity and the convex hull in Poincaré space [36], but this convex hull does not characterize unbounded Voronoi regions in the hyperbolic Voronoi diagram. For example, there is a case in which points in $P_{\max}$ characterized in Theorem 4.8 are not on the boundary of this convex hull. Thus, situation here is very different from that in the Euclidean case. Using results of Onishi and Takayama [40], we have for this case the following theorem corresponding to Theorem 4.6.

Theorem 4.9 *1. Consider the Delaunay triangulation of given points in* $\mathbb{H}$ *in the ordinary Euclidean sense. Delete each edge of the Delaunay triangulation such that there is no circle which passes the two endpoints of the edge, does not contain any given point in its inside, and is contained in* $\mathbb{H}$. *The remaining skeleton is connected, and the Voronoi regions of points incident to the outer-face in this skeleton are unbounded.*

2. *The Voronoi region of a point on the boundary of a convex hull of given points in the ordinary Euclidean manner is unbounded.*

Proof: (1) That skeleton becomes a *Delaunay graph* [40]. The upper edge and interior part of the skeleton is equal to a Delaunay graph because the circumscribed circle is for the triangle of Delaunay triangulation in the ordinary Euclidean manner. Moreover, the deletion of the lower edge of the skeleton and the removed edge of the Delaunay graph are the identity.

When the lower edge of skeleton is removed, the edge is the removed edge of the Delaunay graph [40].

Conversely, suppose an deleted edge, whose end points are $p^{(1)}, p^{(2)}$ and a triangulation which contains that edge on the boundary. Let the rest point of the triangle be p. This triangle is deleted and the lower edge is also erased. We show that the edge is the removed edge of the skeleton. The centers of circles through $p^{(1)}, p^{(2)}$ are on the perpendicular bisector l of the segment. If that circle contains no other given points, then p also is not included. Therefore the center is on l and nearer to the boundary $\sigma = 0$ of the space than is the center of the Euclidean circumscribed circle for the triangle. Thus the circumscribed circle becomes large and is not contained in $\mathbb{H}$. Consequently, there is no circle with the condition.

The Delaunay graph is the dual structure of hyperbolic Voronoi diagram and Voronoi region always contacts with other region, then the connectivity of skeleton is proved.

In addition, the Voronoi region of a point incident to the outer-face in the skeleton is unbounded for upper or intersects with the boundary of the space. In the former case the geodesic can be extended to the upper direction. In the latter case, if the distance is regarded as the parameter, then the length of the geodesic is infinite because of the metric. Thus if the region is tangent to $\sigma = 0$, it is unbounded.

The geodesic segment of the half-circle type that does not cross the other geodesic always comes near $\sigma = 0$. The boundary (geodesic segment) of such a Voronoi region intersects at $\sigma = 0$ and its region becomes unbounded.

(2) is basically implied by (1). □

Thus, in the ∇^*-Voronoi diagram case the convex hull in the η-coordinate system provides partial information for unbounded Voronoi regions, whereas in the hyperbolic Voronoi diagram case the convex hull in the original $[\mu, \sigma]$-plane does. In both cases, to completely characterize the unbounded Voronoi regions, some faces are removed from the convex hull. For this, the hyperbolic Voronoi case provides more intrinsic features, and it would be required to obtain such characterizations in the ∇^*-Voronoi diagram case.

Chapter 5

Delaunay-type Triangulation

In this chapter special triangulations, called *Delaunay* and *Delaunay-type* triangulations are described. These triangulations are useful in the finite element method, mesh generation, etc. We discuss their property and construction, and we explain the relations between these triangulations and Voronoi diagrams.

5.1 Triangulation in Riemannian Space

Triangulation is a partition of a geometric domain into simplices that meet only at shared faces, i.e., for given polygon into simplices and for given surface into triangles. These triangulations are used in the means of computer graphic, mesh generation, finite element method, analysis of manifold, etc.

Firstly, we state that d-dimensional convex hull for a finite set of points is called *d-polytope*. By this object we define the subdivision in the space.

Definition 5.1 (Subdivision) *Suppose V is a finite set of points such that $P = \mathrm{CH}(V)$ is d-polytope. A subdivision of V is a finite collection $S = \{P_1, \ldots, P_m\}$ of d-polytopes such that:*

- *The vertices of each P_i are points in V;*
- *Every points in V is used as a vertex of some P_i;*
- *P is the union of $P_1, \ldots, P_m$;*

  and
- *If $i \neq j$, then $P_i \cap P_j$ is a common face of the boundaries of P_i and P_j.*

Triangulation is a special subdivision and defined like this.

Definition 5.2 (Triangulation) *A subdivision T is a triangulation if each d-polytope P_i of T is a d-simplex, i.e., that is d-polytope with $d+1$ vertices.*

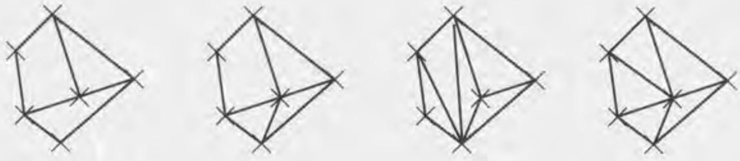

Figure 5.1: Subdivisions (A) not subdivision (B) subdivision (B) triangulation (D) Delaunay triangulation

Since above definition of triangulation depends on *convex hull* in the space, if convex hull is not defined, *triangulation* cannot be also defined. So we suppose that the space has a *global coordinate system* and convex hull can be constructed.

The vertices of triangulation is given in the above definition. However more general triangulation is defined for any surface, for example torus, projective plane, etc. In that triangulation all region are triangles and every point can move around. Therefore the triangulation is a topological object. There is an interesting result for such triangulation in [34]: "for any closed surface, two triangulation are equivalent to each other under diagonal flip, if the number of point is sufficiently large."

There are many triangulations for given points in the domain however Delaunay triangulation is the most famous and useful triangulation. Here, we define Delaunay triangulation.

Definition 5.3 (Delaunay triangulation) *For given set of points P in the d-dimensional Euclidean space, a triangulation of P is the* Delaunay triangulation Del(P), *if no points is included in the circumscribed sphere of any d-simplex of* Del(P).

In the Euclidean space this triangulation is a dual structure of Voronoi diagram, by this relation various theorems are investigated. In particular, two-dimensional Delaunay triangulation has some nice properties [4] :

Figure 5.2: Delaunay triangulation and Voronoi diagram in Euclidean space

- minimizes the maximum radius of a circumscribed circle;
- maximizes the minimum angle;
- minimizes the maximum radius of a minimum enclosing circle;

  and
- maximizes the sum of inscribed circle radii.

The third property is also proved in the high-dimensional Euclidean Delaunay triangulation by *potential function* in [43].

In this chapter we deal with *Delaunay-type triangulation*, i.e., the triangulation like a Delaunay triangulation in some Riemannian spaces. Delaunay-type triangulation in the hyperbolic space is described in Section 5.2. In that space the dual of the hyperbolic Voronoi diagram, called *hyperbolic Delaunay graph*, which is already defined in Section 4.2, is not always triangulation. However that structure has nice properties, we firstly state its properties. In addition, *Delaunay-type triangulation* in that space is defined so that hyperbolic Delaunay graph is included.

In Section 5.4 two Delaunay-type triangulations in the dually flat space, called ∇- and ∇^*-*Delaunay-type triangulations*, are defined. That triangulation is not the dual of ∇-Voronoi diagram but the lower boundary of a certain convex hull. Those triangulations have a nice property, i.e., the radius of maximum minimum enclosing $\nabla(\nabla^*)$-sphere in the $\nabla(\nabla^*)$-Delaunay-type triangulation minimize among all other triangulation by $\nabla(\nabla^*)$-divergence as a measure, respectively.

5.2 Hyperbolic Space

In Section 4.2 we use the Delaunay graph, which is not a triangulation but a graph. In this section we obtain *Delaunay graph* and *Delaunay-type triangulation* in the hyperbolic space (Definition 5.3). The former is a subset of triangulation, but the latter is a subdivision of the convex hull of a set of given points and each dimensional faces exist.

5.2.1 Hyperbolic Delaunay Graph

The hyperbolic Delaunay graph is already defined in Definition 4.3. However we do not described its properties. In here, we state that the graph has so nice in the hyperbolic space.

To explain Delaunay graph *reverse simplex* is defined.

Definition 5.4 *In the d-dimensional hyperbolic space for non-degenerate $(d+1)$ points select d points. Let h, g be a hyperplane and a hyperbolic plane of selected points, respectively (these surfaces are unique for the points). If the unselected point p is contained in the intersection of the halfspaces of h, g, i.e., p stay the upper part of h and is contained in the interior of g, then the point is called* reverse point *and the d-simplex of given points is* reverse

Figure 5.3: Euclidean and reverse simplex

The Delaunay graph has the following property.

Proposition 5.1 *There is no reverse simplex in the Delaunay graph.*

Proof: Firstly we prove this lemma in Poincaré space, which is two-dimensional hyperbolic space. In the upper part of Delaunay graph there is no reverse simplex because that is subgraph of Delaunay triangulation as a face lattice, i.e., if such triangle exists, then that triangulation is not Delaunay triangulation for given points. Thus we deal with only the lower part of Delaunay graph.

This space is regarded as a subset of Euclidean space. Suppose three points $p^{(1)}, p^{(2)}, p^{(3)}$ is given. Let $\mathcal{C}$ be a set of the Euclidean circle which is through $p^{(2)}, p^{(3)}$. The centers of these circles lie on the perpendicular bisector of two points $p^{(2)}, p^{(3)}$. If the triangle is reverse, then x_2-coordinate of the center of the circle becomes negative. Suppose that $p^{(1)}$ move on that perpendicular bisector from infinity of x_2-coordinate. The x_2-coordinate of the center of that circle is equal to 0 if and only if that circle and the geodesic through three points in the Poincaré space are the same. Therefore the center of such circle is not included in Poincaré space, i.e., Voronoi point is also excluded. Thus the corresponding triangle is not included in Delaunay graph.

In the hyperbolic space this lemma is proved by the restriction to the Poincaré space. □

[Remark] The reverse simplex is mostly "skinny", i.e., the ratio of the base to the height is so large for the simplex. In sometime, Euclidean Delaunay triangulation contains such simplices near the boundary and Delaunay graph is made from that triangulation by removing such simplices. In the finite element method it is so good that there is no such skinny simplex, i.e., the Delaunay graph is more nice geometric structure rather than Euclidean Delaunay triangulation.

However removed simplex is not only reverse. Non-reverse triangle is also remove from the Euclidean Delaunay triangulation. Thus the difference Euclidean Delaunay triangulation and Delaunay graph is not only reverse triangulation.

The Delaunay graph is also characterized by the following lemma.

Proposition 5.2 *There is no point of interior of circumscribed circle (respectively hypersphere) of any triangle (respectively d-simplex) in the Delaunay graph.*

Proof: For given $d+1$ points the circumscribed circle in the Euclidean space coincide with the hyperbolic sphere in the hyperbolic space. Since this lemma is proved in the Euclidean space, also in the hyperbolic space. □

Moreover the property about the minimum spanning tree is shown. That tree is defined like this.

Definition 5.5 (Minimum Spanning Tree) *For a finite set of points P suppose a complete weight graph G, whose edge is a geodesic and its weight is given by the hyperbolic distance between two end points. A spanning tree is a minimum spanning tree if the sum of the weight of edges minimize among all spanning tree of G.*

Proposition 5.3 *Delaunay graph contains minimum spanning tree as the hyperbolic distance.*

Proof: The Delaunay graph is the dual structure of hyperbolic Voronoi diagram. In that diagram we prove above lemma i.e., for a given set of points P suppose its hyperbolic Voronoi diagram. The following facts are equivalent for $p^{(i)}, p^{(j)} \in P$:

- The perpendicular bisector for $p^{(i)}, p^{(j)}$ is contained in the hyperbolic Voronoi diagram;
- There is a edge $p^{(i)}, p^{(j)}$, which is a geodesic segment connecting these two points, in the Delaunay graph.

Because of the duality between these structure. In addition, we prove this fact. "For any partition S_1, S_2 of P a minimum geodesic segment l_{12} connecting $p^{(1)} \in S_1$ and $p^{(2)} \in S_2$ is contained in the Delaunay graph." In the other words, $\mathrm{Vor}(p^{(1)})$ and $\mathrm{Vor}(p^{(2)})$ are adjacent. Suppose the l_{12} is a minimum geodesic segment but $\mathrm{Vor}(p^{(1)})$ and $\mathrm{Vor}(p^{(2)})$ are not adjacent. In this case, there is another generator $p^{(3)}$ included in a sphere whose diameter is l_{12}. Let c be the center of that sphere. If $p^{(3)}$ is included in S_1, then

$$d(p^{(2)}, p^{(3)}) \leq d(c, p^{(3)}) + d(c, p^{(2)}) < d(c, p^{(1)}) + d(c, p^{(2)}) = d(p^{(1)}, p^{(2)}).$$

This is a contradiction with the minimum of l_{12}. In case of $p^{(3)} \in S_2$ the contradiction is similarly shown. Thus $\mathrm{Vor}(p^{(1)})$ and $\mathrm{Vor}(p^{(2)})$ are adjacent.

Since for any partition its minimum edge is contained in the hyperbolic Voronoi diagram, the collection of these minimum edges becomes minimum spanning tree. □

This structure has these good properties however is not always triangulation of the convex hull for given points (at times this structure becomes triangulation).

5.2.2 Delaunay and Delaunay-type Triangulation

Delaunay triangulation in the hyperbolic space is defined by replacing the Euclidean space in Definition 5.3 to the hyperbolic space $\mathbb{H}^d$. However the Delaunay triangulation in the hyperbolic space does not always exist.

Example 5.1 For a set of points Delaunay triangulation in the hyperbolic space does not necessarily exist.

For a set of points $P = \{(0,12),(0,1),(\pm 10,11),(\pm 20,1)\}$ in the two-dimensional hyperbolic space. The circumscribed circles in the Euclidean is equal to that in the hyperbolic space (Lemma 2.4). However the circumscribed sphere of $\{(0,1),(20,1),(10,11)\}$ is not included in $\mathbb{H}$ (this circle is included in the Euclidean space and the triangle becomes a element of Delaunay triangle).

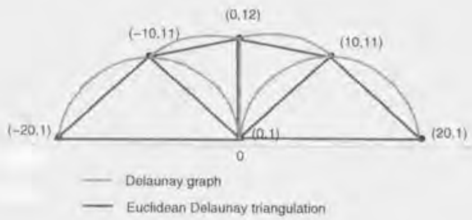

Figure 5.4: Euclidean Delaunay triangulation and hyperbolic Delaunay graph

So we propose a triangulation for a set of points, called *Delaunay-type triangulation*. That is defined by the following algorithm.

Algorithm 5.1 (Delaunay-type Triangulation)

Input : `a set of points` P `in the` d`-dimensional hyperbolic space;`

Output : `Delaunay-type triangulation;`

1. `Construct Delaunay graph H-Del(`P`) and convex hull CH(`P`);`
2. `For ∀` d `points in` P`, suppose minimum enclosing sphere` C `and` d`-simplex` T `by the` d `points;`

```
        Calculate the radius by hyperbolic distance;
        Count the number of included points in the sphere except for the
        d points;
    Suppose 𝒞 = {C = (i, r) ; ∀d points in P };
    /* 𝒞 is the set of minimum enclosing spheres */
3. 𝒯 := { all d-simplices included in the hyperbolic Delaunay graph};
    /* T is the set of d-simplices */
    R := ∪_{T∈𝒯} T; /* regions of hyperbolic space */
4. if (CH(P)=R);
        Output 𝒯; end;
    end;
5. while (𝒞 ≠ ∅) do
        C ∈ 𝒞 s.t.  C is the smallest term of 𝒞 by the order;
        𝒞 = 𝒞 \ C;
        if (C ∩ R = ∅ without boundary)
            𝒯 = 𝒯 ∪ {T}; R = R ∪ T;
            if (CH(P)=R);
                Output 𝒯;
            end;
        end;
    end;
```

The order of C is defined like this: $C_1 = (i_1, r_1) < C_2 = (i_2, r_2)$ if and only if $i_1 < i_2$ or ($i_1 = i_2$ and $r_1 < r_2$).

By this algorithm at least a triangulation is constructed. That triangulation based on minimum enclosing sphere for d-simplex and contains all simplices of the hyperbolic Delaunay graph. That is a kind of greedy algorithm.

Lemma 5.1 *This triangulation contains all simplices of hyperbolic Delaunay graph.*

Proof: The initial $\mathcal{T}$ contains all simplices and these are not removed. Thus the output, which is Delaunay graph, invariably contains all simplices of hyperbolic Delaunay graph. □

However it does not know that Delaunay-type triangulation has other properties. In Euclidean space this algorithm is given the Delaunay triangulation. Because Delaunay graph is equal to Delaunay triangulation in the Euclidean space.

5.3 Poincaré Space

In this section triangulation for given points in the Poincaré space is dealt with. Poincaré space is a subset of Euclidean space as a point set and some properties about triangulation in the two-dimensional Euclidean space was shown, i.e., in that space some properties of triangulation may be proved similarly.

Here, we consider a connectivity of some triangulations by diagonal flip. The edge flipping for triangulation in the Poincaré space is defined as follows.

Definition 5.6 *For any convex quadrangle, that is, convex hull for four points and there is no points in its interior, the operation which change the diagonal of quadrangle is called* edge flipping. *Two triangulation is* flippable *if one can be obtained from the other by a sequence of flips.*

For a class of triangulation of given points following theorem can be proved.

Theorem 5.1 *For given set of points all triangulations without reverse triangle are* flippable *in the Poincaré space. Thus by diagonal flip any triangulation without reverse triangle transforms into others.*

Proof: In the Poincaré space any geodesic is transformed to line by linearization (3.1). Thus all triangulation in the Poincaré space, except reverse triangulation, becomes a certain triangulation in Euclidean space. If there is a reverse triangle, such triangle is *reflected* by linearization. By the reflection some triangles may intersect. However if such triangle is not included in the triangulation, the structure equal to Euclidean. Since all Euclidean triangulation is flippable, by corresponded diagonal flip the triangulation without reverse triangle in Poincaré space also is flippable. □

[Remark] In the three-dimensional hyperbolic space there exists a counter example of this theorem. That example is made from the inverse mapping of Euclidean counter example. Thus in $d(\geq 3)$-dimensional hyperbolic space all triangulation is not flippable.

For the Delaunay graph and Delaunay-type triangulation is the two dimensional space and the angle (Definition 3.3) is also defined. Thus it is the problem that the following properties for Delaunay-type triangulation:

- minimizes the maximum radius of a circumscribed circle;
- maximizes the minimum angle;
- minimizes the maximum radius of a minimum enclosing circle;

  and

- maximizes the sum of inscribed circle radii.

5.4 Dually Flat Space

In this chapter we obtain *Delaunay-type triangulation* in *dually flat space*. So we already described the convex hull (Section 3.2) and the Voronoi diagram (Section 4.3), in those section suppose the existence of global coordinate system. Since these structures are used in this section, we also suppose the existence of global coordinate system in this section. Therefore the triangulation is defined by replacing the Euclidean space in Definition 5.1, 5.2 to the dually flat space.

Moreover the Delaunay triangulation is similarly defined as Euclidean (Definition 5.3). However some parts of the circumscribed sphere of the simplex of the Delaunay triangulation is not included, which parts correspond to removing faces in the ∇(or ∇^*)-Voronoi diagram. Such structure may not be a triangulation since there are some deleted parts. Since the convex hull for given points is included in the space, triangulation, which is a subdivision of the convex hull, is also included. We define *Delaunay-type triangulation* in the dually flat space, i.e., we define a triangulation which is based on the not circumscribed sphere but potential function. Not only the properties of Delaunay-type triangulation but the relations between this triangulation and Voronoi diagram are described. This property already proved in Euclidean space [43] and we prove this theorem based on the paper.

First we define ∇- and ∇*-*Delaunay-type triangulations*. In the dually flat space there exist *potential functions* that can be used to construct Voronoi diagrams. We can also use potential functions to construct the triangulation. For given points consider the θ-coordinate system and suppose a potential function ψ. By adding one axis y to $[\theta]$, we consider $[\theta, y]$ space. Then compute the value of potential function ψ at each point, i.e., lifting points $[\theta^{(i)}, \psi(\theta^{(i)})]$ and construct the ∇-convex hull for these points. When we project the upper envelope to the original space, the projection becomes a triangulation if any d points determine a hyperplane and any $k(> d)$ points are not on a hyperplane where d is the dimension of the space.

The above steps are summed up the following algorithm.

Algorithm 5.2 ($\nabla(\nabla^*)$-Delaunay-type Triangulation)
Input: a set of points in dually flat space;
Output: $\nabla(\nabla^*)$-Delaunay-type triangulation;

1. Lift up given points to potential function $\psi(\varphi)$.
2. Construct the $\nabla(\nabla^*)$-convex hull of these points in the $[\theta, y]([\eta, y])$-coordinate system.
3. Project the lower envelope of the convex hull to $\theta(\eta)$-coordinate system.

Here, we obtain the duality of ∇-Voronoi diagram and ∇*-Delaunay-type triangulation. In Theorem 4.5 we consider that diagram (lower envelope of hyperplane arrangement) and the dual structure *convex hull*. There is a *duality* between the ∇-Voronoi diagram in the θ-coordinate system and the ∇*-Delaunay-type triangulation in the η coordinate system. The duality can be understood as the correspondence between point and hyperplane in the two coordinate systems of dually flat space. The tangent hyperplane of ψ at p in the θ-coordinate system is expressed as

$$y = -\sum_{i=1}^{d} \theta^i \eta_i(p) + \varphi(p)$$

and is transformed to

$$(\eta_1, \eta_2, \cdots, \eta_d, -\varphi(p)).$$

Thus the hyperplane arrangement of given points in the coordinate system is transformed to the hyperplane arrangement whose hyperplane represents the *supporting hyperplane*, that is, the *facet* of the convex hull in the another coordinate. Moreover the projection of the upper envelope of the hyperplane arrangement is the $\nabla(\nabla^*)$-Voronoi diagram, and the projection of the lower envelope of the $\nabla^*(\nabla)$-convex hull is the $\nabla^*(\nabla)$-Delaunay-type triangulation. Therefore there also exists duality between the ∇-Voronoi diagram and the ∇^*-Delaunay-type triangulation.

Theorem 5.2 (Duality) *For given points in a dually flat space with global coordinate system, there is the relations between $\nabla(\nabla^*)$-Voronoi diagram, containing removed faces, and $\nabla^*(\nabla)$-Delaunay-type triangulation, respectively, called* duality *between these structures. The duality is given by transformation $\mathcal{D}$ from $[\eta, y]$ to $[\theta, y]$:*

$$\mathcal{D} : [\eta, -\varphi] \longleftrightarrow y = -\sum_i \theta^i \eta_i(p) + \varphi(p).$$

Moreover, $\nabla(\nabla^*)$-divergence is preserved by $\mathcal{D}$.

Proof: We prove the duality only of the ∇-Voronoi diagram and the ∇^*-Delaunay-type triangulation. Another correspondence that between the ∇^*-Voronoi diagram and the ∇-Delaunay-type triangulation is similarly shown. When removed faces may exist in the ∇-Voronoi diagram, we consider the whole projection of the upper envelope of hyperplane arrangement in θ-coordinate system. We already explained that the structure is transformed to ∇^*-Delaunay-type triangulation.

So we state that the divergence is not changed by $\mathcal{D}$. Suppose a map from the tangent hyperplane of a potential function to the tangent point. This map is a bijection because the potential function is strictly convex. Since $\mathcal{D}$ is also a bijective from point to hyperplane, we can get the bijection from θ to η. Therefore, by the definition of divergence (Definition 2.26), the ∇-divergence is unchanged □

The duality in Euclidean space is easily understood. The two coordinate systems are the same and the two potential functions are also the same. Therefore the duality $\mathcal{D}$ is from $[\xi, y]$ to $[\xi, y]$ and the function from $[\xi]$ to $[\xi]$ is identity. Then the duality can be considered in the one coordinate system.

To describe the properties of Delaunay-type triangulation, we define some geometric structures in the dually flat space.

Definition 5.7 (∇-gravity Point, ∇-circumcenter, ∇-sphere, and ∇-circumscribed Sphere *Suppose points $\{p^{(j)}; j = 1, \ldots, n\}$ in the d-dimensional dually flat space.*

∇-gravity point *A point p is a ∇-gravity point if p attains*

$$\min \sum_{i=1}^{n} D(p^{(i)} \| p). \tag{5.1}$$

∇-circumcenter *Suppose simultaneous equations*

$$D(p^{(i)} \| p) = D(p^{(j)} \| p) \ (\forall i, j = 1, \cdots, d+1) \tag{5.2}$$

for $d+1$ points in the dually flat space. The solution of these equations is called a ∇-circumcenter.

∇-sphere *For a point p in the dually flat space and a positive real number r, the set of point is a ∇-sphere if the ∇-divergence from p to the point of set is r.*

∇-circumscribed sphere *A ∇-sphere for a d-simplex in the d-dimensional dually flat space is a circumscribed sphere if all the vertices of the d-simplex are on the boundary of the sphere.*

The ∇^*-gravity point, the ∇^*-circumcenter, and the ∇^*-sphere are defined by substituting ∇^*-divergence $D^*(\cdot \| \cdot)$ for ∇-divergence $D(\cdot \| \cdot)$.

[Remark] These facts are shown immediately.

- A ∇-circumcenter does not always exist. If the point exists, that becomes the ∇^*-Voronoi point for $(d+1)$ points.
- A ∇-sphere is always included in the space.

The following lemma gives an easy way to calculate the ∇-gravity points.

Lemma 5.2 *Suppose points $\{p^{(j)}; j = 1, \ldots, n\}$ in the d-dimensional dually flat space with global coordinate system. The ∇-gravity point p in the θ-coordinate system can be uniquely determined to be*

$$\theta^j(p) = \frac{1}{n} \sum_{i=1}^{n} \theta^j(p^{(i)}) \tag{5.3}$$

where $\theta^j(p^{(i)})$ is the value of the jth coordinate of $p^{(i)}$.

Proof: Differentiate by η the criterion (5.1)

$$\frac{\partial}{\partial \eta_j} \sum_{i=1}^{n} D(p^{(i)} \| p) = n \cdot \theta^j(p) - \sum_{i=1}^{n} \theta^j(p^{(i)}) \ \ (j = 1, \cdots, d). \tag{5.4}$$

The quadratic differential is positive definite because that is metric (2.21). If there is a solution to the above equations, the point is a ∇-gravity point. The vanishing point is given by equation (5.3). □

[Remark] ∇^*-gravity points are calculated similarly. Thus the point is also expressed by

$$\eta_j(p) = \frac{1}{n}\sum_{i=1}^{n} \eta_j(p^{(i)}). \tag{5.5}$$

In addition, equation (5.5) is the same as equation (2.17). If this lemma for ∇^*-gravity point is limited to the statistical parametric space of exponential family, then the above equation expresses the maximum likelihood estimator for n points (Section 2.2.2).

Moreover, some graphs are defined for a set of points in d-dimensional Euclidean space. So that the set is contained in Euclidean space, suppose that these graphs are embedded in $\mathbb{R}^d$. For example,

Gabriel Graph (GG) A graph whose vertices are points in $\mathbb{R}^d$, with edge (x, y) iff points x and y defined the diameter of an empty sphere.

Relative Neighborhood Graph (RNG) A graph whose vertices are points in $\mathbb{R}^d$, with edge (x, y) iff there exists no points z such that z is closer to x than y is and z is closer to y than x.

There are the following relations for these graphs [17]:

$$\text{EMST} \subseteq \text{RNG} \subseteq \text{GG} \subseteq \text{Del}.$$

EMST is the *Euclidean minimum spanning tree*, which is the minimum spanning tree and whose weight is the Euclidean distance between two end points, and Del is the *Delaunay triangulation* of given points.

Since in the dually flat space the divergence does not satisfy the symmetry of distance, all graphs are not dealt with. That is, GG can be considered, but RNG, and EMST cannot. So the GG in the dually flat space is defined.

Definition 5.8 ($\nabla(\nabla^*)$-Gabriel Graph ($\nabla(\nabla^*)$-GG)) *Suppose a set P of points in the dually flat space. A graph is a* ∇-Gabriel graph *if whose vertex is P and edge (x, y) iff ∇-sphere, whose center is ∇-gravity point c of x, y and radius is ∇-divergence from x to c, is empty, that is, no points are contained in the interior of the sphere. The* ∇^*-Gabriel graph *is defined by replacing ∇ with ∇^*.*

Delaunay-type triangulation satisfies the following theorem.

Theorem 5.3 *For any given points in the dually flat space, the ∇-Delaunay-type triangulation includes the ∇-Gabriel graph. That is,*

$$\nabla\text{-GG} \subseteq \nabla\text{-Del},$$

where ∇-Del *is the* ∇*-Delaunay-type triangulation. There is the same relation for the* ∇^**-Gabriel graph and the* ∇^**-Delaunay-type triangulation.*

Proof: Let (x, y) be a geodesic segment that connects x and y and that becomes an edge of the ∇-Gabriel graph. In Theorem 5.2 we proved the duality of the ∇-Delaunay-type triangulation and the ∇^*-Voronoi diagram with removed faces. Compare the definition of the ∇-GG and of the ∇^*-Voronoi diagram. The set of equi-divergence points to two generators includes the ∇-gravity point of these points, and the ∇-gravity point lies on the ∇-geodesic segment joining generators (see Fig.5.5). That is, because the ∇-gravity point is given by the average of two generators in the θ-coordinate system (Lemma 5.2). Thus this geodesic segment is equal to the edge of graph.

Finally we show the inclusion for any edge of ∇-Gabriel graph. The existence condition of the edge is that there are no points in the sphere whose center is ∇-gravity and whose radius is the divergence. Since there is no points in the sphere, the ∇^*-Voronoi facet exists. That is, there is the geodesic segment connecting the two generators. □

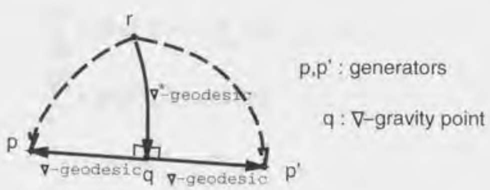

Figure 5.5: Two generators and the Pythagorean theorem in the θ-coordinate system

Here we prove that Delaunay-type triangulation is the "best" of all possible triangulations in the dually flat space. That is, we prove that the ∇-Delaunay-type triangulation minimizes the maximum radius of the *minimum enclosing* ∇*-sphere* by ∇-divergence.

First, we define the *minimum enclosing* ∇*-sphere*.

Definition 5.9 (Minimum Enclosing ∇-Sphere) *Suppose $d+1$ points in the d-dimensional dually flat space. A ∇-sphere is the* minimum enclosing ∇-sphere *if the sphere includes $d+1$ points and the radius is minimized by ∇-divergence from center point among all ∇-spheres including $d+1$ points.*

Lemma 5.3 *For given points $P = \{p^{(j)}; j = 1, \ldots, d+1\}$ in the d-dimensional dually flat space, let X be a linear combination of given points. That is, $X = \sum_{j=1}^{d+1} \lambda_j p^{(j)}$ in the θ-coordinate system where $\lambda_i > 0$, $\sum_i \lambda_i = 1$. The following equation is obtained:*

$$F(X) := \sum_{i=1}^{d+1} \lambda_i D(p^{(i)} \| X) = R - D(X_C \| X) \tag{5.6}$$

where X_C is the ∇-circumcenter for P and $R = D(p^{(j)} \| X_C)$ is constant ($j = 1, \ldots, d+1$) when X_C exists.

Proof:

$$\begin{aligned}
R - D(X_C \| X) &= \sum_{i=1}^{d+1} \lambda_i \{R - D(X_C \| X)\} = \sum_{i=1}^{d+1} \lambda_i \left[D(p^{(i)} \| X_C) - D(X \| X_C)\right] \\
&= \sum_{i=1}^{d+1} \lambda_i \Bigg[\psi(p^{(i)}) + \varphi(X_C) - \sum_j \theta^j(p^{(i)}) \eta_j(X_C) - \psi(X) - \varphi(X_C) + \sum_j \theta^j(X) \eta_j(X_C) \\
&= \sum_{i=1}^{d+1} \lambda_i \left[D(p^{(i)} \| X) + \sum_j \left\{\theta^j(p^{(i)}) - \theta^j(X)\right\} \{\eta_j(X) - \eta_j(X_C)\}\right] \\
&= \sum_{i=1}^{d+1} \lambda_i D(p^{(i)} \| X) + \sum_j \left\{\theta^j(X) - \theta^j(X)\right\} \{\eta_j(X) - \eta_j(X_C)\} \\
&= \sum_{i=1}^{d+1} \lambda_i D(p^{(i)} \| X) = F(X)
\end{aligned}$$

□

A proof of the above equation restricted to statistical parametric space, above equation for Kullback-Leibler divergence, is already shown in [18]. Here we prove it in general for a dually flat space with global coordinate system.

Moreover, by the above equation we can get the maximized point of $F(X)$.

Lemma 5.4 *In Lemma 5.3, if the ∇-circumcenter of the $d+1$ points is included in the d-simplex, $F(X)$ is maximized at the ∇-circumcenter. Otherwise the function is maximized at the boundary of the d-simplex.*

Proof: By Lemma 5.3

$$F(X) = R - D(X_C \| X).$$

Thus the $F(X)$ attains to maximum R at $X = X_C$ if X_C contained in the simplex. If X_C is not included in the simplex, the function becomes minimum at a point of the boundary of the simplex. Therefore suppose a enclosing ∇-sphere, F is maximized at the ∇-circumcenter among the point set $P' \subset P$ on the ∇-sphere as the c-dimensional space where $c+1$ is the number of P'.

In addition, if X_C does not exist in the space, then we consider ∇-circumscribed sphere of the face of the simplex, which contains all vertices of the simplex. The sphere with the smallest radius among such spheres is minimum enclosing sphere for the simplex. In this case the center of the sphere is on the boundary of the simplex. Because $F(X)$ maximize at the center of such sphere for the subset P' of points and λ_i for $P \setminus P'$ equal to 0. □

In addition, we define some functions. For $P = \{p^{(j)}; j = 1, \ldots, n\}$ in the d-dimensional dually flat space the function $f(X)$ is defined at every point X in the ∇-convex hull ∇-CH(P):

$$\lambda_i \geq 0, \ \sum_{i=1}^{n} \lambda_i = 1, \ \sum \lambda_i p^{(i)} = X, \tag{5.7}$$

$$F(X, \lambda) = \sum_{i=1}^{n} \lambda_i D(p^{(i)} \| X), \tag{5.8}$$

$$f(X) = \min_{\lambda} F(X, \lambda). \tag{5.9}$$

Theorem 5.4 *For* $\min_\lambda F(X, \lambda)$ *of a fixed point* X, *the non-zero values of* λ_i *are determined uniquely by the vertices of the Delaunay simplex, which is the simplex of* ∇*-Delaunay-type triangulation, containing the point* X. *Thus* $f(X)$ *is given by Lemma 5.4:*

$$f(X) = f_i(X) = R_i - D(X_{C_i} \| X)$$

where X_{C_i} *and* R_i *are respectively the center and the radius of the minimum enclosing* ∇*-sphere of the simplex.*

Proof: The ∇-Delaunay-type triangulation can be provided by the potential function ψ and the projection of the lower hull of ∇-convex hull (Algorithm 5.2).

Now we consider a point

$$\left(\sum_{i=1}^{n} \lambda_i p^{(i)}, \sum_{i=1}^{n} \lambda \psi(p^{(i)})\right) = (X, F(X, \lambda) + \psi(X)),$$

under the condition (5.7). This point represents all the points of ∇-CH(P). Moreover the minimum of F for X is given by the point with the lowest y-coordinate; therefore, the point lies on the lower-hull of the convex hull. This simplex is included in the ∇-Delaunay-type triangulation containing X. □

Finally we get the theorem about the minimum enclosing ∇-sphere.

Theorem 5.5 *The maximum radius of the minimum enclosing ∇-sphere of the simplex of the ∇-Delaunay-type triangulation, which is the ∇-divergence from the center to the points on the sphere, is equal or less than the maximum radius of the minimum enclosing ∇-sphere of any other triangulation of the set of points.*

Proof: A triangulation $\mathcal{T}$ for a set P of points is considered. The function $F_{\mathcal{T}}(X)$ is defined at each point X in ∇-CH(P) and is the same as the equation (5.6) for the simplex $T \in \mathcal{T}$ that contains the point X. Let $F_{\mathcal{D}}$ be a corresponding function for ∇-Delaunay-type triangulation $\mathcal{D}$. Let $X_{\mathcal{T}}$ and $X_{\mathcal{D}}$ be the points in ∇-CH(P) where $F_{\mathcal{T}}(X)$ and $F_{\mathcal{D}}(X)$ attain their maxima. Moreover, let $R_{\mathcal{T}}$ and $R_{\mathcal{D}}$ be the respectively ∇-divergences from $X_{\mathcal{T}}$ and $X_{\mathcal{D}}$ to the vertex of the simplex.

By Lemma 5.4 and Theorem 5.4 the following relation is proved:

$$R_{\mathcal{T}} = F_{\mathcal{T}}(X_{\mathcal{T}}) \geq F_{\mathcal{T}}(X_{\mathcal{D}}) \geq F_{\mathcal{D}}(X_{\mathcal{D}}) = R_{\mathcal{D}}.$$

Because the first inequality is based on the maxima of $X_{\mathcal{T}}$ for $\mathcal{T}$ and the second is by Theorem 5.4. Therefore we can get the result. □

We proved Theorem 5.5 for ∇-Delaunay-type triangulation, and there is a similar theorem for ∇^*-Delaunay-type triangulation.

Theorem 5.6 *The maximum radius of the minimum enclosing ∇^*-sphere of ∇^*-Delaunay-type triangulation, which is the ∇^*-divergence from the ∇^*-center to the points on the sphere, is equal or less than the maximum radius of the minimum enclosing ∇^*-sphere of any other triangulation of the set of points.*

Proof: The above lemmas of the ∇^* version can be proved by exchanging the role of ∇ and ∇^*. Those lemmas can be used to prove this theorem. □

[**Remark**] Theorem 5.5 includes the Euclidean case. This is proved in [43].

In this section we propose the *Delaunay-type triangulation* and prove some properties. Since this theory is a natural extension of Euclidean computational geometry, that triangulation is also characterized by some other theorems by potential function.

Chapter 6

Applications

Theoretical aspect of Riemannian computational geometry was described in Chapter 3, 4 and 5. That geometry is not only theory but also can be applied to some problems. In this chapter we talk about the geometric clustering and the triangulation of given surface.

Clustering is a classification of similar objects by a certain criterion, which is applied to data analysis, data reduction, pattern recognition, etc. In particular, we deal with *geometric clustering* in Section 6.1. In that clustering a proximate relation is used, for example, Voronoi diagram for given objects, i.e., that space is divided by that geometric structure. In previous researches ([20, 47]) that space is regarded as the Euclidean space and Euclidean geometry is applied. The proximate structure is the *Euclidean* Voronoi diagram. In this thesis, we propose that the space is regarded as the dually flat space and Riemannian geometry is applied. In addition, we consider an improving algorithm of geometric clustering in the dually flat space, called *k-means algorithm*. By that algorithm we can get a nice k-clustering rather than initial clustering. Section 6.1 is considered by project of Imai Laboratory and produced by discussion with Mary Inaba.

In Section 6.2, we deal with a triangulation of surface. One of our aim is a proposition of new mesh generation method. Unfortunately its theory is not established yet. We only state an idea and some parts of such method in that space.

6.1 Geometric Clustering

In this section we describe *geometric clustering* in the dually flat space. So the ordinary clustering is based on the Euclidean space and Euclidean geometry. In this thesis we propose new basis *dually flat space* and *Riemannian geometry* for geometric clustering. This concept is an extension of Euclidean and include various spaces. In particular, we already explained the *statistical parametric space* is included in that space and has closely relations between maximum likelihood method in Section 2.2.2. As the divided space is regarded as the dually flat space or the statistical parametric space, then we use ∇^*-*Voronoi diagram* for the division.

Here, we consider geometric clustering for given points, i.e., for a set of points $P = \{p^{(i)}; i = 1, \ldots, n\}$ P divides into k parts, called k-clustering problem. If the set is contained in the Euclidean space, then it is natural that the Euclidean Voronoi diagram is used to the separation, for example, [20, 47] etc. We use the other space for clustering, i.e., that space including P is regarded as not the Euclidean space but the dually flat space with global coordinate system. In [31, 1] the set of points is regarded as parameters of probability density function. We want to apply such space to clustering. By such method a new clustering may be provided.

When we adopt such space for the k-clustering problem, we consider what criterion is used in the space. In the Euclidean space various criteria are used, for example, sum of squared error and all-pairs sum of squared error in each cluster. The former is dealt with in [20], then proposed an efficient algorithm of k-clustering and an ϵ-approximation 2-cluster algorithm. Since its time complexity is $O(n^{(d+2)k+1})$ and so good rather than previous algorithms, we use the sum of squared error and aim at such bound in this case. The sum of squared error in Euclidean space is defined like this :

$$\min \sum_k \sum_{p \in C_k} d(p, \bar{p}_{(k)})^2 \tag{6.1}$$

where $d(\cdot, \cdot)$ is the distance in the Euclidean space, C_k is a cluster and $\bar{p}_{(k)}$ is gravity point for all points in C_k. Since the square of Euclidean distance corresponds to *divergence* in the dually flat space, we adopt the following criterion for a set of points :

$$\min \sum_k \sum_{p \in C_k} D^*(p \,\|\, \bar{p}^{(k)}) \tag{6.2}$$

where $D^*(\cdot \,\|\, \cdot)$ is the ∇^*-divergence in the dually flat space, C_k is a cluster and $\bar{p}_{(k)}$ is ∇^*-gravity point (Definition 5.7) for all points in C_k. So this criteria is explained by the terms of information theory as follows :

> Suppose k information sources and n observed values from k sources. Which source is the observed value provided?

Since there are some information sources, more detailed estimation may do for observed values rather than single source, i.e., the following algorithm computes the maximum likelihood estimator in each cluster and the sum of the estimators minimizes. In [28, pp.154-156] a similar clustering algorithm is explained as *EM-algorithm* in the probabilistic clustering.

By this criterion we can consider a k-means algorithm in the dually flat space which is a kind of k-means algorithm for the criterion of convex function and its convergence is proved in [49]

Algorithm 6.1 (k-means algorithm in the dually flat space)
Input : set of points P and integer number k.
Output : k-clustering.

1. P':={selected k points from P};

2. Make ∇^*-Voronoi diagram for P'.

3. Calculate ∇^*-gravity point for each Voronoi polygon;
   /* Each Voronoi cell is regarded as one cluster. */
   /* Since the number of polygons is k, then the division becomes k-clustering. */

4. **if** (all ∇^*-gravity point = P')

   then End;

   else $P' := \{\nabla^*$-gravity points$\}$;

5. **goto** 2;

In second step above algorithm the ∇^*-Voronoi diagram is considered however it is not necessary that diagram is actually computed. That is only theoretical object and actually calculate which point is nearest to the generator by the ∇^*-divergence.

Although the termination of this algorithm is proved in [49] and the convexity of divergence, we state the proof.

Proposition 6.1 *Algorithm 6.1 is finished for a set of points in general position.*

Proof: It is trivial that there exists a minimum of criterion (6.2), since the number of clustering for given finite set of points is finite. So we state that the value of criterion (6.2) is decreased by Algorithm 6.1.

Suppose a k-clustering A by ∇^*-Voronoi diagram for k points. Let $F(A)$ be a value of criterion (6.2) for clustering A. Consider a cluster C_k of A. Let $p^{(k)}$ be a generator of C_k and $\bar{p}^{(k)}$ be a ∇^*-gravity point for the whole points of C_k. The following equation is obtained

$$\sum_{p \in C_k} D^*(p \| p^{(k)}) \geq \sum_{p \in C_k} D^*(p \| \bar{p}^{(k)})$$

by the definition of the ∇^*-gravity point. This inequality is proved for all cluster of A. Thus the criterion does not increase by this step.

Moreover suppose a k-clustering B by ∇^*-Voronoi diagram for above ∇^*-gravity points. Compare between A and B. Suppose that a point p moves from a cluster C_l to other C_m. Since the point is near to the generator $p^{(m)}$ of C_m than $p^{(l)}$ of C_l by ∇^*-divergence, p move the cluster (if an equi-divergence point from two generators exists, then this point does not move). Thus the equation $D^*(p\| p^{(m)}) < D^*(p\| p^{(l)})$ is satisfied. By this equation the value of the criterion is always decreased. So we get the inequality

$$F(A) > F(B).$$

Therefore the criterion diminishes by repeating of the algorithm, then the criterion is reached to local minimum and the algorithm is terminated. □

[Remark] A k-clustering for given points is given by Algorithm 6.1. However this clustering is the *local optimal* and the structure depends on the *initial point* (Step 1), i.e., this problem is regarded as an *optimization problem* and some approximation method can be applied, for example, taboo search, simulated annealing, etc. In this section we state the geometric clustering by not ∇-Voronoi diagram but ∇^*-Voronoi. Because the ∇^*-gravity point of each cluster is given by maximum likelihood estimator (Lemma 5.2).

Moreover we describe a family of all discrete distributions in a certain dimension. Since the feature space of text data and the vector space of colors are regarded as this family, these space also is separated by above algorithm. We explain the feature space of text data. For given n text data, select $d+1$ keywords by certain *standards*, compute frequency of keywords in each text data and normalize these vectors as each sum is equal to one. So we can get n vectors in the $d+1$-dimensional dually flat space.

$$\left\{\xi_{(i)} \;\middle|\; 0 < \xi_{(i)j} < 1, \sum_{j=0}^{d} \xi_{(i)j} = 1, i = 1, \cdots, n, j = 0, \cdots, d\right\}$$

This vectors are regarded as d-dimensional discrete distributions, i.e., following distribution is considered : $\mathcal{X} = \{x_0, \ldots, x_d\}, \Xi = \left\{[\xi_1, \ldots, \xi_d] \;\middle|\; \xi_i > 0\ (\forall i = 1, \ldots, d),\ \sum_{i=1}^{d} \xi_i < 1\right\}$

$$p(x_i; \xi) = \begin{cases} \xi_i & i = 1, \cdots, d \\ 1 - \sum_{j=1}^{d} \xi_j & i = 0 \end{cases}.$$

Thus the space of Ξ is equal to $(0,1)^d$. Above equation is rewritten:

$$p(x; \theta) = \exp\left[\sum \theta^i F_i(x) - \psi(\theta)\right],$$

where $F_i(x) = \begin{cases} 1 & (x = x_i) \\ 0 & (x \neq x_i) \end{cases}$, $\theta^i = \log \dfrac{p(x_i)}{p(x_0)}$ and $\psi(\theta) = \log\left\{1 + \sum_{i=1}^{d} \exp \theta^i\right\} = -\log \xi_0$. Therefore the family of those distribution is contained in the exponential family. In the η-coordinate system of this family becomes

$$\eta_i = \int F_i(x) p(x; \theta) dx = p(x_i) = \xi_i.$$

i.e., $[\eta]$ is regarded as the space Ξ. By these calculations the divergence in this space can be computed like this:

$$D(\eta \| \bar{\eta}) = \sum_{i=0}^{d} \bar{\eta}_i \log \frac{\bar{\eta}_i}{\eta_i}.$$

Finally, for a given set of feature vector in the η-coordinate system, ∇^*-Voronoi diagram is computed by Kullback-Leibler divergence and ∇^*-gravity points is calculate by the average of vectors. In the case of vector space of color, weights of each coordinate depending on chosen color should be used.

6.2 Triangulation of Surface

It is said that finite element method and computer graphics are an application of triangulation, since it is one reason that triangulation is used *mesh generation*. Not only triangulation but also mesh generation are investigated by many researchers. There are survey about triangulation and mesh generation in [4, 16]. In particular, in [13] mesh generation by Delaunay triangulation is investigated and in [7, 8] Riemannian metric is used for computing length on the surface however the length is along Euclidean segment not geodesic, i.e., that is only an approximation.

Here, we state our idea for mesh generation. All points on the given surface are separated to three types, i.e., its curvature is positive, zero and negative, which correspond to sphere, plane and *Poincaré space* as a space, respectively. If the surface is skillfully divided into each cluster by the curvature, each region is regarded as sphere, plane or Poincaré space and can be triangulated. Delaunay triangulation in the sphere and in the plane are already described in [35] and [12, 42], respectively, however there is no such good triangulation in the Poincaré space. In this thesis we propose a proximate relation in the hyperbolic space, called *hyperbolic Delaunay graph*. This structure contains minimum spanning tree for given points (Proposition 5.3, i.e., this object has a nice property in the hyperbolic space). In addition, *Delaunay-type triangulation* is defined in Section 5.2, which is a triangulation in the Poincaré space and contains hyperbolic Delaunay graph.

Thus three triangulations in each space are efficiently computed. However there are many problem for this method ;

- computation of mesh points;
- division of the generation points by its curvature;
- composition of each triangulation, etc.

Here, we show the triangulation in Poincaré space is transformed into a surface in three dimensional Euclidean space.

Figure 6.1: Pseudo-sphere in $\mathbb{R}^3$

For a domain $D = \{(u, v) \mid 0 \leq u \leq 2\pi, v \geq 1\} \subset \mathbb{H}$ we define the function $f : D \mapsto \mathbb{R}^3$ as follows:

$$f((u, v)) = \left(\frac{1}{v}\cos u, \frac{1}{v}\sin u, \log(v + w) - \frac{w}{v}\right)$$

where $w = \sqrt{v^2 - 1}$. The image $f(D)$ is a surface on $\mathbb{R}^3$, which is called *pseudo-sphere*. The metric in $\mathbb{R}^3$ naturally introduces the metric on the pseudo-sphere. The domain $D \subset \mathbb{H}$ and $f(D)$ is isomorphic as the Riemannian manifold. Hence, the hyperbolic Voronoi diagram and a triangulation on $\mathbb{H}$ are regarded as the Voronoi diagram and triangulation on the pseudo-sphere in $\mathbb{R}^3$ without changing distance, respectively.

In this section we only explain an idea of mesh generation and the correspondence between the Poincaré space and the pseudo-sphere. More research is necessary to an implementation of such mesh generation.

Chapter 7

Conclusion

In this thesis we have dealt with computational geometry in Riemannian space, which is called *Riemannian computational geometry*; a description of the properties of the convex hull, the Voronoi diagram and the Delaunay-type triangulations in hyperbolic space and in dually flat space; and the proposition of efficient constructive algorithms. These structures can be calculated by computer and applied to real problems.

In Chapter 3 we described the convex hull as the simplest object amongst those treated, whose concept can be considered in the space where a unique minimizing geodesic joins any two points. However such a structure is not always determined uniquely and is not always computable in a general Riemannian space. We show that the convex hull in the special case of a flat space with global coordinate system can be constructed (Section 3.2). In hyperbolic space, the convex hull is also efficiently computed by a linearization method. In Section 3.5 we propose a class of Riemannian space, called *linearizable space*, which includes flat space with global coordinate system and hyperbolic space. The convex hull for a given set of points in these spaces is efficiently computable and constructed by a Euclidean algorithm. In these spaces, the geodesic segment coincides with the Euclidean segment, and the convex hull is included in the space. However, there are some problems remaining. For example, "Is the convex hull computable in non-linearizable space?" and, "Is there a flat and non-linearizable space ?".

We explained the Voronoi diagram in Riemannian spaces (Chapter 4). That structure in hyperbolic space is determined by the distance with Levi-Civita connection, the perpendicular bisector is a half-sphere, and the collection of geodesics. Moreover, the sphere in the hyperbolic space coincides with the Euclidean. Thus, for a given set of points, the circumscribed sphere is the same if that sphere is contained in the space. By this fact, when that sphere is included, the part has the same structure as the Euclidean. Otherwise, that part is removed. The hyperbolic Voronoi diagram is efficiently computable using these properties. For Voronoi diagrams in dually flat space, called ∇- and ∇^*-Voronoi diagrams, we use *divergence* instead of distance. There are two diagrams, because the divergence is non-symmetric, since the diagrams are a projection of a certain hyperplane arrangement. That diagrams can be computed by an algorithm of the Euclidean Voronoi diagram and the removal of faces (Section 4.3). That correspondence is proved, since the relation between potential function and distance is extended to the relation between potential functions and *divergences*. By this property the algorithm for computation can be designed. We also state the relationship between that diagram in the statistical parametric space of normal distribution and in the Poincaré space in Section 4.4. Moreover we state the higher-order Voronoi diagram in each space.

In Chapter 5 we mainly explained Delaunay triangulation. Since it is not necessarily the case that Delaunay triangulation exists in these spaces, we propose a triangulation, which is called *Delaunay-type triangulation* and which shares some of the properties of Delaunay triangulation. The Delaunay graph, the dual structure of the hyperbolic Voronoi diagram, has nice characteristics but is not a triangulation in the space. A triangulation in that space, which contains the Delaunay graph and is based on a minimum enclosing sphere, is defined. However, its properties are not yet known. We show that there is a flippable class of triangulation in the Poincaré space. Since this space is two dimensional, some other properties of triangulation in the Euclidean plane may be proved. Moreover, the Delaunay-type triangulation in the dually flat space is also considered. That is defined by a *potential function* and has characteristics of the Euclidean Delaunay triangulation, concerning the minimum enclosing sphere - maximal minimum enclosing sphere of the Delaunay-type triangulation minimized amongst all triangulations in the dually flat space. Further research is needed to uncover other properties of the triangulation.

In addition, we explained the applications of these structures in Section 6. For two problems, *geodesic clustering* and *surface triangulation*, we apply the ∇-Voronoi diagram and the triangulation of Poincaré space, respectively. The former is a geometric clustering for a set of points. Suppose these vectors are embedded in the Euclidean space, then the measure should depend on the Euclidean metric. If those are included in the statistical parametric space or the dually flat space, then we should use the divergence as a measure and the ∇^*-Voronoi diagram. In this case we adopt the ∇^*-Voronoi diagram not ∇-Voronoi, because the ∇^*-Voronoi has the closest relationship to the maximum likelihood method. In Section 6.2 we state an idea for mesh generation, which is based on the curvature of the points on the surface. Moreover we state that the triangulation of the Poincaré space maps to the surface in three dimensional space without changing the distance - a nice triangulation of the surface is easily constructed if Delaunay-type triangulation is used. We intend to propose a new mesh-generation method when this topic has been further researched.

In this thesis, some efficiently computable geometric structures, convex hull, Voronoi diagram and Delaunay-type triangulation in both hyperbolic space and dually flat space, are defined and investigated. In these spaces, other structures may be considered, for example, tilings, visibility, shortest path problem, etc. It is most important to note that geometric structures in Riemannian space can be efficiently computed, which is interesting and is the main contribution of this thesis. The research has been undertaken from both a mathematical and a computational point of view. These fields have so many topics that are worthy of study.

References

[1] S. Amari : *Differential Geometrical Methods in Statistics.* Lecture Notes in Statistics, Vol.28, Springer-Verlag, New York, 1985.

[2] S. Amari : Differential Geometry of a Parametric Family of Invertible Linear Systems - Riemannian Metric, Dual Affine Connections and Divergence. *Mathematical Systems Theory,* Vol. 44, 1987, pp.53-82.

[3] S. Amari and H. Nagaoka : *Method of Information Geometry* (in Japanese). Iwanami Shoten, Tokyo, 1993.

[4] M. Bern and D. Eppstein : Mesh Generation and Optimal Triangulation. In D.-Z. Du and F. K. Hwang, editors, *Computing in Euclidean Geometry, 2nd Edition,* World Scientific, Singapore, 1995, pp.47-123.

[5] J. D. Boissonat, A. Cérézo, O. Devillers, M. Teillaud : Output-Sensitive Construction of the Delaunay Triangulation of Point Lying in Two Planes. *International Journal of Computational Geometry & Applications,* Vol. 6, No. 1, 1996, pp.1-14.

[6] J. D. Boissonat, M. Yvinec : *Algorithmic Geometry.* Cambridge University Press, Cambridge, 1998.

[7] H. Borouchaki, P. L. George, F. Hecht, P. Laug, E. Saltel : Delaunay Mesh Generation Governed by Metric Specifications. Part I. Algorithms. *Finite Elements in Analysis and Design,* Vol. 25, 1997, pp.61-83.

[8] H. Borouchaki, P. L. George, B. Mohammadi : Delaunay Mesh Generation Governed by Metric Specifications. Part II. Applications. *Finite Elements in Analysis and Design,* Vol. 25, 1997, pp.85-109.

[9] B. H. Bowditch : Some Results on the Geometry of Convex Hulls in Manifolds of Pinched Negative Curvature. *Comment. Math. Helvetici*, Vol. 69, 1994, pp.49-81.

[10] K. L. Clarkson and P. W. Shor : Applications of Random Sampling in Computational Geometry, II. *Discrete Comput. Geom.*, Vol. 4, 1989, pp.387-421.

[11] T. M. Cover and J. A. Thomas : *Elements of Information Theory*. Wiley-Interscience, New York, 1991.

[12] H. Edelsbrunner : *Algorithms in Combinatorial Geometry*. Springer-Verlag, Berlin, 1987.

[13] H. Edelsbrunner and T.-S. Tan : A Upper Bound for Conforming Delaunay Triangulations. *Discrete Comput. Geom.* Vol. 10, 1993, pp.335-347.

[14] P. E. Ehrlich and H-C. I. Hof : Dirichlet Regions in Manifolds without Conjugate Points. *Comment. Math. Helvetici.*, Vol. 54, 1979, pp.642-658.

[15] L. P. Eisenhart : *Riemannian Geometry*. Princeton Univ. Press, Princeton, 1949.

[16] P. L. George : *Automatic Mesh Generation*. Weily, New York, 1991.

[17] J. E. Goodman and J. O'Rourke edited : *Handbook of Discrete and Computational Geometry*. CRC Press, New York, 1997.

[18] Y. Horibe : *Information Entropy, 2nd Edition*, (in Japanese). Morikita Syuppan, Tokyo, 1997.

[19] H. Imai, M. Iri and K. Murota : Voronoi Diagrams in the Laguerre Geometry and Its Applications. *SIAM J. Comput.*, Vol.14, 1985, pp.93-105.

[20] M. Inaba, N. Katoh and H. Imai : Application of Weighted Voronoi Diagrams and Randomization to Variance-based k-clustering. *Proc. 10th ACM Symposium on Computational Geometry*, 1994, pp.332-339.

[21] J. Itoh : The Length of a Cut Locus on a Surface and Ambrose's Problem. *J. Differential Geometry*, Vol.43, 1996, pp.642-651.

[22] J.Itoh : Riemannian Metric with Fractal Cut Locus. *Preprint*.

[23] U. H. Ki and N. G. Kim : Ruled Real Hypersurfaces of a Complex Space Form. *Acta Mathematica Sinica*, New Series. Vol 10, No.4, 1994, pp.401-409.

[24] S. Kobayashi and K. Nomizu : *Foundations of Differential Geometry I & II*. Interscience Publishers, 1969.

[25] S. Kojima : Knot, Three-dimensional Manifold and Hyperbolic Geometry (in Japanese). *Sūgaku*, Vol. 49, No. 1. 1997, pp.25-37.

[26] D.-T. Lee : On k-nearest Neighbor Voronoi Diagrams in the Plane. *IEEE Trans. Comput.* C-31, 1982, pp.478-487.

[27] M. Mazón and T. Recio : Voronoi Diagrams on Orbifolds. *Computational Geometry : Theory and Applications*, Vol. 8, No. 5, 1997, pp.219-230.

[28] B. Mirkin : *Mathematical Classification and Clustering*. Nonconvex Optimization and Its Applications, Vol.11, Kluwer Academic Publishers, Boston, 1996.

[29] M. K. Murray and J. W. Rice : *Differential Geometry and Statistics*. Monographs on Statistics and Applied Probability, Vol.48, Chapman & Hall, London, 1993.

[30] M. Näätänen and R.C. Penner : The Convex Hull Construction for Compact Surfaces and the Dirichlet Polygon. *Bull. London Math. Soc.*, Vol.23, 1991, pp.568-574.

[31] H. Nagaoka and S. Amari : Differential Geometry of Smooth Families of Probability Distributions. *METR*, 82-7, University of Tokyo, 1982.

[32] Y. Namikawa : A New Compactification of the Siegel Space and Degeneration of Abelian Varieties I. *Math. Ann.*, Vol. 221, No 2, 1976, pp.97-141.

[33] Y. Namikawa : A New Compactification of the Siegel Space and Degeneration of Abelian Varieties II. *Math. Ann.*, Vol. 221, No 2, 1976, pp.201-241.

[34] S. Negami : Diagonal Flips in Triangulations of Surfaces. *Discrete Mathematics*, 1994, pp.225-232.

[35] A. Okabe, B. Boots, K.Sugihara : *Spatial Tessellations Concepts and Applications of Voronoi Diagrams*. John Weily, New York, 1992.

[36] K. Onishi : Riemannian Computational Geometry — The Convex Hull and Voronoi Diagram in Hyperbolic Space —. *Submitted*, 1998.

[37] K. Onishi and H. Imai : Voronoi Diagram in Statistical Parametric Space by Kullback-Leibler Divergence. *Proc. 13th ACM Symposium on Computational Geometry*, Communication Session, 1997, pp.463-465.

[38] K. Onishi and H. Imai : Voronoi Diagram for an Exponential Family of Probability Distributions in Information Geometry. *JAPAN-KOREA Joint Workshop'97 on Algorithm and Computation*, Kyushu University, Fukuoka, pp.1-8, 1997.

[39] K. Onishi and H. Imai : Riemannian Computational Geometry — Voronoi Diagram and Delaunay-type triangulation in dually flat space —. *Submitted*, 1998.

[40] K. Onishi and N. Takayama : Construction of Voronoi Diagram on the Upper Half-plane. *IEICE Trans. on Fundamentals*, Vol.E79-A, No.4, 1996, pp.533-539.

[41] P. Petersen : *Riemannian Geometry*, Springer, New York. 1998.

[42] F. P. Preparata and M. I. Shamos : *Computational Geometry*, Springer-Verlag, New York, 1985.

[43] V. T. Rajan : Optimality of the Delaunay Triangulation in $\mathbb{R}^d$. *Proc. 7th ACM Symposium on Computational Geometry*, 1991, pp.357-363.

[44] C. R. Rao : Information and Accuracy Attainable in the Estimation of Statistical Parameters, *Bull. Calcutta. Math. Soc.*, Vol.37., 1945, pp.81-91.

[45] R. T. Rockafellar : *Convex Analysis*. Princeton University Press, Princeton, 1970.

[46] S. Sadakane, H. Imai, K. Onishi, M. Inaba, F. Takeuchi and K.Imai : Voronoi Diagrams by Divergences with Additive Weights. *Proc. 14th ACM Symposium on Computational Geometry*, Video Session, 1998, pp.403-404.

[47] T. Schreiber : A Voronoi Diagram Based Adaptive K-means-type Clustering Algorithm for Multidimensional Weighted Data. In *Computational Geometry –Methods, Algorithms and Applications*, Vol. 553 of *Lecture Notes in Comput. Sci.*, Springer-Verlag, New Yorks, 1992, pp.265-275.

[48] R. Seidel : Constructing Higher-dimensional Convex Hulls at Logarithmic Cost per Face. *Proc. 18th ACM Symposium on Theory of Computing*, 1986, pp.404-413.

[49] S. Z. Selim and M. A. Ismail: K-Means-Type Algorithms: A Generalized Convergence Theorem and Characterization of Local Optimality. *IEEE Transactions on Pattern Analysis and Machine Intelligence*, Vol.PAMI-6, No.1 (1984), pp.81–87.

[50] D. D. Sleator, R. E. Tarjan, W. P. Thurston, William : Rotation distance, Triangulations, and Hyperbolic Geometry. *J. Amer. Math. Soc.* Vol.1 , no. 3, 1988, pp.647-681.

[51] K. Tanabe and T. Tsuchiya : Dynamical Systems Associated with Karmarkar's Method for Linear Programming. *Preprint*, Institute of Statistical Mathematics, 1987.

[52] W. P. Thurston : *Three-dimensional Geometry and Topology*. Vol 1. Princeton University Press, Princeton, 1997.

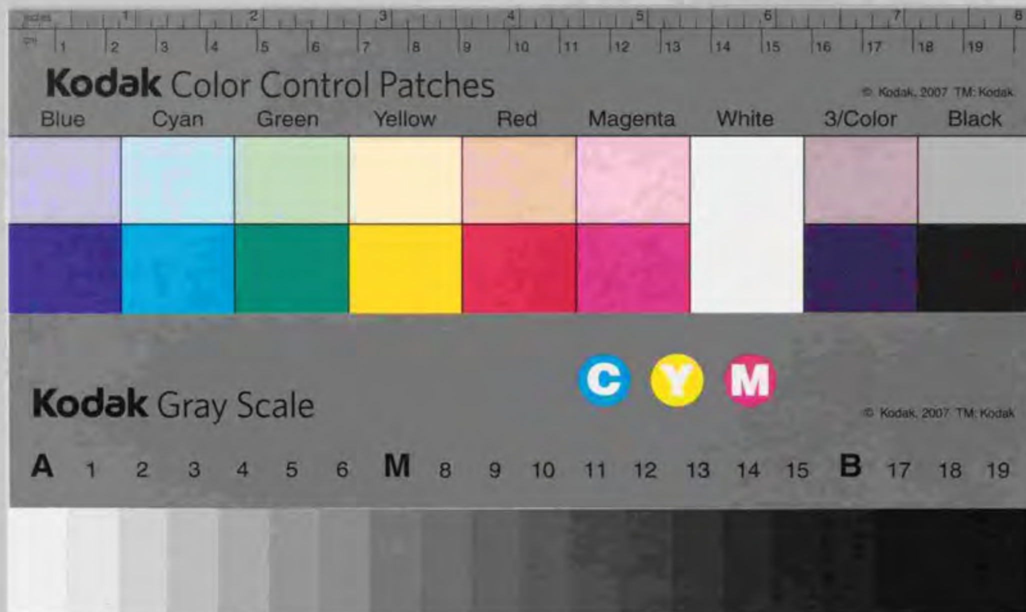
Kodak Color Control Patches
© Kodak, 2007 TM: Kodak
Blue Cyan Green Yellow Red Magenta White 3/Color Black
C Y M
Kodak Gray Scale
© Kodak, 2007 TM: Kodak
A 1 2 3 4 5 6 M 8 9 10 11 12 13 14 15 B 17 18 19